SEISMIC RESPONSE CONTROL OF A BUILDING USING PASSIVE DEVICES

BY

VIJAY M. CHACHAPARA

09MCL003

NIRMA UNIVERSITY
INSTITUTE OF TECHNOLOGY

DEPARTMENT OF CIVIL ENGINEERING

AHMEDABAD-382481

May 2011

SEISMIC RESPONSE CONTROL OF A BUILDING USING PASSIVE DEVICES

Major Project

Submitted in partial fulfillment of the requirements

For the degree of

Master of Technology in Civil Engineering

(Computer Aided Structural Analysis & Design)

By

VIJAY M. CHACHAPARA

09MCL003

तमसो मा ज्योतिर्गमय

NIRMA UNIVERSITY

INSTITUTE OF TECHNOLOGY

DEPARTMENT OF CIVIL ENGINEERING

AHMEDABAD-382481

May 2011

Declaration

This is to certify that

a. The thesis comprises my original work towards the Degree of Master of Technology in Civil Engineering (Computer Aided Structural Analysis and Design) at Nirma University and has not been submitted elsewhere for a degree.

b. Due acknowledgement has been made in the text to all other material used.

Vijay M. Chachapara

Certificate

This is to certify that the Major Project entitled "Seismic Respose Control of a Building using Passive Devices" submitted by Vijay M. Chachapara (09MCL003), towards the partial fulfillment of the requirements for the degree of Master of Technology in Civil Engineering (Computer Aided Structural Analysis and Design) of Nirma University, Ahmedabad is the record of work carried out by him under my supervision and guidance. In my opinion, the submitted work has reached a level required for being accepted for examination. The results embodied in this major project, to the best of my knowledge, haven't been submitted to any other university or institution for award of any degree or diploma.

Dr. S.P. Purohit
Guide and Associate Professor,
Department of Civil Engineering,
Institute of Technology,
Nirma University, Ahmedabad

Dr. P. H. Shah
Professor and Head,
Department of Civil Engineering,
Institute of Technology,
Nirma University, Ahmedabad

Dr K Kotecha
Director,
Institute of Technology,
Nirma University,
Ahmedabad

Examiner

Date of Examintion

Abstract

Earthquake is one of the major natural hazards to life on the earth and have affected people and structure of every continent. The damaged caused by earthquake is mostly associated with man mad structures. Hundreds of earthquakes (small or big) are affecting regularly acroses the world and hence, it is necessary that structures should be designed to resist earthquake forces, so as it reduces the loss of lives. Three basic technologies are currently in practice to protect buildings from damaging earthquake effects. These are Base Isolation, Passive Energy Dissipation Devices and Active Control Devices. In passive energy dissipation systems the motion of structure is controlled by adding devices which modifies stiffness, damping or both. Passive energy dissipation devices are found effective against winds and earthquake induced motion, and operates on principles such as, yielding of metals, frictional sliding and deformation of viscoelastic (VE) solids or fluids.

The present study is an attempt to understand the behavior of passive energy dissipation devices and its effectiveness in response reduction under different types of excitation. The work composed of characterizing passive devices, like Viscous, Viscoelastic (VE), and Metallic Yield dampers, under sinusoidal motion and random earthquake excitations through commercially available tool MATLAB. Earthquake events used in this studies are El Centro(1940), Loma Prieta (1989), Northridge (1994), and Kobe (1995) time histories. A three storey shear building has been considered to find out the effectiveness of various passive dampers. Lump mass model is adopted in order to obtain, mass matrix and stiffness matrix. Damping is assumed to be Rayleigh's damping and damping matrix is determined considering 5 % critical damping coefficient for all modes. Equation of motion for multi degree of freedom system with passive devices are derived. These equations are solved using numerical method like Newmark-Beta for building without passive device, i.e,. uncontrolled and with passive devices, i.e,. controlled building under the different earthquake excitations through MATLAB. Response quantities like displacement, velocity, acceleration, inter storey

drift and damper force have been extracted for uncontrolled and controlled building. The response quantities of uncontrolled building have been compared with the controlled building in order to establish it's effectiveness.

Parametric study of three storey building equipped with viscous and viscoelastic damper have been carried out, by changing the damping co-efficient and required damping ratio respectively. Results indicate that extra amount of damping and stiffness provided by different passive damper directly influence the responses by reducing it. From the study, it can be reveals that all the response quantities like maximum displacement, maximum velocity, maximum acceleration and maximum inter storey drift are reduces by half as compare to uncontrolled building. It has been found that, viscous damper are more effective under the Northridge type of earthquake excitations, however viscoelastic and ADAS damper are suitable for Loma Prieta type of earthquake excitations.

Acknowledgements

I would first of all like to thanks **Dr. S. P. Purohit**, Guide M.Tech. Department of Civil Engineering (CASAD), Institute of Technology, Nirma University, Ahmedabad whose keen interest and excellent knowledge base helped me to carry out the dissertation work. His constant support and interest in the subject equipped me with a great understanding of different aspects of the required architecture for the project work. He has shown keen interest in this dissertation work right from beginning and has been a great motivating factor in outlining the flow of my work.

My sincere thanks and gratitude to **Prof. G. N. Patel**, Formerly Professor, Department of Civil Engineering, **Dr. P. V. Patel**, Professor, Department of Civil Engineering, and **Prof. N. C. Vyas**, Professor, Civil Engineering Department, Institute of Technology, Nirma University, Ahmedabad for his continual kind words of encouragement and motivation throughout the Dissertation work.

I further extend my thanks to **Dr. P. H. Shah**, Head, Department of Civil Engineering, Institute of Technology, Nirma University, Ahmedabad and **Dr K Kotecha**, Director, Institute of Technology, Nirma University, Ahmedabad for providing all kind of required resources during my study.

I would like to thank The Almighty, my family and all my friends, for supporting and encouraging me in all possible ways throughout the dissertation work.

- Vijay M. Chachapara
09MCL003

Abbreviation Notation and Nomenclature

ADAS .... Added Damping and Stiffness
DVA .... Dynamic Vibration Absorber
EQ .... Earthquake
FEMA .... Federal Emergency Management Egency
PGA .... Peak Ground Acceleration
PGV .... Peak Ground Velocity
PGD .... Peak Ground Displacement
sgm .... Signum Function
RCC .... Reinforced Cement Concrete
SDOF .... Single Degree of Freedom
SR .... Stiffness Ratio of Metallic Damper
TADAS .... Triangular Plate Added Damper
VE .... Viscoelastic
a .... Amplitude of Motion
m .... Mass Matrix of Building
k .... Stiffness Matrix of Building
c .... Damping Matrix of Building
f_{ck} .... Characteristic Strength of Concrete
f_y .... Characteristic Strength of Steel
E_d .... Energy Dissipation per Cycle
γ_0 .... Shear Strain Amplitude
V .... Volume of the Viscoelastic Material
P(t) .... Force in an Energy Dissipation Damper as a Function of Time
C_d .... Co-efficient of Damper
α .... Velocity Exponent of Viscous Damper
$\tau(t)$ .... Shear Stress as a Function Time
$\gamma(t)$ .... Shear Strain as a Function Time
f .... Circular Frequency in Radians per Seconds

G' .... Storage Modulus of Viscoelastic Material

G'' .... Loss Modulus of Viscoelastic Material

K_d .... Damper Stiffness

$F(t)$ .... Force in VE Damper as a Function of Time

A .... Shear Area of Viscoelastic Material

t .... Thickness of Viscoelastic Damper

ζ .... Required Damping Ratio of Building

ς .... Target Added Damping Ratio

ξ .... Inherent Damping Ratio of Building

ω .... Fundamental Frequency of Building

P_y .... Yield Force of Metallic Yield Damper

Δ_y .... Yield Displacement of Metallic Yield Damper

k_a .... ADAS Damper Element Stiffness

Contents

List of Tables

List of Figures

Chapter 1

Introduction

1.1 General

Earthquakes are one of the major natural hazards to life on the earth and have affected countless cities and villages on almost every continent. The damaged caused by earthquakes are mostly man mad structures. Hundreds of small earthquake occurs around the world every day. Some of them are so minor that humans cannot feel them, but seismographs and other sensitive machines can record them. Every year, earthquakes take the lives of thousands of people, and destroy property worth billions. Therefore, it is necessary that structures are designed to resist earthquake forces, in order to reduce the loss of life. Earthquake engineering has gain lots of attention and structural design has a lot since past years, one can design safe structures which can safely withstand earthquakes of reasonable magnitude.

Conventional seismic design attempts to make buildings that do not collapse under strong earthquake shaking, but may sustain damage to non-structural elements and to some structural members in the building. This may cause the building to be non-functional after the earthquake, which may be problematic in some structures, like hospitals, which need to remain functional after an earthquake. Special techniques are required to design buildings such that they remain practically undamaged even in a severe earthquake. Damage in the structures are due to vibrations that arise from external forces like earthquake, wind forces, machine vibrations, or many other sources. However inherent or natural damping in structure helps to a some extent vibrations caused due to earthquake etc. But, for structures subjected to strong motions, the inherent damping in the structure is not sufficient to mitigate the structural response. All vibrating structures dissipate energy due to internal stressing, rubbing, cracking, plastic deformations, and so on; the larger the energy dissipation capacity the smaller the amplitudes of vibration. Some structures have very low damping on the order of 1% of critical damping and consequently experience large amplitudes of vibration even for moderately strong earthquakes. In this regard, many researchers have studied, developed and tested different supplemental damping techniques.

Three basic technologies are used to protect buildings from damaging earthquake effects. These are Base Isolation, Passive Energy Dissipation Devices and Active Control Devices. The concept behind base isolation is to detach (isolate) the building from the ground in such a way that earthquake motions are not transmitted up through the building or at least greatly reduced. In passive energy dissipation systems the motion of structure is controlled by adding devices to structure in the form stiffness, mass and damping. Passive energy dissipation devices can be effective against winds and earthquake induced motion, and generally operates on principles such as, yielding of metals, frictional sliding and deformation of viscoelastic (VE) solids or fluids. An active control system is one in which an external source powers control actuator that apply forces to the structure in a prescribed manner. These forces can be used to both add stiffness, damping and dissipate energy in the structure. Figure 1.1 shows the classification of structural protective systems.

In order to control the vibration response of buildings during seismic earthquakes, energy absorbing passive damping devices is most commonly used for dissipation of energy. Nowadays there are a number of types of manufactured dampers available in the market. Some of these include Friction, Yielding, Viscoelastic and Viscous Dampers. An effective damping system can result in higher levels of safety and comfort; and can also lead to considerable savings in total cost of a building.

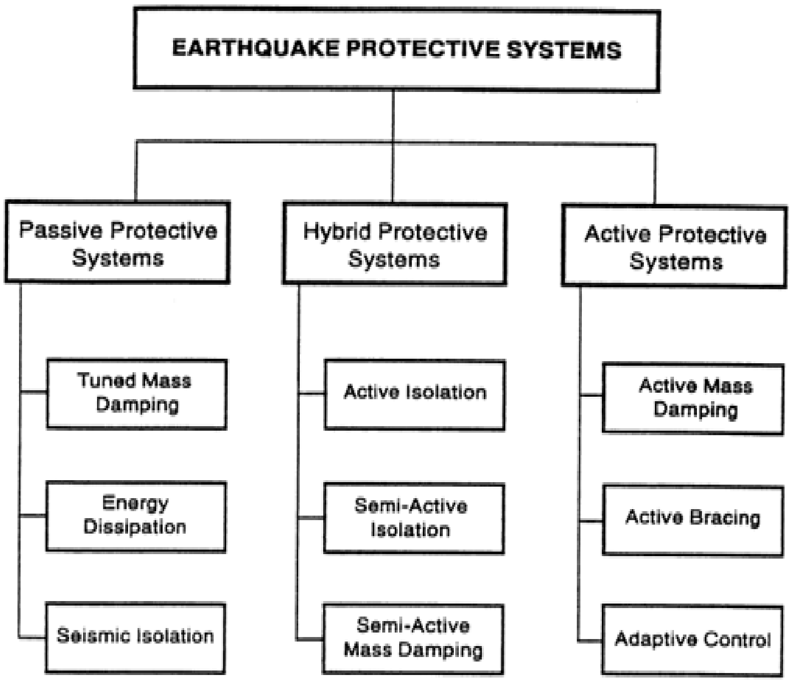

Figure 1.1: Earthquake Protective Systems

1.2 Background

Recently, concept of structural control has employed for a safer and economical design of the structural system using active control, passive control, and hybrid control devices, These devices yields reduction in response of buildings subjected to earthquake ground motions. Passive control devices were developed the earliest and have been used more commonly in practice for seismic design because they require minimum maintenance and need no external power supply to operate.

The concept of structural control as currently defined can trace its roots back more than 100 years to John Milne, a professor of engineering in Japan, who built a small house of wood and placed it on ball bearings to demonstrate that a structure could be isolated from earthquake shaking. The development of linear system theory and its application to the field of vibration, and in particular structural dynamics, required much of the first half of the twentieth century. The driving force for much of this development was the internal combustion engine, used in both automobiles and airplanes, which inherently produced significant dynamic force levels at connection points. It was during the 2nd world war that concepts such as vibration isolation, vibration absorption, and vibration damping were developed and effectively applied to aircraft structures.

1.3 Objective of Study

The main objective of present study is to study response reduction of building subjected to various earthquake excitations using passive energy dissipation devices like viscous damper, viscoelastic damper, and metallic yield damper. Also, compare the performances of controlled building with respect to uncontrolled structure. The specific objectives stated as follows:

- To study passive energy dissipation devices and their principle. Study in detail mathematical modeling of these devices, and understand the influence of various model parameters.

- To obtain the response of passive energy devices like viscous and viscoelastic damper subjected to sinusoidal and different earthquake ground excitations, in order to characterize them.

- Consider three storey shear building and obtain damping matrix. Also, obtain uncontrolled response of the building under various earthquake excitations.

- Obtain seismic response of a three story shear building attached with passive devices like Viscous, Viscoelastic, and metallic yield dampers subjected to various earthquake excitations, and extract the response quantities like displacement, velocity, acceleration, and inter storey drift for controlled building using numerical method through MATLAB.

- Analyze results obtain for uncontrolled building and compare with results of controlled building.

1.4 Scope of Work

Following is the scope of work:

- Carry out extensive literature review on implementation of passive devices for structural control of the building.
- Study, in detail, various mathematical models used for various passive energy dissipation devices.
- Compile various types of earthquake ground motion acceleration history data.
- Response characterization of damper under sinusoidal and random excitation.
- Discrete(lumped mass) model formulation of the building.
- Formulation and solution of equation of motion for building with and without passive energy dissipation devices using numerical method like Newmark-Beta through MATLAB.
- Extract response quantities like interstorey drift, displacement, velocity, acceleration, damper force etc.

1.5 Organization of Report

The Major Project is divided into eight chapters. They are as follows:

Chapter 2 deals with the details of literature review of various technical papers. It focuses on the mathematical model, behavior and properties of different passive energy dissipation devices.

Chapter 3 consists study and characterization of passive devices. like viscous, viscoelastic and metallic yield damper. Also it deals with the simulation of damper responses for viscous and viscoelastic damper under sinusoidal and random excitations. Various earthquake excitations used to obtain damper responses are El Centro(1940), Loma Prieta (1989), Northridge (1994), and kobe (1995).

Chapter 4 includes Formulation and solution of equation of motion for building with and without passive devices using Newmark-Beta method under the four different excitations through MATLAB. Extraction of the response quantities for uncontrolled building like inter storey drift, displacement, velocity, acceleration and damping force.

Chapter 5 includes the shear building equipped with viscous damper using Newmark-Beta under four different earthquake excitations through MATLAB. It includes extraction of the response quantities. i.e., inter storey drift, displacement, velocity, acceleration and damping force. These response quantities are compared with the uncontrolled structure.

Chapter 6 includes the shear building response by adding viscoelastic damper using Newmark-Beta under the four different earthquake excitations through MATLAB. Design of VE damper and parametric study are carried out for different value of required damping ratio. Extraction of the response quantities like inter storey drift, displacement, velocity, acceleration and damping force are obtained.

Chapter 7 includes the three storey shear building response by adding metallic damper using numerical method like Newmark-Beta under the different earthquake excitations through MATLAB. Comparison of response quantities are carries out for uncontrolled and controlled building.

Chapter 8 includes the summary of the study, conclusions & future scope of work.

Chapter 2

Literature Survey

2.1 General

Design for strength alone does not necessarily ensure that the building will respond dynamically in such a way that the comfort and safety of the occupants is maintained. For example, during the 1989 Loma Prieta earthquake, a 47-story Building in San Francisco experienced peak accelerations of about 0.1% g in the basement and 0.45% g on the top floor, which indicates that harmful accelerations in the upper stories can result from strong ground accelerations. Similar comments can be made regarding the behavior of structures during the Northridge and Kobe earthquakes. In fact, the requirements for strength and for safety can be conflicting. Thus, alternate means of increasing the resistance of a structure while maintaining desirable dynamic properties, based on the use of various active, semiactive, passive, and hybrid control schemes, offers great promise. This literature review provides glimpse of research related to passive energy dissipating devices.

2.2 Literature Review

Various papers have been referred for basic understanding of passive devices considered in buildings, their mathematical modeling, behavior and available applications of passive dampers. Some of the important papers are summarized below.

G. W. Housner et al. [1] presented a concise point of departure for researchers and practitioners alike wishing to assess the current state of the art in the control and monitoring of civil engineering structures, and provides a link between structural control and other fields of control theory, Pointing out both differences and similarities, and points out where future research and application efforts are likely to prove fruitful. The paper deals with sufficient details of passive energy dissipation devices and their model, active control, hybrid and semiactive control systems, sensors for structural control, smart material systems, health monitoring, damage detection. Toward and it discusses potential research area and needs.

A. Mortezaei and S.M. Zahrai [**2**] presented that the performance of passive energy dissipation systems depends significantly on the characteristics of near-field ground motion pulses. Work focused on the viscoelastic (VE) dampers to be used as energy-absorbing devices in buildings. Detailed and systematic investigation on the performance of passive energy dissipation systems during near-field ground motions has been carried. The analytical studies of the model structures exhibiting the structural response reduction due to these VE devices are presented. A nonlinear time history analysis is carried out under strong ground motion records from near-field and far-field earthquakes for a 5-story, 10-story and 15-story reinforced concrete building. Top story relative displacements as well as the top story absolute accelerations, and base shear values indicate that these VE dampers when incorporated into the superstructure reduce the earthquake response significantly in proportion to the amount of damping supplied in these devices.

Energy dissipation per cycle of VE damper can be expressed as:

$$E_d = \pi \gamma_0^2 G_1 \eta V \tag{2.1}$$

where γ_0 is the shear strain amplitude, η is the loss factor ($\eta = G_2/G_1$), G_1 is the storage modulus, G_2 is the loss modulus, V is the volume of VE material (V=$n_v A_v h_v$), n_v is the number of VE layer, A_v and h_v are the area and the thickness of VE layer, respectively. If the storage modulus G_1 and the loss factor η are determined, the stiffness k_d and the damping C_d of VE dampers can be written as

$$k_d = \frac{n_v G_1 A_v}{h_v} \tag{2.2}$$

$$C_d = \frac{n_v G_1 A_v \eta}{h_v \omega} \tag{2.3}$$

Julius Marko et al. [3] focuses on the comprehensive study on the seismic mitigation of medium rise frame-shear wall structures using embedded dampers. Two building structures with embedded viscoelastic(VE) and friction dampers in different configurations and placed in various locations throughout the structure were subjected to five different earthquake loadings. Another study treated seismic mitigation by using six different damping systems, namely friction and VE diagonal dampers, friction and VE chevron brace dampers, hybrid friction-VE dampers and lower toggle VE dampers. These damping systems were embedded into six different placements (one at a time) within cut outs of shear walls to mitigate the seismic response of medium rise building. A VE damper was modeled as a linear spring and dash-pot in parallel (i.e., Kelvin Model) where the spring represents stiffness and the dashpot represents damping.

Finite element techniques were used to model the dampers and the structures to obtain the dynamic responses under five different earthquake excitations, using time history analysis. Damper properties such as stiffness, damping coefficient, location, configuration and size were varied and results for displacement and accelerations at top storey were obtained. A direct integration dynamic analysis was selected to obtain the response of the structure under seismic loading. The response of the structure is obtained for selected time steps of the input earthquake accelerogram through ABAQUS/Standard that uses implicit time integration.

B. Samali and K. C. S. Kwok [4] discussed about the use of viscoelastic dampers in reducing wind and earthquake induced motion of building structures. The methodology for the design of viscoelastic dampers used were as given by Abbas and Kelly, briefly and is described here. Abbas and Kelly proposed simplified analytical models consisting of a Single Degree of Freedom (SDOF) model using a rigid brace and a two-DOF model with a deformable brace to capture the response of viscoelastically damped structures as shown in Figure 2.1. Extensive parametric

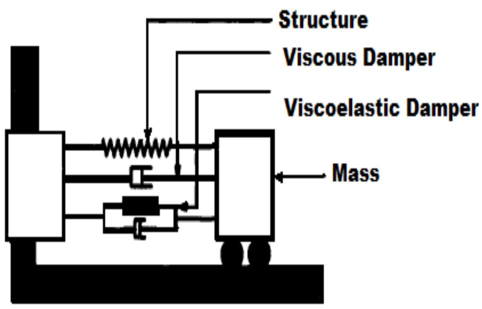

Figure 2.1: Rigid Brace Model for Viscoelastically Damped Structure

analysis show that the addition of viscoelastic dampers consistently reduces the displacement demands and thus decreases or eliminates the nonlinear response in the primary structure. The resulting inter storey drift demand is related to the volume of the viscoelastic material and the stiffness of the bracing to be provided at each storey. The braces may be provided in any configuration and are designed to remain elastic during a design earthquake. The design process was illustrated with the design of viscoelastic dampers and associated braces for a nine-storey moment resisting steel frame. Extensive nonlinear time-history analysis of a viscoelastically-damped frame subjected to different earthquake ground motions showed significant reduction in the storey shear force and peak inter storey drift. It has been shown that about 85% of input energy is dissipated through viscoelastic devices.

E. Yazdan Panah et at. [5] presented the analysis of building structures equipped with viscous brace damper system and subjected to strong earthquake excitation. The analysis was carried out by considering nonlinear time history, inherent damping coefficient and brace-damper dissipation system. An attempt has been made to analyze 15-storey steel rigid frame connected to viscous brace damper. Following equation was used to find out the force in viscous damper.

$$P(t) = C|\dot{u}(t)|^{z} \tag{2.4}$$

Where u(t) and C are displacement across the damper and damping coefficient respectively, z is damping exponent with the practical range of 0.2 to 2.0.
Figure 2.2 shows a single-degree-of-freedom frame structure with viscous damper is connected to braces.

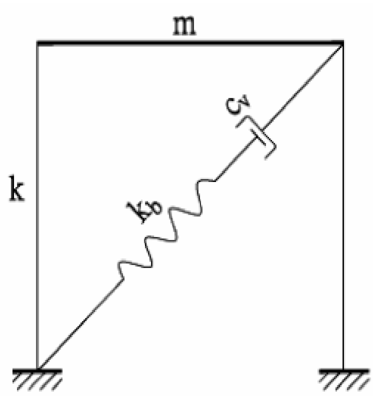

Figure 2.2: A SDOF Frame Equipped with Viscous Brace Damper

Chuan Xia and Robert D. Hanson [6] presented the study of the metallic yield devices, the steel-plate added damping and stiffness (ADAS) device. Yield force, yield displacement, strain-hardening ratio, ratio of the device stiffness to the bracing member stiffness, and ratio of device stiffness to structural story stiffness without the device in place have been identified as the most important parameters to characterize the performance of this device. They selected the bilinear model to represent the ADAS device inelastic behavior because of its mathematical simplicity and its ability to account for both strain hardening and hysteretic behavior. The hysteretic energy dissipated by the device in a loading cycle, as shown in Figure 2.3, is a function of the yield force, P_y, the yield displacement, Δ_y, and the ductility ratio, $\mu = (\Delta/\Delta_y)$.

$$W_b = 4P_y\Delta_y(\mu - 1) \tag{2.5}$$

The objective of the study was to study the influence of ADAS element parameters on the inelastic response of a 10-story cross-braced moment frame, and a 10-story moment frame.

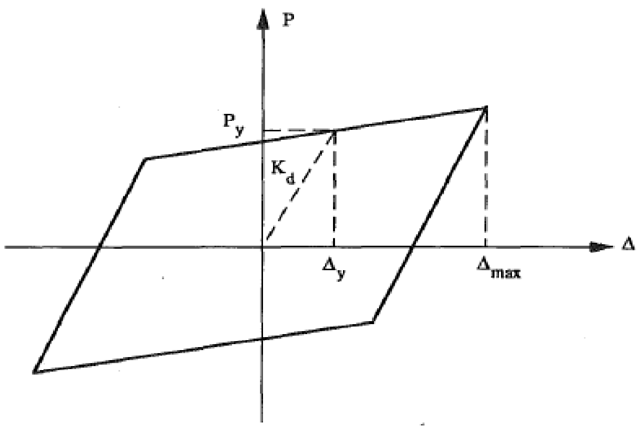

Figure 2.3: Bilinear Model for ADAS Device

S. M. S. Alehashem et al. [7] focuses on metallic dampers such as Added Damping and Stiffness (ADAS) and Triangular Added Damping and Stiffness (TADAS). They investigated the behavior and performance of steel structures equipped with ADAS and TADAS metallic dampers and compared with conventional earthquake-resisting steel structures such as Centrally Braced Frame (CBF), CHEVRON and Eccentrically Braced Frame (EBF) systems from the performance and behavior point of view. In this work, a bilinear curve (with strain hardening of 3 %) is used.

To compare different systems, they selected a ten-story building. The studied building is a steel frame with symmetrical plane, 5m span both way, and 3.2m story height. Bracings are set in outside frames of building and in each frame two spans are braced. In designing EBF system, short link (shear link) is used and considering designing codes, bracing spans are chosen such that gravitational loads is not placed on link beams. Dynamic analysis of the structures is carried out by DRAIN-2DX, the analysis is carried on a single frame (outer frame) which is equipped with one of the earthquake resisting systems. For designing systems equipped with ADAS and TADAS dampers, first a moment resistant frame is designed. This frame is designed for the minimal base shear force recommended by UBC97 considerations. For designing ADAS dampers, specification of ADAS dampers tested by Whittaker et al [8], are used and for TADAS, specifications of TADAS dampers tested by Tsai et al [9], are used.

S. M. S. Alehashem et al., have concluded that, the induced base shear force of the systems equipped with ADAS and TADAS under El Centro, Hachinohe and Taft earthquakes shows approximately 50 % decrease comparing with EBF systems, 60 % comparing with CBF system and 70 % comparing with CHEVRON systems. Inter Storey Drift for systems equipped with ADAS and TADAS dampers and EBF systems in the height of the building is almost uniform.

2.3 Summary

In this chapter, review of relevant literature is carried out. The review of literature includes, mathematical modeling, hysteresis behavior and properties of various passive dampers. Basic concept of analysis of damper added structure are carried out.

Chapter 3

Passive Control Systems

3.1 Introduction

Dynamic load produces vibration in the structure which causes the damage or collapse of the structure. A large amount of energy is imparted into structure during these vibrations. To reduce these vibrations it becomes important for the structure to absorb or dissipate energy. Research is under way to reduce the response of the structures resulting due to dynamic loading. A widely considered strategy consists of incorporating external elements to the structure to control its dynamic response. The branch of Structural Engineering that deals with such concepts is called Structural Control.

The function of seismic passive energy dissipation system is to reduce structural response due to earthquake, wind and other dynamic loads. Passive control system develops control forces at the point of attachment of the system. The power needed to generate these forces is provided by the motion of the points of attachment during dynamic excitation. Passive energy dissipation systems encompass a range of materials and devices for enhancing damping, stiffness and strength, and can be used both for natural hazard mitigation and for rehabilitation of aging or deficient structures.

In recent years, serious efforts have been undertaken to develop the concept of energy dissipation or supplemental damping into a workable technology and a number of such devices have been installed in structures throughout the world [10, 11]. In general, they are all characterized by a capability to enhance energy dissipation in the structural systems to which they are installed. This may be achieved either by conversion of kinetic energy to heat, or by transferring of energy among vibrating modes. The first method includes devices that operate on principles such as frictional sliding, yielding of metals, phase transformation in metals, deformation of viscoelastic solids or fluids, and fluid orificing. The latter method includes supplemental oscillators, which act as dynamic vibration absorbers.

3.2 Classification of Energy Dissipation Devices

Passive energy dissipaters may be simply classified as,

1) Displacement Dependent Devices

- Friction Damper
- Metallic Damper

2) Velocity Dependent Devices

- Viscous Damper
- Solid and Fluid Viscoelastic Damper

3) Dynamic Vibration Absorber

- Shape-Memory Alloys
- Tune Mass or Tune Liquid Oscillator Type Damper

3.2.1 Displacement Dependent Devices

Displacement-dependent devices dissipate energy through sliding friction, like friction dampers, or through the inelastic behavior of the damper elements, like metallic dampers because their energy dissipation depends primarily on relative displacements within the device and not on their relative velocities. A variety of hysteretic devices has been proposed and developed to enhance structural safety. The majority of these devices generate rectangular hysteresis loop. This indicates that behavior of friction dampers is close to that of coulomb friction. The simplest models of hysteretic behavior involve algebraic relation between force and displacement. Hence, hysteretic devices are often called displacement dependant.

3.2.2 Velocity Dependent Devices

Velocity dependent devices like viscous and VE elastic dampers dissipate energy through deformation of VE polymers, deformation of viscous fluids, or fluid orificing. Their energy dissipation depends on both relative displacements and relative velocities within the device. Velocity-dependent devices provide damping and stiffness to the structures while displacement dependent devices provides stiffness and energy dissipations takes place under moderate ground motions only.

3.2.3 Dynamic Vibration Absorber

A dynamic vibration absorber (DVA) is a typical example of a passive controller. It consists of an auxiliary mass-spring system which tends to neutralize the vibration of a structure to which it is attached. The basic principle of operation is vibration out of phase with the vibration of such structure, thereby applying a counteracting force. An absorber is only effective at its natural frequency which must be tuned to coincide with the forcing frequency. The example of DVA are shape memory alloy and tune mass damper. Tune mass damper consists of a secondary mass with properly tuned spring and damping elements, providing a frequency-dependent hysteresis that increases damping in the structure.

Table 3.1: Passive Devices and its Principle of Operation

Type	Device	Principle of operation
Hysteretic	Metallic yielding	Yielding of metals
	Friction	Frictional sliding
VE	VE solids	Deformations of VE polymers
	Viscous and VE fluids	Deformation of viscous fluid

Table 3.1 shows the supplemental energy dissipation devices and its principle of operation. Arrangement of viscoelastic damping system in building structure is shown in Figure 3.1.

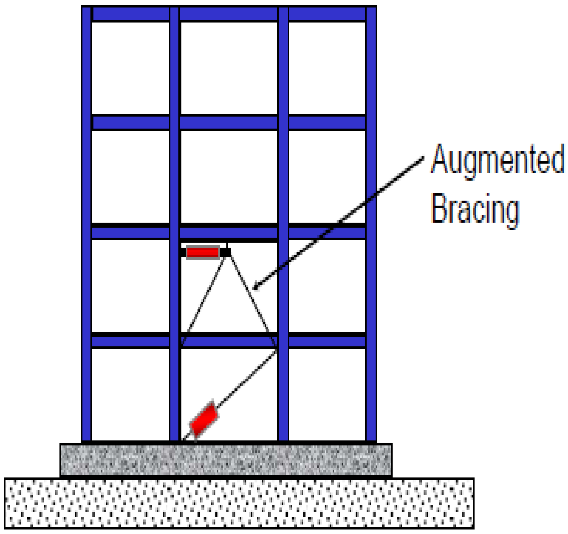

Figure 3.1: Damper Placement within Structure

In the next section, major focus is to study effectiveness of the Viscous, VE and metallic yielding damper are consider in mitigating the responses. However, before that characterization of such damper is essential, in order to understand the dynamics of the dampers. Therefore, damper are subjected to sinusoidal motion and four different characteristics of earthquake motions. The earthquake events used in characterization are El Centro (1940), Loma Prieta (1989), Northridge (1994), and Kobe (1995) time histories.

3.3 Viscous Fluid Damper

Viscous dampers are known as effective energy dissipation devices improving structural response to earthquakes. Fluid viscous dampers are fluid-filled cylinders with two chambers that are separated by a moving piston with directional orifices, and an accumulator chamber. As the head moves longitudinally within the shaft, viscous fluid flows from one chamber to the other. The force in the damper is a result of the pressure differential between chambers, which is a function of the orifices in the piston head and the velocity of the piston head [12, 13]. The damping force developed by the viscous damper depends on the physical properties of the fluid used in the damper. The most common type of viscous fluid damper and its parts are shown in Figure 3.2. It can be seen that by simply moving the piston rod back and forth, fluid is orificed through the piston head orifices, generating damping force. It dissipates energy through movement of the piston in the highly viscous fluid. If the fluid is purely viscous (for instance, Newtonian), then the output force of the damper is directly proportional to the velocity of the piston.

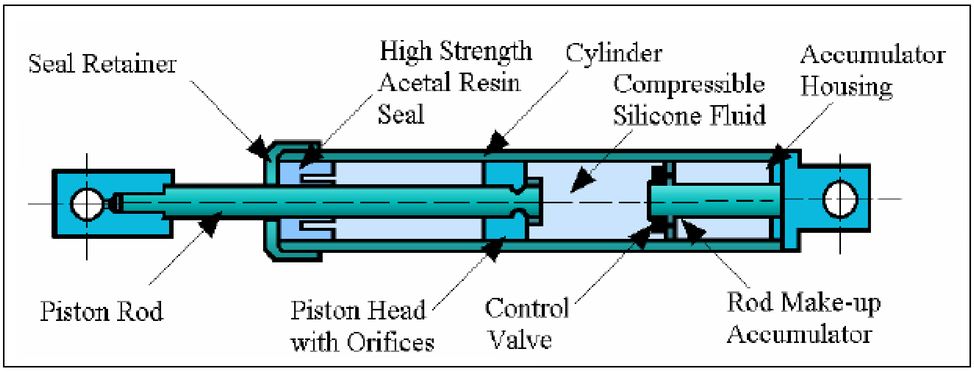

Figure 3.2: Viscous Fluid Damper [13]

If a given structure requires certain total macroscopic damping, to implement this damping will involve dividing the total damping by the number of dampers used. The end result is a maximum force and damping function for each individual damper.

3.3.1 Mathematical Model and Behavior

Different mathematical models have been proposed in literature to predict the behavior of viscous devices. Figure 3.3 shows a classical Maxwell model, in which dashpot and spring elements are joined in series. However, for typical structural applications the viscous damper can be modeled as a simple dashpot element in which the damping force is directly proportional to the velocity of the piston as given in Figure **??**.

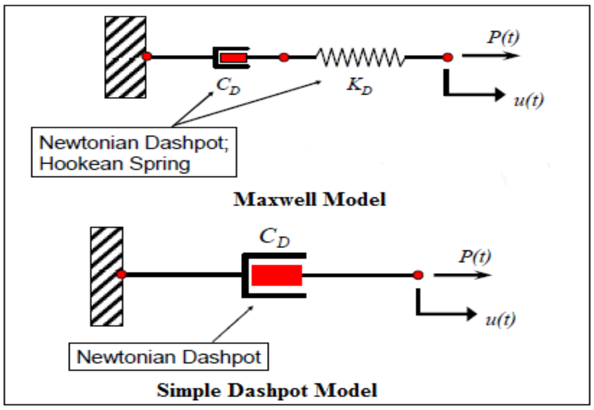

Figure 3.3: Simple Dashpot and Maxwell Model for Viscous Damper

The force in the fluid viscous damper may be expressed as [14],

$$P(t) = C_d|\dot{u}|^{\alpha} sgn(\dot{u}) \tag{3.1}$$

Where, C_d is the damping coefficient for the damper, α is the velocity exponent for the damper that ranges from 0.1 to 2, $\dot{u}$ is the relative velocity between each end of the device, and sgn is the signum function that, defines the sign of the relative velocity term. A value of $\alpha = 1.0$ represents the linear viscous damper. Structural dampers usually have α values ranging from 0.3 - 1.0. The main advantage of the linear viscous dampers is that there is very little interaction between damper forces and structural forces. Maximum structural forces occur at maximum displacement, at which the damper forces are zero because the deformational velocity in the damper is near zero. The value of the resisting force in linear viscous fluid damper varies with respect to the translational velocity of the damper at any point in time is given by,

$$P(t) = C_d \dot{u}(t) \tag{3.2}$$

Where, $P(t)$ is the resistance force for linear viscous damper. C_d and u are the damping coefficient and displacement of the dampers respectively.
The energy dissipation by the damper can be find out from the following equation,

$$E_D = \int |P(t)| du \tag{3.3}$$

The area contained within the hysteretic loop present in Figure 3.4, measures the energy dissipated per cycle in the viscous damper.

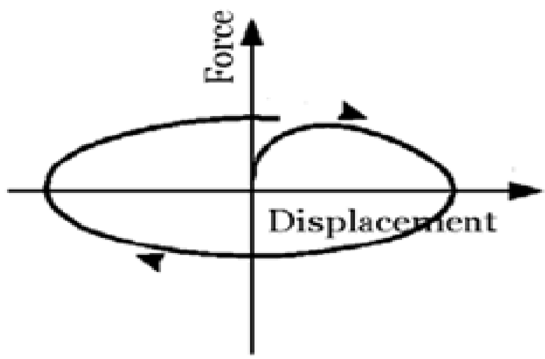

Figure 3.4: Hysteresis Loop for Viscous Damper [11]

3.3.2 Response of Viscous Damper

The cyclic response of fluid viscous damper is dependent on the velocity of motion, may be dependent on the amplitude and frequency of motion; and is generally depend on the operating temperature. Fluid viscous device may be modeled using a spring and dashpot in series, i, e., Mexwell Model. Force in the linear fluid viscous damper may be given by Equation 3.2

3.3.2.1 Response of Damper Subjected to Sinusoidal Input

In the present study of characterization, the damping coefficient of viscous fluid damper (C_d=160 $\frac{N.S}{mm}$) is considered as given in literature. The plots of Force Vs Time, Force Vs Displacement, and Force Vs Velocity of viscous damper subjected to sinusoidal excitations with frequency of 1 Hz and different value of amplitude ('a' = 20, 35, 30, 35 and 40 mm) are shown in Figure 3.5. Similarly, these curves of viscous damper subjected to sinusoidal excitations with varying frequency (1, 1.16, 1.32, 1.48, and 1.64 Hz) and 20 mm amplitude are shown in Figure 3.6. Force time

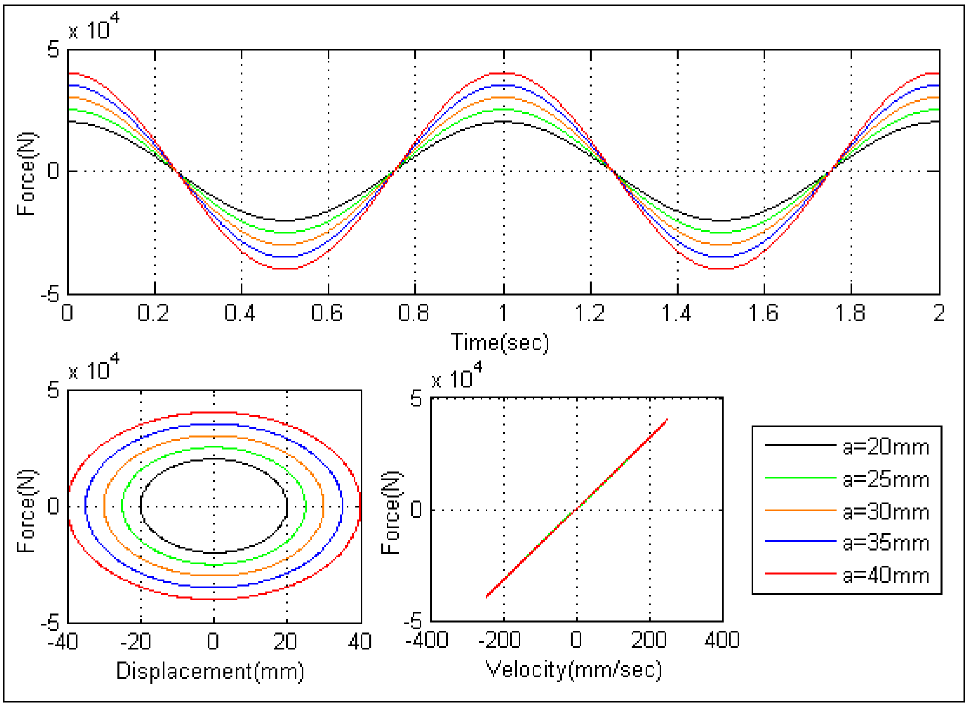

Figure 3.5: Response For Different Amplitude of Motion

history as shown in Figure 3.5 indicates that with increase in amplitude, damper force also increases. It is clear from force-displacement plot that curve is perfect oval. The energy dissipates is equal to area under an oval. It is evident from Figure 3.5 that force-velocity plot of viscous damper is linear in nature. Similarly, force time history shown in Figure 3.6 shows that damper force increases with increase in frequency of excitation. Force Vs displacement plot in Figure 3.6 indicates that curve is

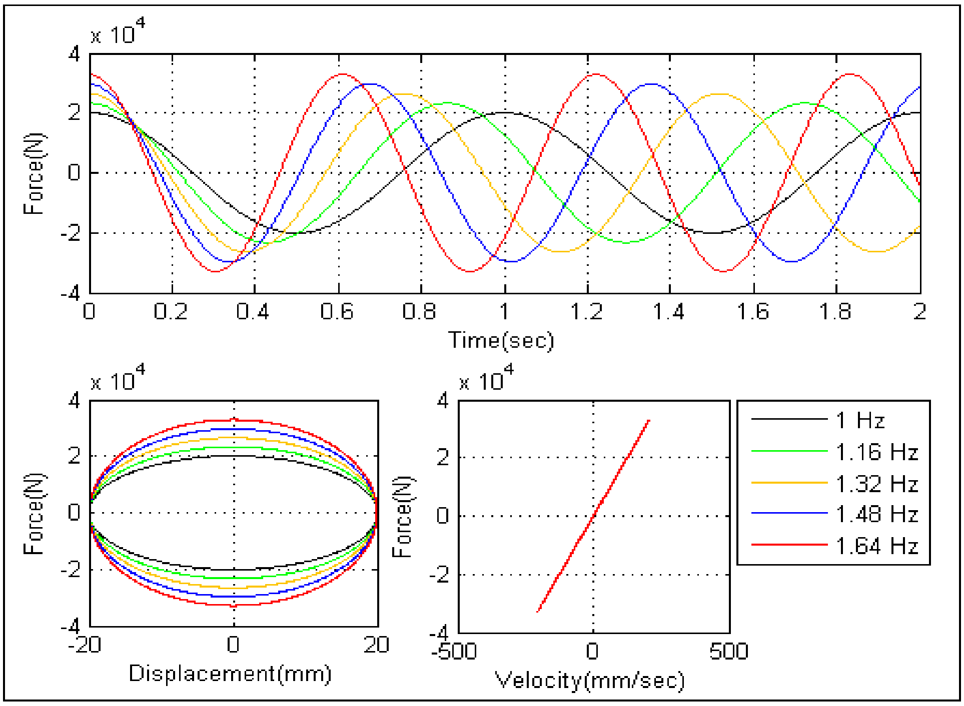

Figure 3.6: Response For Different Excitation of Frequency

perfectly oval. Area under this oval is equal to energy that dissipates. As compares to sinusoidal input of varying amplitude and fixed frequency, dissipation of energy is less for damper subjected to varying frequency and fixed amplitude like, earlier, force-velocity plot reveals that force-velocity relation is linear in nature.

3.3.2.2 Response of Damper Subjected to Earthquake Input

In general, earthquakes have different properties such as Peak Ground Acceleration (PGA), Peak Ground Velocity (PGV), Peak Ground Displacement (PGD), duration of strong motion and ranges of dominant frequencies; hence they have different influence on the structures. In order to ensure that the chosen mitigation procedure is effective under different types of excitations, four well-known earthquake records are used in this study. The time history data was taken from "Pacific Earthquake Engineering Research Institute" (PEER). The earthquake time history records, which are selected for this study to investigate the dynamic response of viscous damper models are summarized in Table 3.2. Plot of acceleration with respect to time for different earthquake time histories are shown in Figure 3.7. In this study same properties of viscous damper are considered as used in case of damper subjected to sinusoidal input. In simulation of viscous damper under different earthquake excitations, input of earthquake ground velocity is used. Force Vs Time, Force Vs Displacement, and Force Vs Velocity relationship to understand the behavior of viscous damper under earthquake excitations are given in Figure 3.8 to Figure 3.11.

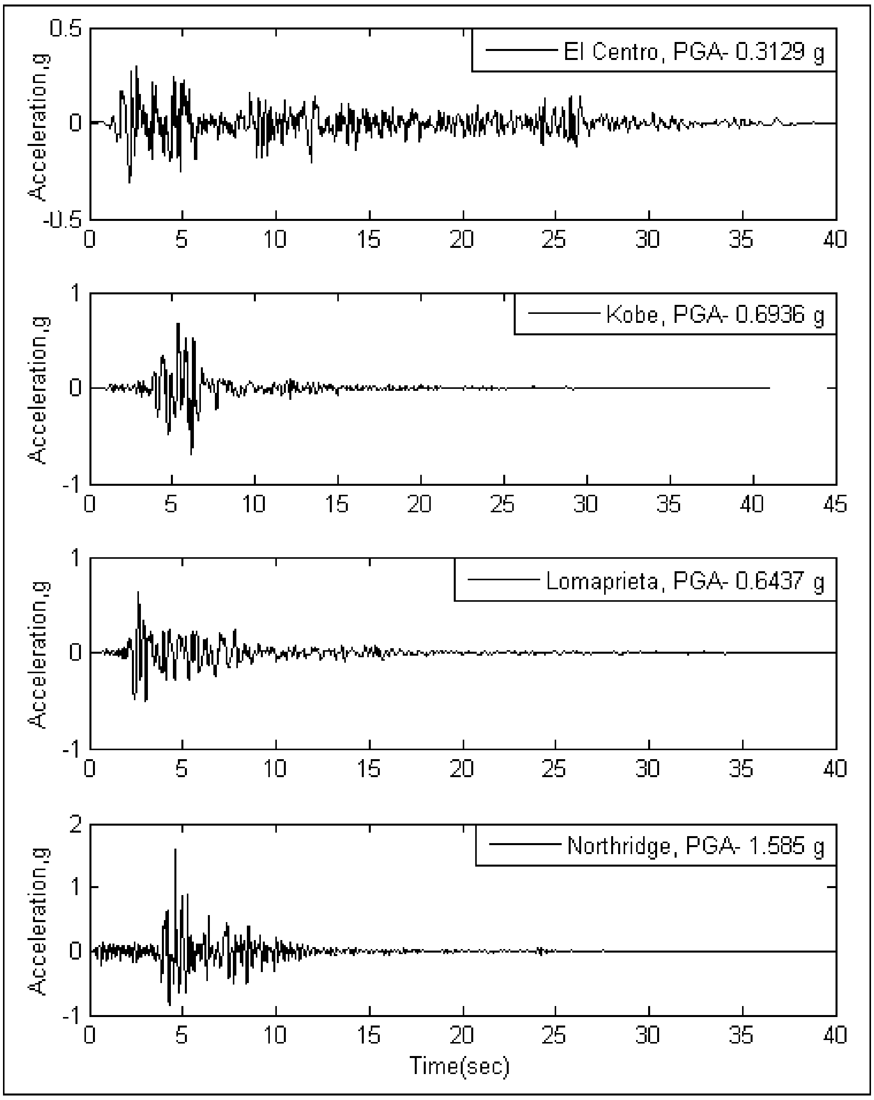

Figure 3.7: Earthquake Time History

Table 3.2: Time History Data for Various Earthquakes

Earthquake	Year	PGA(g)	PGV(cm/sec^2)	PGD(cm)	Damping
El centro	1940	0.3129	43.8	18.3	0.05
Kobe	1995	0.6936	37.3	9.52	0.05
Loma prieta	1989	0.6437	94.8	41.18	0.05
Northridge	1994	1.585	103.9	23.8	0.05

Force time history of viscous damper under the El Centro earthquake excitations is shown in Figure 3.8. It indicates that, resisting force value of viscous damper are varying with respect to time. The value 47.69 kN, 0.133 m, and 0.29 m/sec are the maximum damper force, displacement and velocity under the EL Centro excitations respectively. From, force time history of El Centro excitation, it is reveals that strong motion duration is between (2-7) sec and (10.5-14.5) sec observed. In figure 3.8, Force Vs Displacement plot shows that area within hysteresis loop gives energy dissipation of viscous damper under the El Centro Excitation. Force Vs Velocity plot shows the damper force is linear in nature.

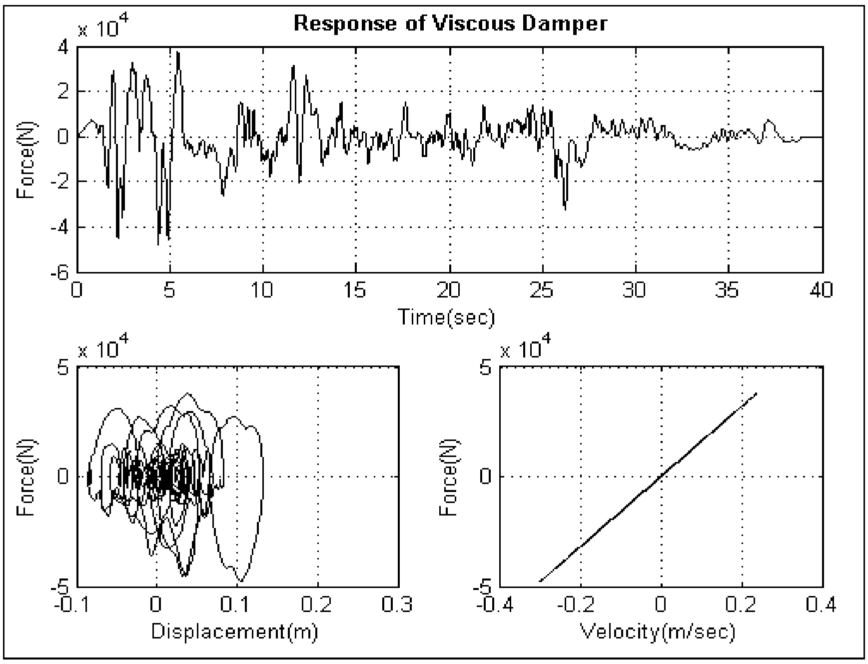

Figure 3.8: Response under 0.3129 g El Centro Earthquake

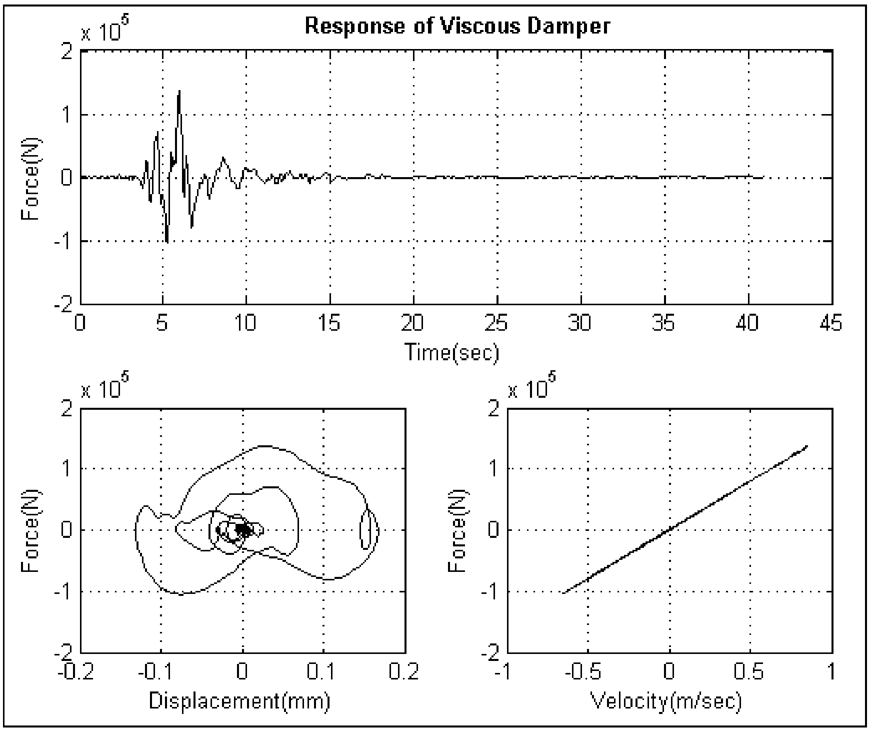

Figure 3.9: Response under 0.6936 g Kobe Earthquake

Force time history of viscous damper under the Kobe earthquake excitations is shown in Figure 3.9. It indicates that, resisting force value of viscous damper are varying with respect to time. The value 136.4 kN, 0.1675 m, and 0.852 m/sec are the maximum damper force, displacement and velocity under the Kobe excitations respectively. From, force time history of Kobe excitation, it is reveals that strong motion duration is between (3-7.5) sec observed. In figure 3.9, Force Vs Displacement plot shows that area within hysteresis loop gives energy dissipation of viscous damper under the Kobe Excitation, there is less number of cycles produces as compare to El Centro earthquake. Force Vs Velocity plot shows the damper force is linear in nature. Force time history as shown in Figure 3.10 indicates that damper force are varying with respect to time under loma Prieta earthquake. The value 88.290 kN, 0.108 m, and 0.5518 m/sec are the maximum damper force, displacement and velocity under the Loma Prieta excitations respectively. From, force time history of Loma Prieta excitation, it is reveals that strong motion duration is between (2.5-7.5) sec observed.

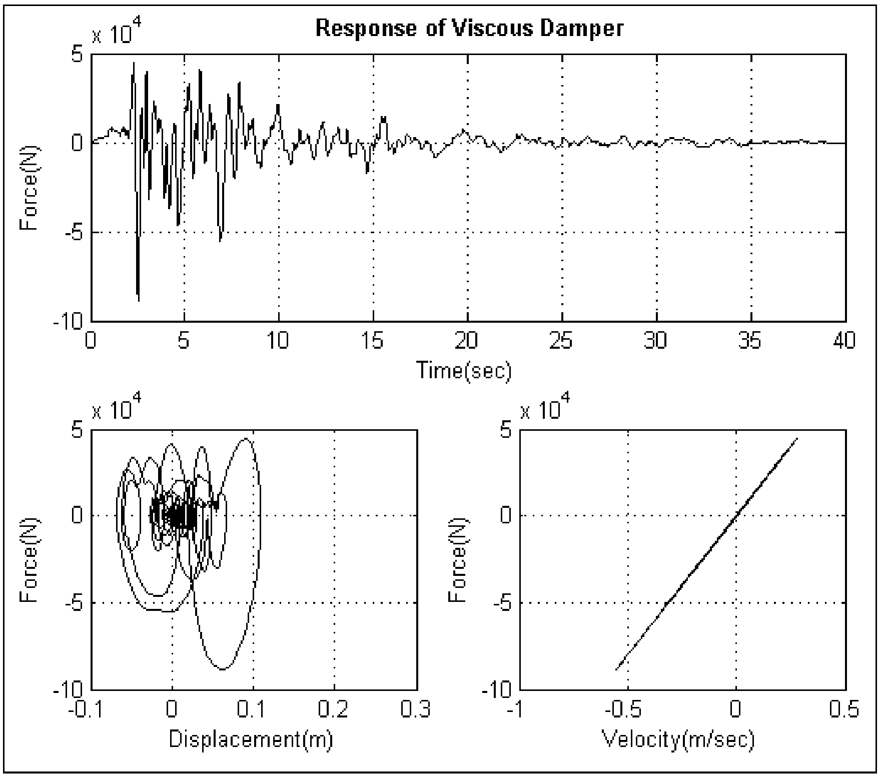

Figure 3.10: Response under 0.6437 g Loma Prieta Earthquake

Figure 3.11 shows the Force Vs Time, Force Vs Displacement, and Force Vs Velocity plots of viscous damper response under the Northridge Earthquake. The value 89.23 kN, 0.0606 m, and 0.557 m/sec are the maximum damper force, displacement and velocity under the Loma Prieta excitations respectively. From, force time history of Northridge excitation, it is reveals that strong motion duration is between (2-8) sec observed, which is maximum from all four earthquake. In this figure total area under the hysteresis loops are shown, which is indicates total energy dissipates under the Northridge earthquake. Force Vs Velocity plot shows that the damper force is linear in nature. From all the earthquake, maximum damper force 136.4 kN is maximum under the El Centro earthquake.

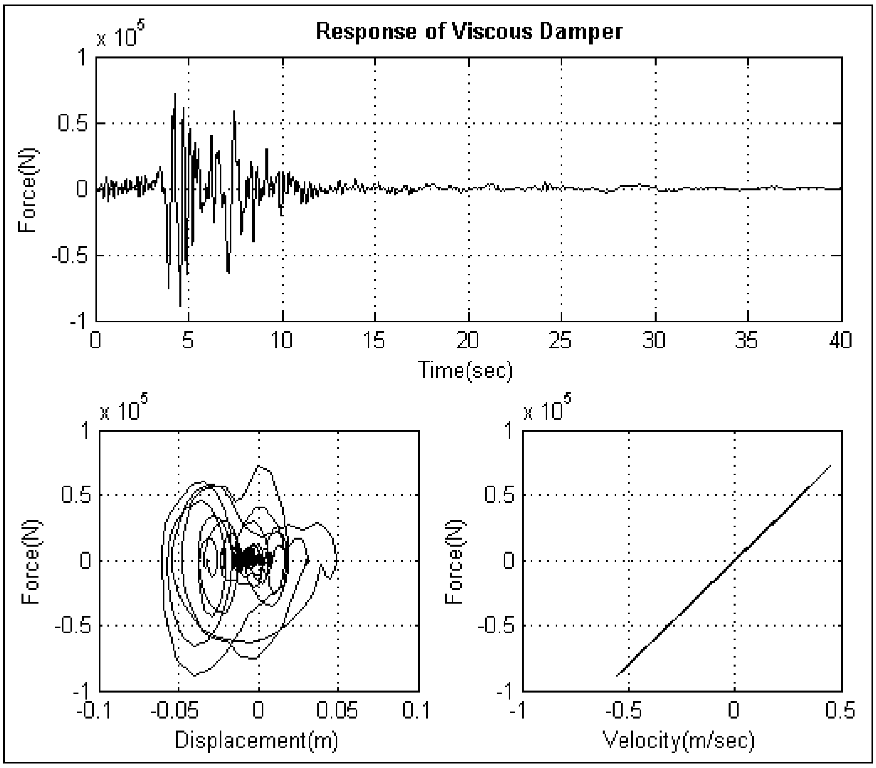

Figure 3.11: Response under 1.585 g Northridge Earthquake

3.4 Viscoelastic (VE) Damper

Application of viscoelastic damper to civil engineering structures appears to have begun in 1969 when 10,000 VE dampers installed in each of the twin tower of the World Trade Center in New York to help resist wind loads (Mohmoodi et al.,1969). For seismic applications, larger damping increases are usually required in comparison with those required for mitigation of wind- induced vibrations. VE materials used in structural application are typically copolymers or glassy substances which dissipate energy when subjected to shear deformation. A typical VE damper is shown in Figure 3.12, which consists of viscoelastic layers bonded with steel plates. When mounted in structure, shear deformation and hence energy dissipation takes place. The structural vibration induces relative motion between the outer steel flanges and the center plate.

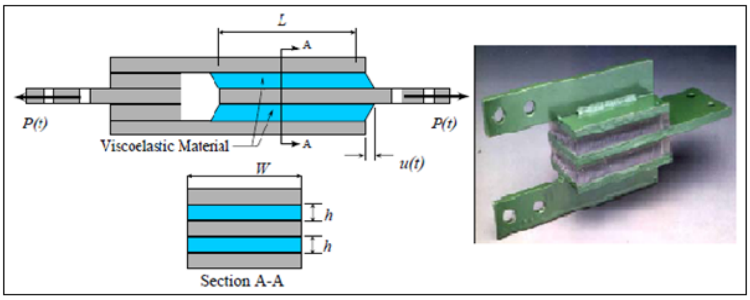

Figure 3.12: Viscoelastic Damper [15]

3.4.1 Mathematical Model and Behavior

The addition of dampers into a structure not only increases the stiffness of the structure but also provides a significant amount of damping. It is thus necessary to take into account such changes in the analysis and design of the structure with added dampers. Furthermore, the increased application of velocity-dependent dampers in structures will depend on the availability of simplified methods for the analysis and design. Energy is dissipated through large shear strains in the viscoelastic material. Implementation of viscoelastic dampers causes a small increase in structural stiffness due to the inherent storage stiffness of the viscoelastic material. One of the primary advantages of the viscoelastic dampers is that they dissipate energy under all levels of ground motion. As suggested in the FEMA-273 [14] guidelines, solid viscoelastic devices may be modeled using a classical Kelvin Model in which a linear spring is placed in parallel with a viscous dashpot, as shown in Figure 3.13.

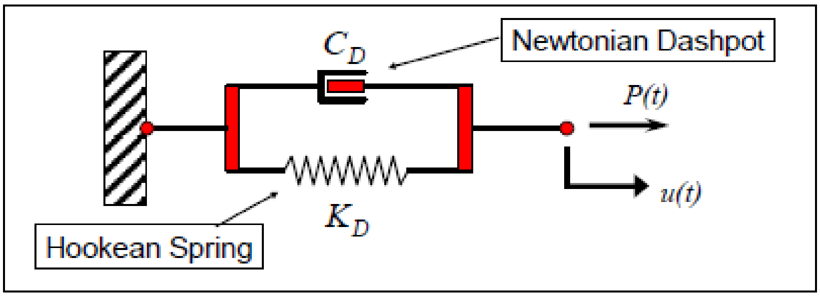

Figure 3.13: Kelvin Model for Viscoelastic Damper

Most of the the mechanical properties of viscoelastic materials are rather complex and may vary with environmental temperature and excitation frequency. The best method of evaluating the properties of the damper is to generate the hysteresis loop by subjecting the center part of the damper to a periodic displacement then plotting this and the corresponding shear force on an x-y recorder as shown in Figure 3.14 for one cycle. The area of the hysteresis loop represents the actual energy lost or

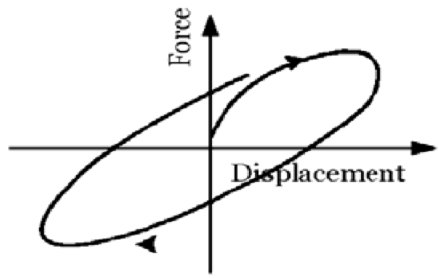

Figure 3.14: Hysteresis Loop for Viscoelastic Damper

damped. This energy is related to VE properties. The main VE material properties used in designing the VE devices are the shear storage modulus, G', which provides the elastic shear stiffness of the material, and the shear loss modulus, G'', which represents the velocity dependent devices or viscous stiffness of material. The main stress strain material relation can be expressed as:

$$\tau(t) = G'\gamma(t) \pm G''\dot{\gamma}(t)/f \tag{3.4}$$

Where $\tau(t)$ is the shear stress as a function of time, t; $\gamma(t)$ is the shear strain as a function of time; and f is the circular frequency in radians per sec. Stress strain relation is an ellipse with a nonzero slope. The slope is associated with G' term, and the area of the ellipse is related to the G'' term. Thus a simple relationship between the energy dissipated by VE materials and viscous dampers can be established.

Abbas et al., (1993) defines the stiffness coefficient K_d and damping coefficient C_d for a viscoelastic damper. Force - displacement relationship of viscoelastic device may be expressed,

$$F(t) = K_d(x) + C_d(\dot{x}) \tag{3.5}$$

In Which,

$$K_d = \frac{G'A}{t} \tag{3.6}$$

$$C_d = \frac{G''A}{ft} \tag{3.7}$$

Where, A is the shear area of VE material, t is the thickness of VE material, f is the loading frequency of VE damper, G' is the shear storage modulus, G'' is the shear loss modulus and T is temperature.Loss factor, η, is define as a ratio of the shear loss modulus to the shear storage modulus, (η=G''/G'). The following expressions can be used to obtain the moduli of the VE material as defined by Abbas et al.,(1993):

$$G' = 16.0f^{0.51}\gamma^{-0.23}e^{72.46/T} \tag{3.8}$$

$$G'' = 18.5f^{0.51}\gamma^{-0.20}e^{73.89/T} \tag{3.9}$$

where, γ is the shear strain. Temperature variations will have an effect on damper properties as evident from equations.

3.4.2 Response of VE Damper

Damping is the resistance offered by a body to the motion of the vibratory system. The resistance may be applied by a liquid or solid internally or externally. In general all engineering materials dissipate energy during cyclic deformations. Some materials such as rubber and plastics, dissipate much more energy per cycle of deformation than others, such as steel and aluminum. Under cyclic loads, the relation between the stress and strain forms hysteresis loops. These hysteretic loops are very useful in understanding the damping and energy dissipation capacity of the any damping systems or material.

For this study, VE damper size (A=50.8mm $\times$ 38.1mm) and thickness (t=7.62mm) is consider as specified in literature [15]. Damper properties storage modulus (G'=958370.25 N/m^2), loss modulus (G''=1151423.25 N/m^2) and loss factor(η=1.2) are taken for excitation frequency 1 Hz, ambient temperature 24^0 C and damper strain 20 %. From these data stiffness coefficient (k_d=468.85 N/mm) and damping coefficient (C_d=93.093 N$\cdot$Sec/mm) for a viscoelastic damper are calculated using Equation 3.6 and 3.7 respectively. The plot of Force Vs Time, Force Vs Displacement, and Force Vs Velocity of VE damper subjected to sinusoidal excitations with fixed frequency of 1 Hz and different value of amplitude (a= 0.75, 1, 1.25, 1.50, 1.75 and 2 mm) are obtained out through MATLAB as shown in Figure 3.15. By considering the same damper dimension and properties, simulation of the damper response under sinusoidal excitations for 1 mm amplitude and different excitation of frequencies (1, 1.16, 1.32, 1.48, 1.64 and 1.80 Hz) are carried out and the same are shown in Figure 3.16.

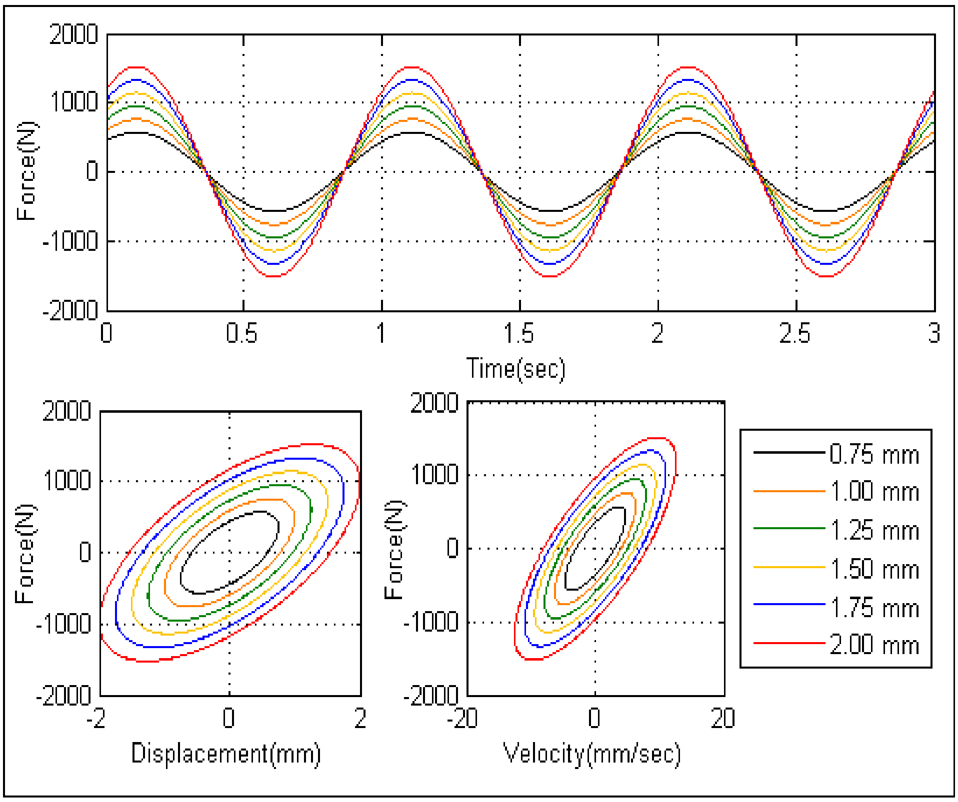

Figure 3.15: VE Dampers Response For Different Amplitude of Motion

It is evident from Figure 3.15 that with increase in amplitude of excitation damper force also increases. Force Vs Displacement and Force Vs Velocity plots shows hysteresis nature of the VE damper. From, Figure 3.16 shows that with increase in excitation

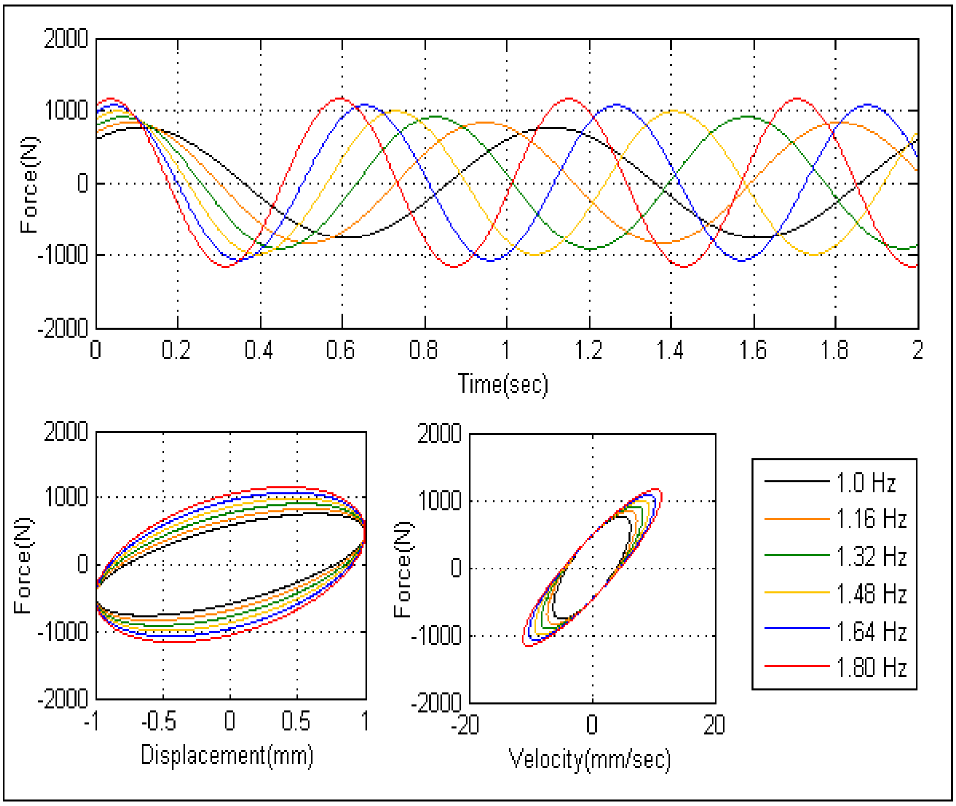

Figure 3.16: VE Dampers Response For Different Excitation of Frequency

of frequency damper force also increases. Force Vs Displacement and Force Vs Velocity plots shows hysteresis nature of the VE damper.

The earthquake time history records, which are selected for this study to investigate the dynamic response of VE damper models are summarized in Table 3.2 with Peak Ground Acceleration (PGA), Peak Ground Velocity (PGV), Peak Ground Displacement (PGD) and damping. In this study same properties of VE damper are consider that have been used for earlier study. Force Vs Time, Force Vs Displacement, and Force Vs Velocity relationship to understand the behavior of VE damper are obtained through MATLAB, which is given in Figure 3.17 to 3.20.

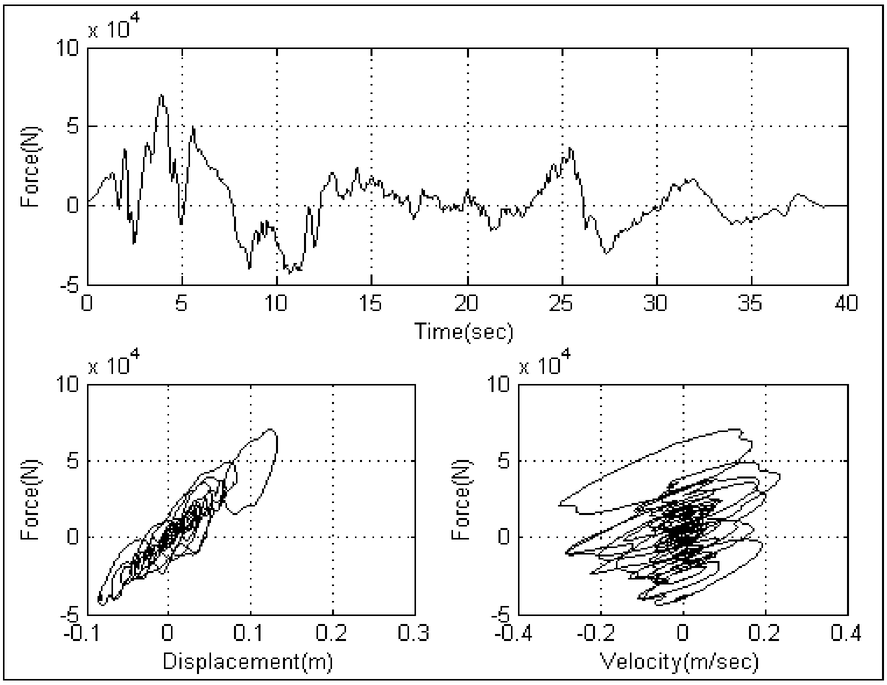

Figure 3.17: VE Damper Response under 0.3129 g El Centro Earthquake

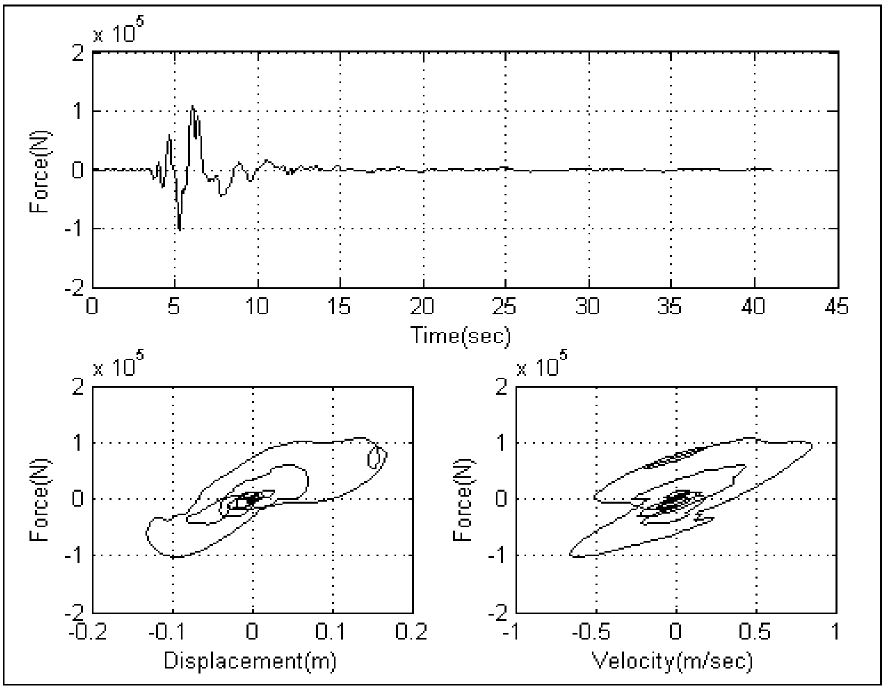

Figure 3.18: VE Damper Response under 0.6936 g Kobe Earthquake

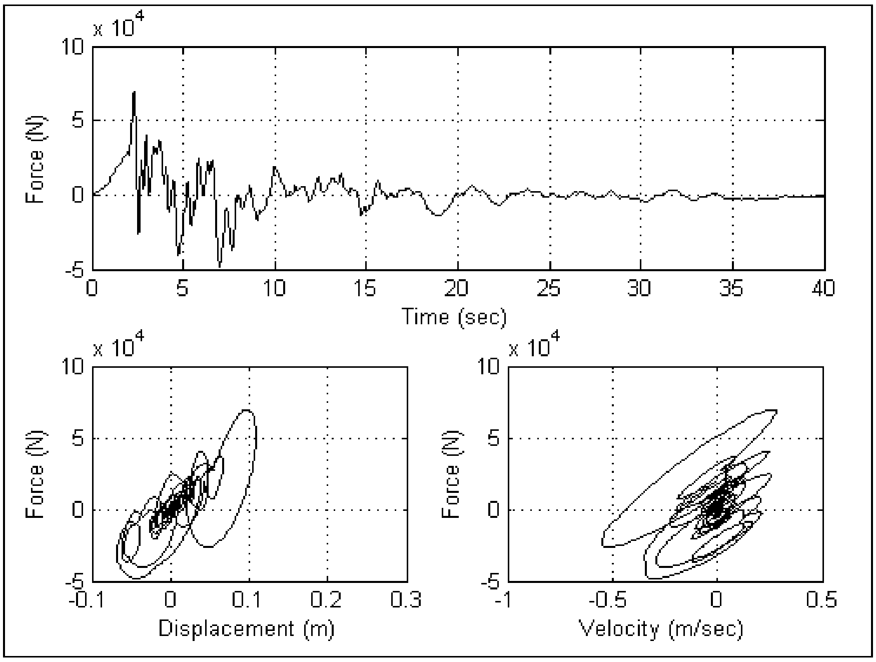

Figure 3.19: VE Damper Response under 0.6437 g Loma Prieta Earthquake

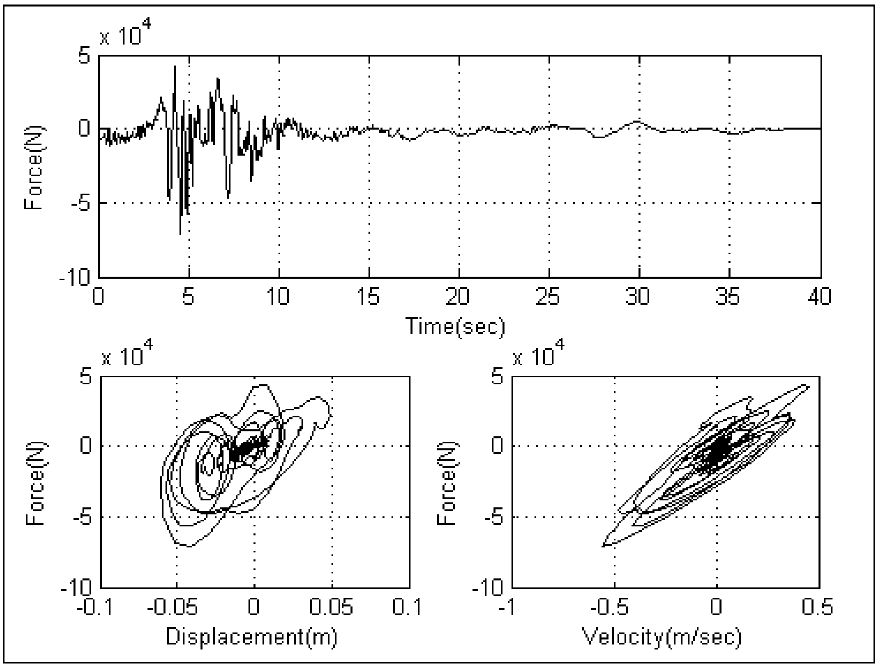

Figure 3.20: VE Damper Response under 1.585 g Northridge Earthquake

Force time history as shown in Figure 3.17 to 3.20 indicates that damper force are varying with respect to time under all the earthquake. From Force Vs Time History maximum damper forces are obtain, which is 70.43 kN, 107.3 kN, 69.75 kN, and 71.07 kN for El Centro, Kobe, Loma Prieta, and Northridge earthquake excitations respectively. Force Vs Displacement plot shows that area within hysteresis loop gives energy dissipation of viscous damper under the all earthquake excitations. Force Vs Velocity plot also shows the hysteresis loops are developed under the all earthquake excitations.

3.4.3 Temperature Effects on VE Damper

To understand the behavior of VE damper under different ambient temperature Type B and C damper configuration is selected based on the experimental work carried by Change et al [15], and these experiment results are compare with the simulation result obtain through MATLAB. Type B and C dampers are of similar VE materials but different in dimension. The Force-Deformation curve of damper Type B (Area=2 in×1.5 in,t=0.3 in) and Type C (Area=6 in×3 in, t=0.15 in) subjected to sinusoidal excitations with frequency 3.5 Hz and 5 % damper strain at ambient temperature 24^0C and 42^0C are shown in Figure 3.21. For Type B dampers storage modulus (G'=251.1 psi) and loss modulus (G''=301.3 psi) are taken at 24^0C ambient temperature and 3.5 Hz frequency, from that stiffness coefficient (k_d=5.02 kip/inch) and damping coefficient (C_d=0.27 kip sec/inch) are determined for a viscoelastic damper using Equation 3.6 and Equation 3.7 respectively. Similarly at 42^0C Type B damper properties storage modulus (G'=89.8 psi) and loss modulus (G''=94.3 psi) are taken and from that stiffness coefficient (k_d=1.796 kip/inch) and damping coefficient (C_d=0.08576 kip sec/inch) are determined. Type C dampers storage modulus (G'=28.2 psi) and loss modulus (G''=24.6 psi) are taken at 24^0C ambient temperature and 3.5 Hz frequency, from that stiffness coefficient (k_d=6.77 kip/inch) and damping coefficient (C_d=0.268 kip sec/inch) are determined for a viscoelastic damper.

Similarly at 42^0C Type C damper properties storage modulus (G'=15.6 psi) and loss modulus (G''=9.8 psi) are taken and from that stiffness coefficient (k_d=3.744 kip/inch) and damping coefficient (C_d=0.106 kip sec/inch) are determined.

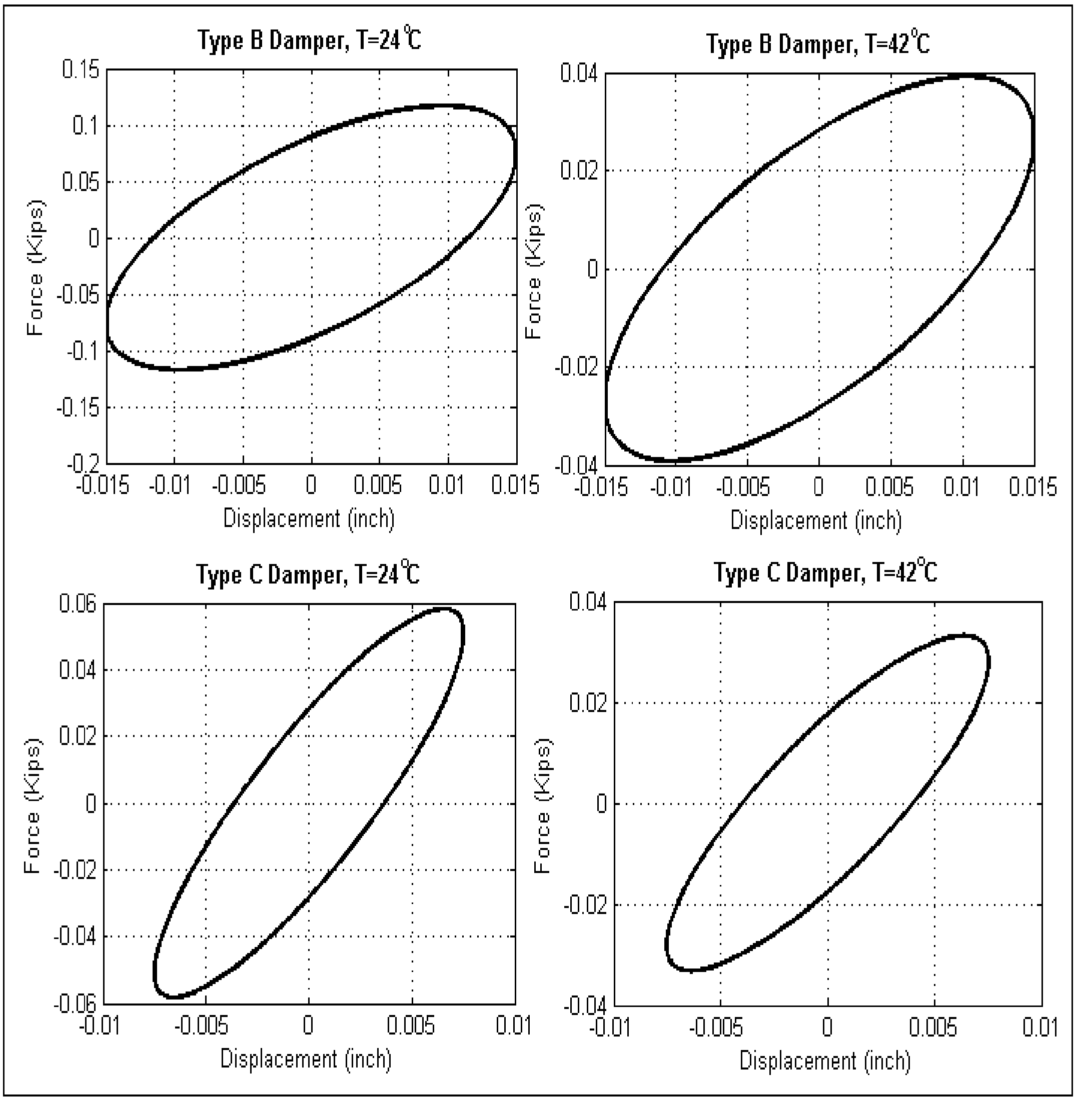

Figure 3.21: Force-Deformation Relationships, Analytical (3 Hz, 5 % Strain)

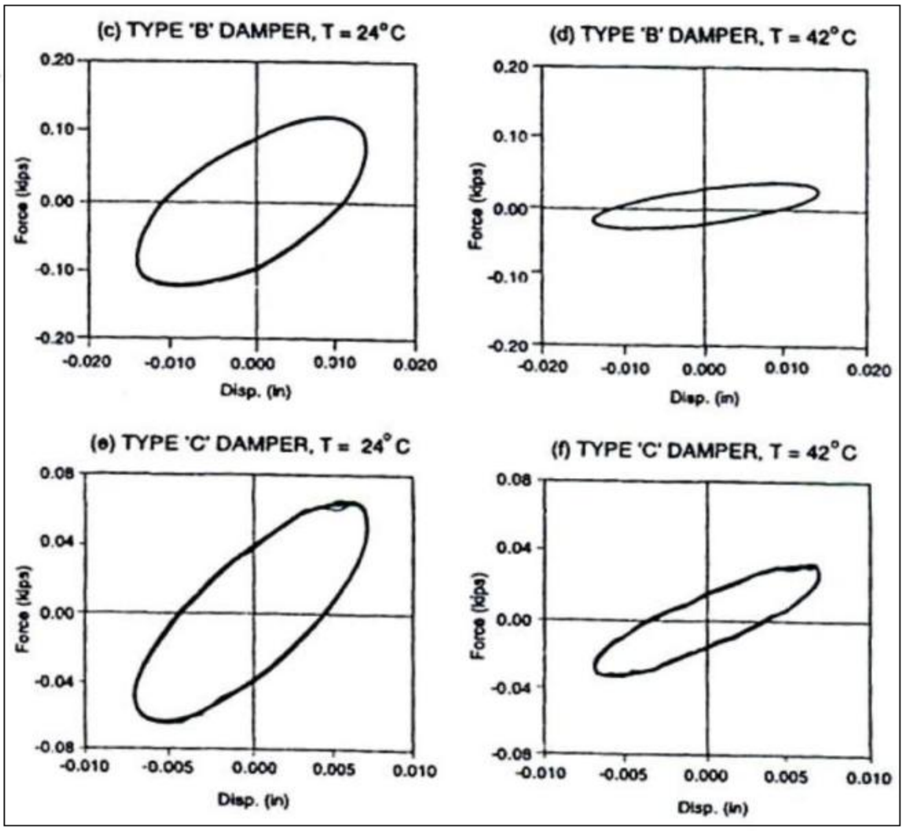

Figure 3.22: Force-Deformation Relationships, Experimental (3 Hz, 5 % Strain) [15]

Force-Deformation relationship of simulation of Type B and Type C VE dampers are shown in Figure 3.21, and experimental results given by Change et al,.[15] is shown Figure 3.22. It shows that all of the hysteresis loops are fairly rounded in shape, indicating that the dampers can effectively dissipate energy. It is seen from Figure 3.22 that the damper stiffness and the amount of energy dissipation in one cycle decreases for both types of damper with increasing ambient temperature. The percent reductions in energy dissipation capacity due to the change in ambient temperature from 24^0C to 42^0C are 70 % and 60 % respectively, for Types B and C dampers. From the above result, it is clear that one has to take into account the effect of ambient temperature and excitation frequency for an effective design of VE dampers in building structure.

3.5 Metallic Damper

The idea of utilizing added metallic energy dissipators within a structure to absorb a large portion of the seismic energy began due to work by J. M. Kelly et al [16]. Metallic dampers uses mild steel or other metals which can sustain many cycles of stable hysteretic yielding behavior to dissipate the input energy. A wide variety of different types of devices that utilize flexural, shear or longitudinal deformation modes into the plastic range have been developed. One of the effective mechanisms available for the dissipation of energy input to a structure from an earthquake is through inelastic deformation of metals. A number of devices have been given in the literature. The Bechtels Added Damping and Stiffness (ADAS) and Triangular-plate Added Damping and Stiffness (TADAS) dampers have been found particularly suitable for the retrofit of existing structures as well as the construction of new structures. A typical X-shaped plate damper or added damping and stiffness (ADAS) device is shown in Figure 3.23. ADAS elements consist of multiple X-shaped mild steel configured in parallel between top and bottom boundary element which is design in a building such that the storey drift causes top of the device to move horizontally relative to the bottom. ADAS device can be easily replaced after earthquake. In order to effectively include these devices in the design of an actual structure, one must be able to characterize their expected nonlinear force-displacement behavior under cyclic load [17].

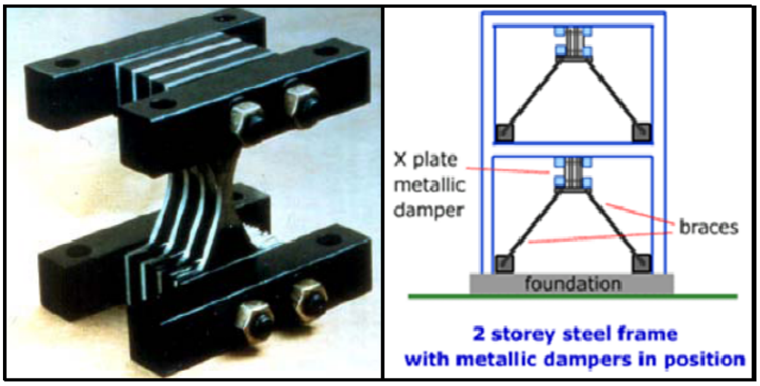

Figure 3.23: X-Shaped ADAS Device [8]

3.5.1 Mathematical Model and Behavior

The response of metallic damper is a function of its geometry and its mechanical characteristics of the metal from it is manufactured. The primary factors affecting ADAS element behavior are; device elastic stiffness, yield strength and yield displacement. For effectively include these devices in the design of an actual structure, one must be able to characterize their expected hysteretic behavior under arbitrary cyclic loading. Usually, metallic devices dissipate energy through a mechanism that is independent of the rate of load frequency, number of load cycles or variation in temperature. In addition, hysteresis devices have high resistance to fatigue. Metallic dampers utilizes the yielding of metals as the dissipative mechanism. Hysteretic behavior of a metallic yielding device is shown in Figure 3.24. The steel-plate added damping and stiffness

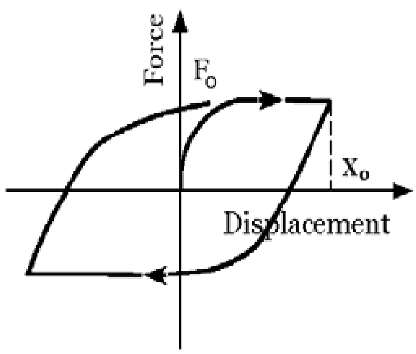

Figure 3.24: Hysteresis Loop for Metallic Damper [11]

(ADAS) device is a mechanism of steel plates to designed for installation in a building frame such that the relative story drift causes the top of the device to move horizontally relative to the bottom, as shown in Figure 3.25, due to yielding of steel plates, the ADAS device can dissipate energy during an earthquake. Figure 3.25 shows the combination of a yielding metallic element and the bracing members that support the device is called as the device-brace assembly. The horizontal stiffness of the ADAS element, K_a, is a function of the lateral stiffness of the bracing members, K_b, and the

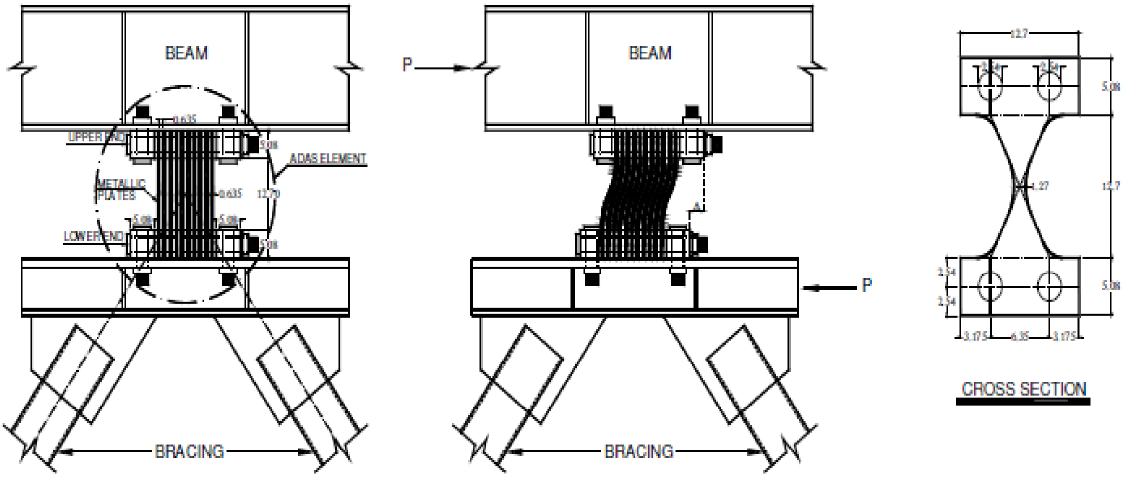

Figure 3.25: The behavior of ADAS damper during earthquake (all dimensions in centimeter) [8]

device initial stiffness, K_d,

$$K_a = \frac{K_b K_d}{K_b + K_d} = \frac{K_d}{1 + \frac{1}{\frac{B}{D}}} \tag{3.10}$$

where B/D is the ratio between the bracing and device stiffness,

$$\frac{B}{D} = \frac{K_b}{K_d} \tag{3.11}$$

Another quantity of interest is the Stiffness Ratio (SR) defined as the ratio of device-brace assembly stiffness to the stiffness of the building story without applying ADAS element, K_s as,

$$SR = \frac{K_a}{K_s} \tag{3.12}$$

The yield force of the yielding metals , denoted by P_y, is based on the yield displacement of the device Δ_y, as:

$$P_y = K_d \times \Delta_y \tag{3.13}$$

For design purposes, this equation can be expressed in terms of the parameters SR and B/D by considering Equations 3.10 and 3.12 in Equation 3.13 as:

$$P_y = SR \cdot K_s[1 + \frac{1}{\frac{B}{D}}]\Delta_y \tag{3.14}$$

Equation 3.14 shows the interrelationship of ADAS device parameters of the assumed bilinear model. It can be observed that in a given structure the behavior of a metallic yielding element is governed by four key parameters, i.e., the yielding load, the yield displacement of the metallic device, and the stiffness ratios SR and B/D. However, later three of these variables are independent since the fourth one can be determined from Equation 3.14.

The ratio of damper element stiffness to structural storey stiffness 'SR', and the ratio of damper yield force to total structure force, 'g' can be used to calculate the equivalent viscous damping using the following formula.

$$\beta = \frac{W_D}{4\pi W_S} \tag{3.15}$$

Where, W_D is the total energy dissipation under the hysteresis loop which at a displacement Δ is calculated as,

$$W_D = 4P_y(\Delta - \Delta_y) \tag{3.16}$$

where Δ_y is the yield deformation of the damper $= P_y/K_d$.

The strain energy, W_S is calculated as,

$$W_S = \frac{1}{2}(K_S\Delta + K_d\Delta_y) \tag{3.17}$$

from Equation 3.16 and 3.17, the equivalent viscous damping ratio is determine as,

$$\beta = \frac{2P_y(\Delta - \Delta_y)}{\pi(K_S\Delta + K_d\Delta_y)} \tag{3.18}$$

3.6 Summary

This chapter deals with the detail of mathematical model of passive dampers like viscous, viscoelastic, and metallic damper. To understand the behavior of viscous and viscoelastic damper, characterization of this dampers have been carried out through MATLAB under the sinusoidal and different earthquake excitations, namely El Centro, Kobe, Loma Prieta, and Northridge excitations, and Force Vs time, Force Vs Displacement, and Force Vs Velocity plots are obtained.

Chapter 4

Three Storey Shear Building Problem

4.1 General

The chapter deals with the dynamic analysis of 3 - storey RC framed building through MATLAB. In Subsequent section, equation of motion for the building without any passive devices, termed as 'uncontrolled building' are derived. Also, other sections discuss in detail derivation of dynamic equation of motion for building with passive devices like viscous, VE and metallic damper. Response quantities like displacement, velocity, acceleration, inter storey drift are determine under four different earthquake ground motion.

4.2 Building Configuration

- No. of Storey = G+2 Storey
- Story Height = 3 m
- Slab Thickness. = 120 mm
- No. of Bays in X-Direction = 3

- No. of Bays in Y-Direction = 3
- Bay Width in X-Direction = 4 m
- Bay Width in Y-Direction = 4 m
- Column Size = 0.3 m × 0.3 m
- Beam Size = 0.23 m × 0.3 m
- f_{ck}= 25 N/mm^2 (M 20 grade of concrete)
- f_y = 415 N/mm^2 (Fe 415 grade of steel)
- Live Load on Typical Storey = 3 KN/m^2

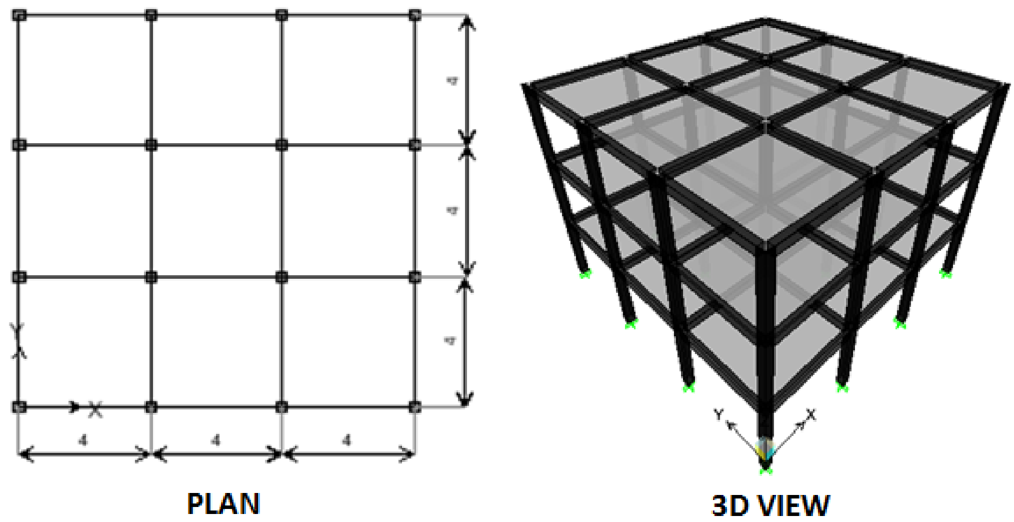

Figure 4.1: Three Storey Buildings Plan and 3D View

The building is symmetric in plan. Dynamic properties of the building like mass matrix and stiffness matrix is determined using lumped mass modeling approach. Inherent damping of the building is assumed to be Rayleigh's damping (proportional damping), It is determined considering damping for first two mode is 5 % of critical damping. Detailed calculation of mass, stiffness and damping matrices are given in Appendix-A.

4.3 Equation of Motion for Uncontrolled Building

Consider a three storey reinforced concrete (RC) building as shown in Figure 4.1. One can replace the distributed mass or inertia of the building by a finite number of lumped masses or rigid bodies. The masses are assumed to be connected by mass-less elastic damping members. Linear or angular coordinates (degree of freedom) are used to describe the motion of the lumped masses, such model are called lumped masses or discrete mass model and is used in present study. Note that, 3-D building is a continuous system and this requires infinite numbers of degree of freedom to describe the motion of the building. However, simple assumptions like slab is considered as rigid diaphragm help in deriving simplified model with limited degree of freedom . Figure 4.2 shows the simplified model of building with degree of freedom associated for present study.

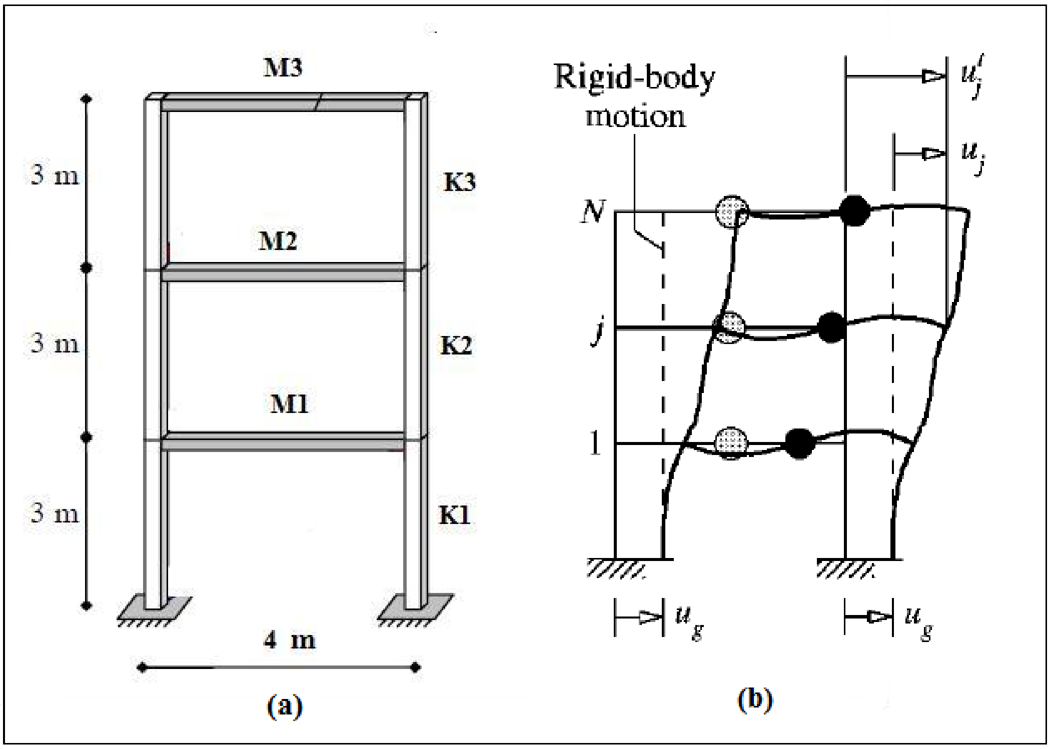

Figure 4.2: Three Storey Building: a) Lumped Mass Model, b)Building Frame under Ground Excitation

The equation of motion of uncontrolled building subjected to earthquake induced ground motion are derived first, to visualize elastic, damping, and inertia forces. In the building , the beam and floor system are considered rigid (infinitely stiff) in flexure, and several factors are neglected while deriving simplified model, like axial deformation of the beam and columns, and the effects of axial force on the stiffness of the columns. The mass is distributed throughout the building, but it is idealize as concentrated at the floor levels. The building as shown in Figure 4.2, has lump mass at each floor level and has three degree of freedoms: the lateral displacements u_1, u_2 and u_3 of the three floors in the direction of the x-axis.

According to D'Alembert's principle, with inertia forces included, a dynamic system is in equilibrium at each time instant. Each inertia force is equal to the product of mass times its acceleration and acts opposite to the direction of acceleration. The displacement of ground is denoted by u_g, the total or absolute displacement of mass by u^t; and the relative displacement between the mass and ground by u at each instant of time, these displacements are related by,

$$u^t(t) = u(t) + u_g(t) \tag{4.1}$$

Such equations for all the N masses can be combined in vector form:

$$u^t(t) = u(t) + u_g(t)l \tag{4.2}$$

Where the influence vector 'l' represents the displacement of the masses resulting from the static application of a unit ground displacement.

The equation of motion for the building of Figure 4.2 subjected to earthquake excitation can be derived by concept of dynamic equilibrium from the free body diagram including the inertia force. The equation of dynamic equilibrium is,

$$f_I + f_D + f_S = 0 \tag{4.3}$$

Only the relative motion u between the mass and the base due to structural deformation produces elastic and damping forces. Thus for a linear system the damping force is,

$$f_D = c\dot{u} \tag{4.4}$$

And elastic resisting force is,

$$f_S = ku \tag{4.5}$$

The inertia force f_I is related to the total acceleration $\ddot{u}^t$ at the mass by,

$$f_I = m\ddot{u}^t \tag{4.6}$$

Substituting Equation 4.4, 4.5 and 4.6, in equation 4.3, and using equation 4.2.,

$$m\ddot{u}^t + c\dot{u} + k(u) = 0 \tag{4.7}$$

$$m\ddot{u}(t) + c\dot{u}(t) + ku(t) = -ml\ddot{u}_g(t) \tag{4.8}$$

Equation 4.8 is known as the equation of motion for the building subjected to earthquake excitation. Where $\ddot{u}_g(t)$ is the ground acceleration and m, c, and k are the mass, damping and stiffness matrix respectively. For building with n degree of freedom, the size of matrix $[m]$, $[c]$, and $[k]$ is $n \times n$.

4.4 Equation of Motion for Building with Passive Devices

The addition of dampers into a building not only increases the stiffness of the structure but also provides a significant amount of damping [11]. This added stiffness and damping helps in reducing the response of the building when subjected to earthquake excitation. For a shear building with added passive dampers subjected to earthquake excitation, the equation of motion of the system combining building and dampers can be written as,

$$m\ddot{u}(t) + c\dot{u}(t) + ku(t) = -ml\ddot{u}_g(t) - BF \tag{4.9}$$

where,
m, k, and c are the mass, stiffness and damping matrices of the building respectively.
u = The vector of the relative displacements of the floors of the building.
l = Influence vector.
$\ddot{u}_g$ = The earthquake acceleration excitation.
B = The matrix derived based on placement of passive devices in the building.
$F = [F_1,\ F_2,\ F_3\ .....\ F_n]^T$ is the vector of control forces produced by passive dampers, Here n is the number of floor of the building.

The control force F for linear viscous fluid dampers with damping coefficient c_d is given by Equation 3.2. The equations of motion of the multi-story structure with viscous damper under the external excitation that is earthquake ground motion, then p_{eff} = -ml$\ddot{u}_g$(t), in which $\ddot{u}_g$(t) is the earthquake ground acceleration and 'l' is an identity matrix so Equation 4.11 can then be expressed as,

$$m\ddot{u}(t) + c\dot{u}(t) + ku(t) = -ml\ddot{u}_g(t) - Bc_d\dot{u}(t) \tag{4.10}$$

$$m\ddot{u}(t) + (c + Bc_d)\dot{u}(t) + ku(t) = -ml\ddot{u}_g(t) \tag{4.11}$$

Equation 4.11 is the equation of motion for multi degree of structure with viscous damper. Depending on the damper diameter and orifice area, the damping co-efficient c_d can be determined and is an important variable in Equation 4.11. In Equation 4.11, c represent the matrix due to structural inherent damping and B$\cdot c_d$ represent the additional damping due to viscous damper in the building.

Similarly for viscoelastic damper, the control force F produces due to stiffness coefficient k_d and damping coefficient c_d are given in Equation 3.5. The equation of motion for the multi degree of freedom shear type building with viscoelatic damper can then be expressed as,

$$m\ddot{u}(t) + c\dot{u}(t) + ku(t) = -ml\ddot{u}_g(t) - B[k_d(u) + c_d\dot{u}(t)] \tag{4.12}$$

$$m\ddot{u}(t) + (c + Bc_d)\dot{u}(t) + (k + Bk_d)u(t) = -ml\ddot{u}_g(t) \tag{4.13}$$

In this equation 4.13, k and c are the matrix due to structural storey stiffness and structural inherent damping, respectively. B$\cdot k_d$ and B$\cdot c_d$ are the matrix due to the addition of viscoelastic dampers stiffness and damping respectively, in the building.

The control force produces by metallic yield damper with damper stiffness K_d is given in Equation 3.12. The equation of motion for the building with metallic yield damper can then be expressed as,

$$m\ddot{u}(t) + (c + c_{eq})\dot{u}(t) + (k + Bk_a)u(t) = -ml\ddot{u}_g(t). \tag{4.14}$$

where, m, c, and k are the mass, damping, and stiffness matrices of the structure. c_{eq} is matrix determine by the equivalent viscous damping contribution due to addition of metallic yielding damper, and Bk_a is the matrix forming due to damper element stiffness.

4.5 Solution of Equation of Motion using Numerical Method

Analytical solution of equation of the motion for a multi degree of freedom system is usually not possible if the excitation-applied force or ground acceleration varies arbitrarily with time. Such problem can be solved by the numerical time-stepping methods for integration of differential equations. There are two basic approaches to numerically evaluate the dynamic response. The first approach is numerical interpolation of the excitation and the second is numerical integration of the equation of motion. Both approaches are applicable to linear systems but the second approach is related to non-linear systems.

Many numerical integration methods are available for the solution of equation of motion specified in previous section. All the numerical integration method have two basic characteristics. First, they do not satisfy differential equation at all time t, but only at discrete time intervals, say Δ(t) apart. secondly, within each time interval Δ(t), a specific type of variation of the displacement u, velocity $\dot{u}$,and acceleration $\ddot{u}$ is assumed. Thus, several numerical integration methods are available depending on the type of variation assumed for u, $\dot{u}$ and $\ddot{u}$ within each time interval Δt.

4.5.1 Time stepping Methods

Equation of motion in the case of base excitation due to earthquake is given as,

$$m\ddot{u}(t) + c\dot{u}(t) + ku(t) = -m\ddot{u}_g(t) \tag{4.15}$$

Now, subject to initial conditions u_0=$u(0)$; and $\dot{u_0}$=$\dot{u}(0)$ usually the system is assumed to have a linear damping, but other forms of damping such as nonlinear damping can be considered. The applied force at discrete time intervals and the time increment Δt_i = t_{i+1} - t_i is usually take to be constant, although this is not necessary. The response is determine at discrete time instants t_i, denoted as time i; the displacement, velocity, and acceleration at the i^{th} step are denoted by u_i, $\dot{u}_i$ and $\ddot{u}_i$ respectively. These values are assumed to satisfy Equation 4.15 at time $i:$ as,

$$m\ddot{u}_i + c\dot{u}_i + ku_i = p_i \tag{4.16}$$

Where ku_i is the resisting force at time i; for linearly elastic but would depend on the prior history of displacement and velocity at time i if the system were inelastic. In subsequent section numerical procedure is presented, which enable us to determine the response quantities u_{i+1}, $\dot{u}_{i+1}$ and $\ddot{u}_{i+1}$ at time (i+1) step that satisfy Equation 4.15 at time i+1:

$$m\ddot{u}_{i+1} + c\dot{u}_{i+1} + ku_{i+1} = p_{i+1} \tag{4.17}$$

If the numerical procedure is applied successively with $i = 0, 1, 2, 3,$....The time stepping procedure gives the desired response at all times with the known initial conditions u_0 and $\dot{u}_0$.

Types of Time Stepping Methods

Three types of time stepping procedures are as follows:

1) Method based on the interpolation of the excitation function.

2) Method based on finite difference expressions for the velocity and acceleration.

3) Method based on the assumed variation of acceleration.

In a direct integration method, the system of equation of motion is integrated successively by using step by step numerical method. No transformation of equation of motion is needed prior to integration and using difference formulas that involve one or more increments of time usually approximates time derivatives. Basically two principle approaches used in the direct integration method: Explicit and implicit schemes. In an explicit scheme, the response quantity are expressed in terms of previously determined value of displacement, velocity, and acceleration. In an implicit scheme the difference equations are combine with the equation of motion, and the displacements are calculated directly by the solving the equation.

4.5.2 Newmark Beta Method [18,19]

The well known Newmark direct integration method is quite often used to compute the structural response, and hence in this section we intend to formulate a procedure that incorporates the Newmark type numerical scheme in solving the equation of motion with and without passive devices under the earthquake excitations.

The Newmark Beta integration method is based on the assumption that the acceleration varies linearly between two instants of time. Two parameter α and β are used in this method, which can be suit the requirement of the particular problem. Newmark [18] presented a family of time-step methods for the solution of structural dynamics problem for both blast and seismic loading. In order to illustrate the use of this numerical integration method, consider the solution of linear dynamic equilibrium equations of motion as given in Equation 4.17. Newmark developed a family of time-stepping methods based on the following equations:

$$\dot{u}_{i+1} = \dot{u}_i + [(1-\gamma)\Delta t]\ddot{u}_i + (\gamma \Delta t)\ddot{u}_{i+1} \tag{4.18}$$

$$u_{i+1} = u_i + (\Delta t)\dot{u}_i + [(0.5-\beta)(\Delta t)^2]\ddot{u}_i + [\beta(\Delta t)^2]\ddot{u}_{i+1} \tag{4.19}$$

Newmark used Equations 4.17, 4.18 and 4.19 iteratively for each time step, for each displacement DOF of the structural system. The parameter β and γ define the variation of acceleration over a time step and determine the stability and accuracy characteristics of the method. Typical selection for γ is 1/2 and $1/6 \leq \beta \leq 1/4$ is satisfactory from all point of view, including that of accuracy. These two equations, combined with the equilibrium Equation 4.17 at the end of the time step, provide the basis for computing u_{i+1}, $\dot{u}_{i+1}$ and $\ddot{u}_{i+1}$ at time (i+1) from the known u_i, $\dot{u}_i$ and $\ddot{u}_i$ at time i. Iteration is required to implement these computations because the unknown $\ddot{u}_{i+1}$ appears in the right side of Equation 4.18 and 4.19. The parameter γ and β indicate how much acceleration enters into the displacement and velocity equations at the end of the interval Δt. Therefore, γ and β are chosen to obtain the desired integration accuracy and stability. When $\gamma = 1/2$ and $\beta = 1/6$, Equations 4.18 and

4.19 correspond to the linear acceleration method. When $\gamma = 1/2$ and $\beta = 1/4$, this correspond to the assumption that the acceleration remain constant. The complete algorithm using the Newmark Beta integration method is given in Table 4.1.

Table 4.1 Newmark's Direct Integration Method[19]

---

1) Initial calculation

(1.1) Form static stiffness matrix [k], mass matrix [m] and damping matrix [c]

(1.2) Specify integration parameter γ and β

(1.3) Select Δt

(1.4) Specify initial conditions u_0, $\dot{u}_0$, $\ddot{u}_0$

(1.5) $\ddot{u}_0 = \frac{p_0 - c\dot{u}_0 - ku_0}{m}$

(1.6) Calculate constants, a = $\frac{1}{\beta\Delta t}$m + $\frac{\gamma}{\beta}$c; and b = $\frac{1}{2\beta}$m + Δt($\frac{\gamma}{2\beta}$-1)c.

(1.7) Calculate modified stiffness, $\widehat{k}$ = k + $\frac{\gamma}{\beta\Delta t}$c + $\frac{1}{\beta(\Delta t)^2}$m.

2) Calculation for each time step, *i*

(2.1) $\Delta\ \widehat{p_i} = \Delta p_i$ + a$\dot{u}_i$ + b$\ddot{u}_i$

(2.2) $\Delta u_i = \frac{\Delta\widehat{p}_i}{\widehat{k}}$

(2.3) $\Delta\ \dot{u}_i = \frac{\gamma}{\beta\Delta t}\Delta u_i$ - $\frac{\gamma}{\beta}\ \dot{u}_i$ + Δt(1-$\frac{\gamma}{2\beta}$)$\ddot{u}_i$.

(2.4) $\Delta\ \ddot{u}_i = \frac{1}{\beta(\Delta t)^2}\Delta u_i$ - $\frac{1}{\beta\Delta t}\ \dot{u}_i$ - $\frac{1}{2\beta}\ddot{u}_i$

(2.5) $u_{i+1} = u_i + \Delta u_i$, $\dot{u}_{i+1} = \dot{u}_i + \Delta\dot{u}_i$ and $\ddot{u}_{i+1} = \ddot{u}_i + \Delta\ddot{u}_i$

3) Repetition for the next time step. Replace *i* by *i* + 1 and implement steps 2.1 to 2.5 for the next time step.

For the ground acceleration excitation $\ddot{u}_g$(t), replace p_i by -m$\ddot{u}_{gi}$ in Table 4.1. The computed u_i, $\dot{u}_i$, and $\ddot{u}_i$ gives response value like displacement, velocity and acceleration relative to the ground. We can find out the total velocity and total acceleration from $\dot{u}_i^t = \dot{u}_i + \dot{u}_{gi}$ and $\ddot{u}_i^t = \ddot{u}_i + \ddot{u}_{gi}$, respectively.

4.6 Response of Uncontrolled Shear Building

In this section, response of uncontrolled shear building is obtained under four different types of earthquakes excitations. Earthquake excitation considered are, El Centro, Loma Prieta, Kobe, and Northridge, where first two excitation are strong motion type while later two excitation are pulse type motion. In order to obtain response quantity equation of motion given by Equation 4.8 is solved using Newmark-Beta method discussed in Section 4.5 through writing code in MATLAB. Response quantities like displacement, acceleration, inter storey drift and velocity are extracted for a shear building.

4.7 Result and Discussions

Table 4.1 shows the maximum response quantity obtained for uncontrolled building under El Centro earthquake excitation.

Table 4.1: Response Quantity under El Centro (PGA-0.3129g) EQ

Storey	**Max.Displ** (m)	**Max.Velo** (m/sec)	**Max. Accel** (m/sec^2)	**Inter Storey Drift** (m)
1	0.010	0.197	5.476	0.011
2	0.018	0.327	7.107	0.008
3	0.023	0.386	8.382	0.005

It is evident that maximum displacement, maximum velocity, and maximum acceleration increases with storey numbers. i,e,. maximum response occurs at top storey of the building. However, inter storey drift is maximum at lower storey and decreases with storey numbers. Time history plot of response quantities like, displacement, acceleration and velocity is obtained. Figure 4.3 shows time history plot of displacement, velocity and acceleration for top storey of the building. It is seen that maximum displacement is 23 mm, maximum velocity is 38.6 cm/sec and maximum acceleration is 838 cm/s^2. It is also observed that, response quantities shows increased response when frequency of earthquake excitation increases.

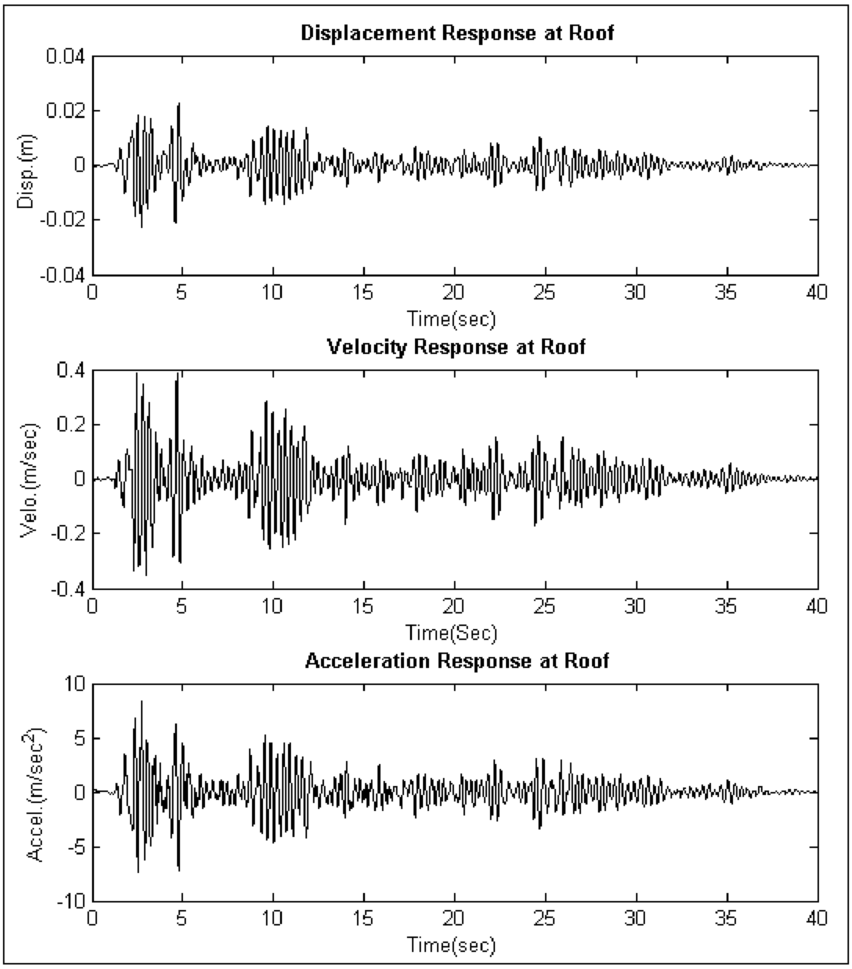

Figure 4.3: Uncontrolled Building Response at Roof under El Centro EQ Excitation

Similarly, response quantity like displacement, velocity, and acceleration are also obtained for uncontrolled building under Kobe, Loma Prieta, and Northridge earthquake excitations. Table 4.2 to 4.4 shows that maximum displacement, maximum velocity, and maximum acceleration increases with storey numbers, however inter storey drift is maximum at lowest storey and decreases with storey numbers.

Table 4.2: Response Quantity under Kobe (PGA-0.6936g) EQ

Storey	**Max.Displ** (m)	**Max.Velo** (m/sec)	**Max. Accel** (m/sec^2)	**Inter Storey Drift** (m)
1	0.026	0.422	9.673	0.031
2	0.045	0.692	14.623	0.024
3	0.055	0.792	17.823	0.012

Table 4.3: Response Quantity under Lomaprieta (PGA-0.6437g) EQ

Storey	**Max.Displ** (m)	**Max.Velo** (m/sec)	**Max. Accel** (m/sec^2)	**Inter Storey Drift** (m)
1	0.029	0.553	10.279	0.029
2	0.051	1.007	16.791	0.023
3	0.062	1.251	21.119	0.012

Table 4.4: Response Quantity under Northridge (PGA-1.585g) EQ

Storey	**Max.Displ** (m)	**Max.Velo** (m/sec)	**Max. Accel** (m/sec^2)	**Inter Storey Drift** (m)
1	0.044	0.770	16.318	0.044
2	0.078	1.508	25.418	0.034
3	0.095	1.904	31.330	0.017

Figure 4.4 to 4.6 shows the time history of building at roof under the Kobe, Loma Prieta, and Northridge, respectively. From Figure 4.4, it is seen that maximum displacement is 55 mm, maximum velocity is 79.2 cm/sec and maximum acceleration is 1782.3 cm/s^2. It is also observed that, response quantity shows increased response when frequency of earthquake excitation increases. Time history under the Loma Prieta earthquake are shown in Figure 4.5, it is seen that maximum displacement is 62 mm, maximum velocity is 125 cm/sec and maximum acceleration is 2111.9 cm/s^2.

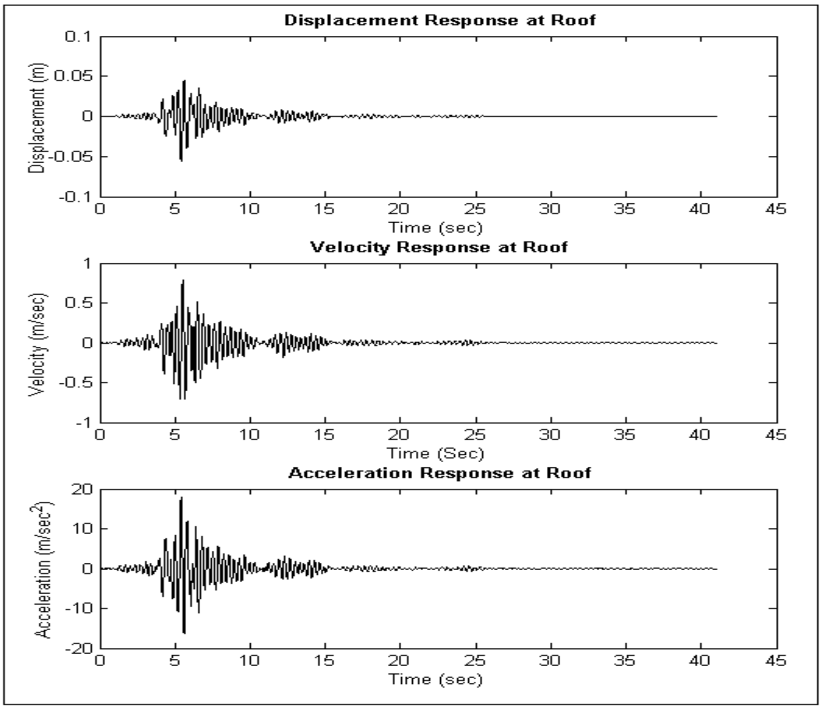

Figure 4.4: Uncontrolled building Response at Roof under Kobe EQ Excitation

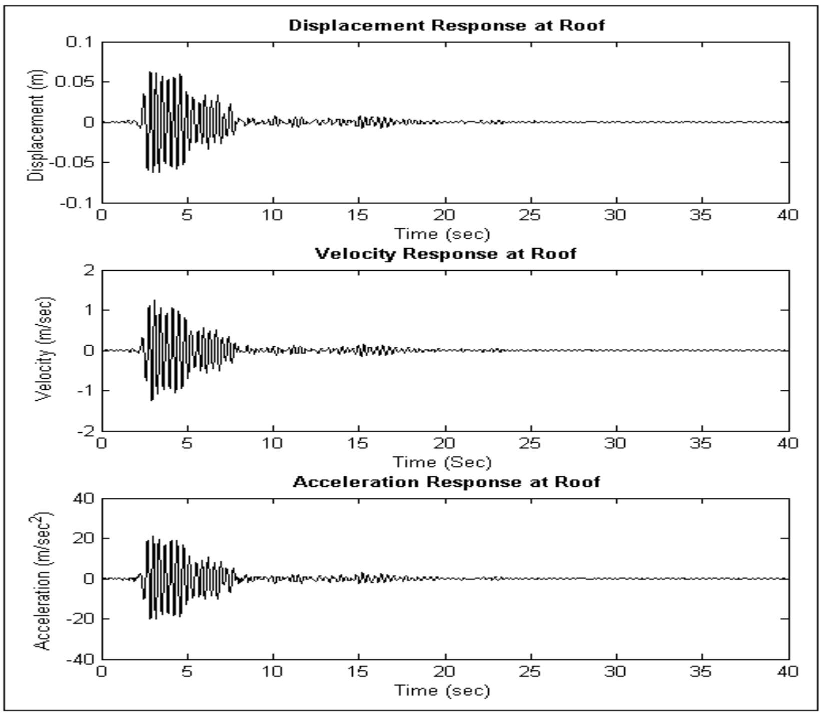

Figure 4.5: Uncontrolled building Response at Roof under Loma Prieta EQ Excitation

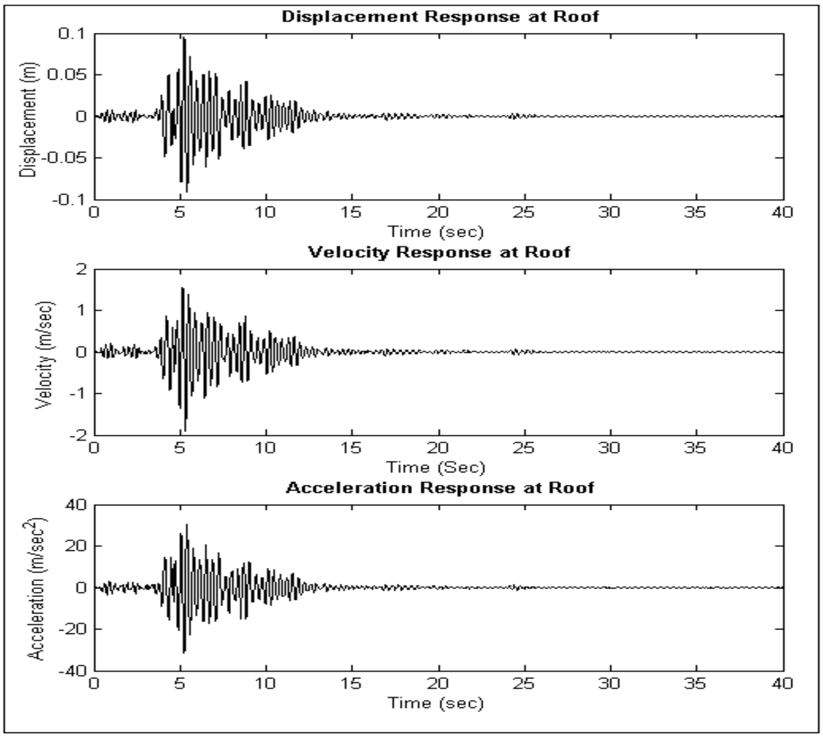

Figure 4.6: Uncontrolled building Response at Roof under Northridge EQ Excitation

Figure 4.6 shows time history plot of displacement, velocity and acceleration for top storey of the building. It is seen that maximum displacement is 95 mm, maximum velocity is 190.4 cm/sec and maximum acceleration is 3133.0 cm/s^2. It is also observed that, response quantities shows increased response when frequency of earthquake excitation increases.

4.8 Summary

The chapter deals with the dynamic response of uncontrolled shear building. Equation of motion for uncontrolled and controlled building with passive ddevices like viscous, vicoealstic and metallic damper are derived. Using Newmark-Beta method response quantiies of building are find out like maximum displacement, maximum velocity, maximum accleration and inter storey drift under the four different earthquake excitations.

Chapter 5

Response of Building using Viscous Damper

The chapter deals with the response of shear building using viscous damper. The time history direct integration method Newmark-Beta is used to find out the response quantity of controlled structure. Algorithm of Newmark-Beta method given in Table 4.1, is used to find out the different response quantities through MATLAB. Extraction of different response quantities are given in subsequent sections.

Viscous dampers are considered as the supplemental devices of choice to reduce the structural response. It is assumed that these devices do not contribute to the overall stiffness of the building. The value of the resisting force in viscous fluid devices is linear. Therefore, their force-deformation is characterized by a viscous dashpot with mathematical model given by Equation 3.2. The building considered here acts like a bare frame as no brick infills are considered as shown in Figure 4.1, and damping allocated is 5 % of critical. For parametric study a shear building has been considered as given in Section 4.2, which was converted into a lump mass model. From this lump mass model mass matrix, stiffness matrix and damping matrix is determined, which is given in Appendix-A. For response of controlled structure, a viscous damper is connected as diagonally at the first storey as shown in Figure 5.1.

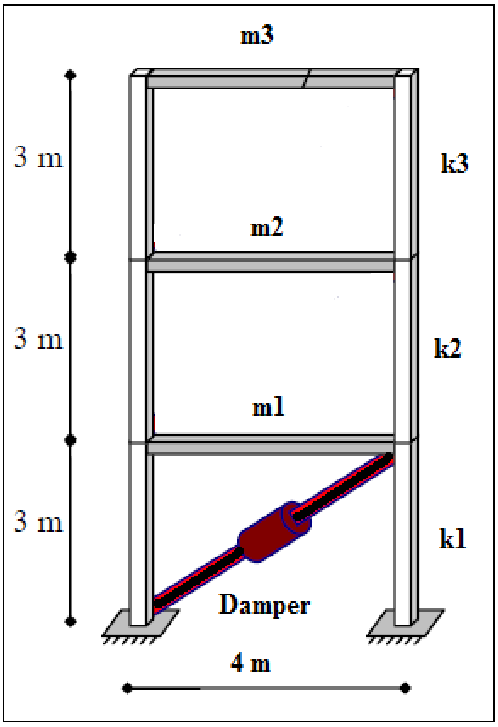

Figure 5.1: A structure with passive damper

5.1 Parametric Study

To understand the influence of viscous damper in reducing different response quantities, parametric study has been carried out. For parametric study damping co-efficient is assumed is varied as 10, 20, 30, 40, 50, 60 70, 80, 90 and 100 $kN \cdot sec/cm$. From these damping co-efficient, it is possible to find out the damping ratio supplied by the devices. (from the formula given in FEMA 273). The equation of motion for multi degree of freedom structure with viscous damper is given in Equation 4.11. This equation of motion is solved using numerical method Newmark-Beta as per Table 4.1 for four different types of earthquake excitations through MATLAB. The response quantities like relative displacement, relative velocity, absolute acceleration and damper forces for different value of damping co-efficient 'C_d' are calculated. The earthquake excitations used in this study are given in Table 3.2.

5.2 Results and Discussion

This section presents the results obtained through direct integration method Newmark-Beta of three storey R.C. frame building with velocity dependent energy dissipation device (Viscous damper). The response of R.C frame building in the form of relative displacement, relative velocity, absolute acceleration, and damper force are obtained. Efficiency of these damping systems is investigated for four earthquake excitation of different peak acceleration value, namely El Centro, Kobe, Loma Prieta and Northridge. The undamped structural response was found out as discussed in Section 4.6 of chapter 3 in order to compare its results with the results of the building embedded with viscous damping system. There are various ways of assessing seismic response, but computation of top storey response is a reasonable measure of the overall effect of seismic response. The reduction in the top storey velocity, acceleration, and damping force at first storey of the building are also investigated for four types of earthquake excitations.

5.2.1 Comparison of Displacement Response

The results of displacement response of uncontrolled and controlled building for four earthquake excitation of different peak acceleration value, namely El Centro, Kobe, Loma Prieta and Northridge are given in Table 5.1 to 5.4 respectively. The graphical representations of comparison of displacement response for uncontrolled and controlled structure are presented in Figure 5.2. From results, it is evident that displacement of top storey is highest, so comparison of displacement is done at top of the building.

Table 5.1: Relative Displacement under El Centro (PGA-0.3129g) EQ Excitation

Cd	Maximum Storey Displacement (m)					
$kN \cdot sec/cm$	1^{st}	% Red.	2^{nd}	% Red.	Roof	% Red.
10	0.0091	12.9	0.0159	13.9	0.0190	16.4
20	0.0073	30.5	0.0139	24.6	0.0168	26.1
30	0.0070	33.5	0.0123	33.2	0.0150	34.1
40	0.0063	40.3	0.0110	40.3	0.0135	40.5
50	0.0061	42.1	0.0107	42.1	0.0128	43.8
60	0.0059	44.1	0.0104	43.3	0.0126	44.8
70	0.0056	46.2	0.0102	44.6	0.0123	45.9
80	0.0054	48.4	0.0099	46.0	0.0121	47.0
90	0.0052	50.6	0.0097	47.4	0.0118	48.1
100	0.0049	53.3	0.0094	48.8	0.0116	49.2
Uncontrolled	0.010	0.0	0.0184	0.0	0.0228	0.0

Table 5.2: Relative Displacement under Kobe (PGA-0.6936g) EQ Excitation

Cd	Maximum Storey Displacement (m)					
$kN \cdot sec/cm$	1^{st}	% Red.	2^{nd}	% Red.	Roof	% Red.
10	0.0251	2.28	0.0445	2.05	0.0542	1.95
20	0.0214	16.53	0.0380	16.45	0.0464	16.07
30	0.0188	26.73	0.0334	26.53	0.0410	25.80
40	0.0168	34.57	0.0301	33.82	0.0371	32.86
50	0.0153	40.52	0.0275	39.42	0.0342	38.16
60	0.0140	45.53	0.0255	43.83	0.0319	42.24
70	0.0129	49.61	0.0239	47.36	0.0302	45.43
80	0.0121	53.06	0.0226	50.24	0.0288	47.97
90	0.0113	56.09	0.0215	52.62	0.0276	50.03
100	0.0106	58.79	0.0206	54.61	0.0267	51.72
Uncontrolled	0.0257	0.00	0.0455	0.00	0.0553	0.00

Table 5.3: Relative Displacement under Lomaprieta (PGA-0.6437g) EQ Excitation

Cd	Maximum Storey Displacement (m)					
$kN \cdot sec/cm$	1^{st}	% Red.	2^{nd}	% Red.	Roof	% Red.
10	0.0248	13.71	0.0440	13.67	0.0533	14.68
20	0.0221	23.23	0.0396	22.28	0.0482	22.91
30	0.0197	31.51	0.0358	29.63	0.0439	29.83
40	0.0177	38.57	0.0327	35.84	0.0403	35.59
50	0.0159	44.68	0.0300	41.07	0.0373	40.36
60	0.0144	49.94	0.0278	45.49	0.0348	44.34
70	0.0131	54.50	0.0259	49.18	0.0327	47.69
80	0.0120	58.44	0.0243	52.31	0.0309	50.52
90	0.0110	61.90	0.0229	54.98	0.0294	52.90
100	0.0101	64.94	0.0218	57.28	0.0282	54.88
Uncontrolled	0.0288	0.00	0.0509	0.00	0.0625	0.00

Table 5.4: Relative Displacement under Northridge (PGA-1.585g) EQ Excitation

Cd	Maximum Storey Displacement (m)					
$kN \cdot sec/cm$	1^{st}	% Red.	2^{nd}	% Red.	Roof	% Red.
10	0.0366	16.63	0.0663	15.34	0.0811	15.02
20	0.0302	31.23	0.0555	29.17	0.0680	28.74
30	0.0257	41.59	0.0476	39.31	0.0588	38.44
40	0.0225	48.77	0.0423	46.07	0.0530	44.49
50	0.0198	54.89	0.0377	51.84	0.0489	48.80
60	0.0180	59.02	0.0346	55.83	0.0454	52.44
70	0.0165	62.37	0.0323	58.72	0.0425	55.52
80	0.0152	65.33	0.0306	60.99	0.0400	58.13
90	0.0141	67.94	0.0290	62.96	0.0386	59.58
100	0.0131	70.23	0.0277	64.67	0.0377	60.49
Uncontrolled	0.0439	0.00	0.0784	0.00	0.0955	0.00

For controlled building with viscous damper a reduction of 16.4%, 1.95%, 14.68% and 15.02% in roof displacement is observed, when co-efficient of damping 'C_d' is 10 $kN \cdot sec/cm$ for El Centro, Kobe, Loma Prieta and Northridge earthquake excitations, respectively, with respect to uncontrolled structure. But for Kobe earthquake only 1.95% roof displacement reduction is observed, which is very less as compare to other three earthquake excitations for C_d=10 $kN \cdot sec/cm$. When co-efficient of damping 'C_d'=100 $kN \cdot sec/cm$, reduction of 49.2%, 51.72%, 54.88% and 60.49% in roof displacement is observed for El Centro, Kobe, Loma Prieta and Northridge earthquake excitation, respectively. It is observed that, reduction in displacement up to 50% is achieved when viscous damper with co-efficient of damping C_d=100 $kN \cdot sec/cm$ is used, under four different types of earthquake excitations.

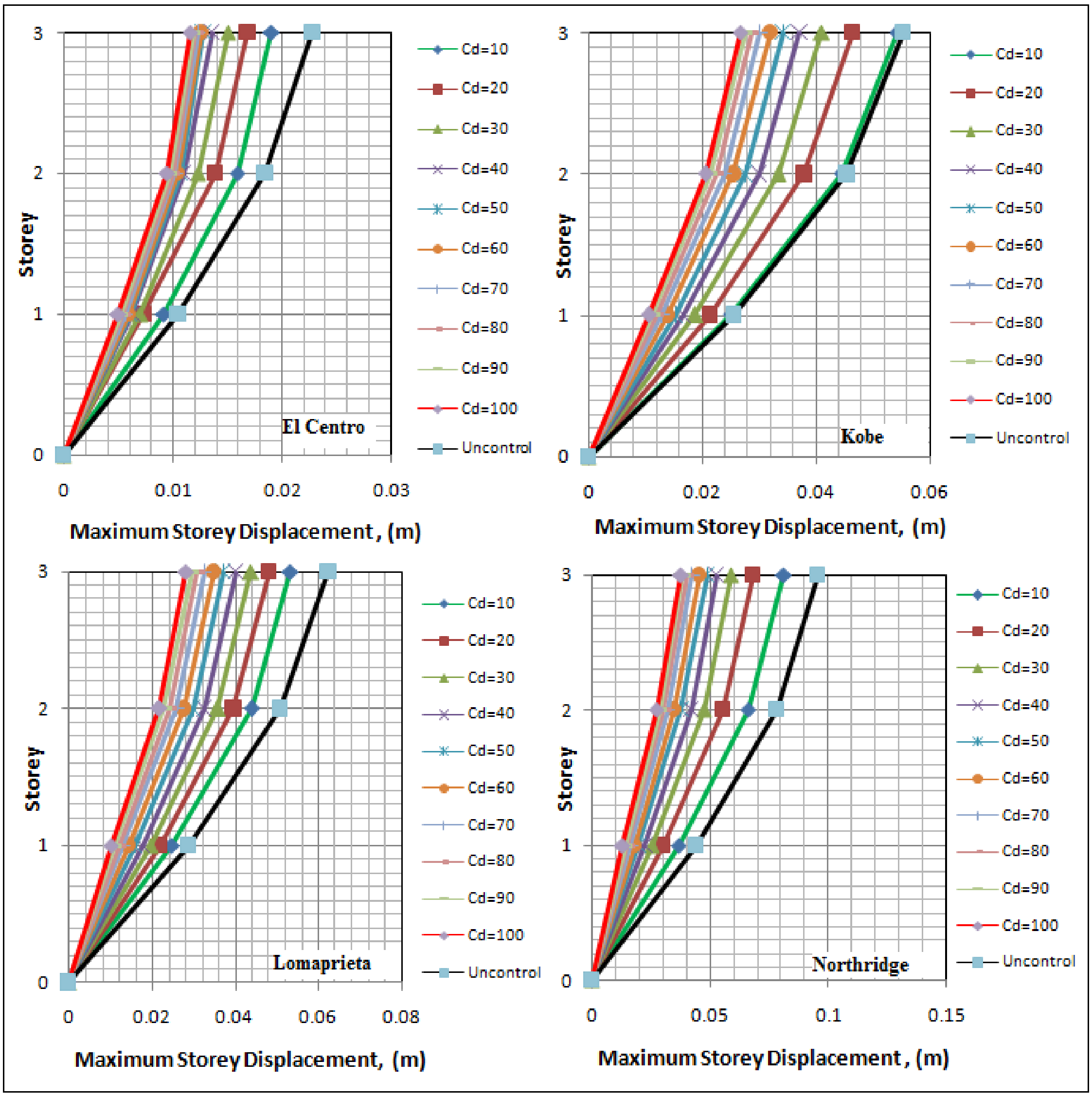

Figure 5.2: Comparison of Displacement for Different EQ Excitation

5.2.2 Comparison of Velocity Response

The results of Velocity response of uncontrolled and controlled building for four earthquake excitation of different peak acceleration value, namely El Centro, Kobe, Loma Prieta and Northridge are given in Table 5.5 to 5.8, respectively. The graphical representations of comparison of velocity for uncontrolled and controlled structure are presented in Figure 5.3.

Table 5.5: Relative Velocity under El Centro (PGA-0.3129g) EQ Excitation

Cd	Maximum Storey Velocity (m/sec)					
$kN \cdot sec/cm$	1^{st}	% Red.	2^{nd}	% Red.	Roof	% Red.
10	0.1671	15.0	0.2845	12.9	0.3455	10.4
20	0.1444	26.5	0.2504	23.3	0.3086	20.0
30	0.126	35.9	0.2245	31.3	0.2983	22.7
40	0.1107	43.7	0.2158	33.9	0.2902	24.8
50	0.0982	50.0	0.2076	36.4	0.2825	26.8
60	0.092	53.2	0.2003	38.7	0.2756	28.6
70	0.0863	56.1	0.1939	40.6	0.2708	29.8
80	0.0808	58.9	0.1892	42.1	0.2666	30.9
90	0.0758	61.4	0.1851	43.3	0.263	31.8
100	0.0712	63.8	0.1816	44.4	0.2598	32.7
Uncontrolled	0.1965	0.0	0.3266	0.0	0.3858	0.0

Table 5.6: Relative Velocity under Kobe (PGA-0.6936g) EQ Excitation

Cd	Maximum Storey Velocity (m/sec)					
$kN \cdot sec/cm$	1^{st}	% Red.	2^{nd}	% Red.	Roof	% Red.
10	0.400	5.30	0.671	3.12	0.776	2.04
20	0.323	23.49	0.550	20.49	0.640	19.18
30	0.269	36.33	0.468	32.34	0.552	30.34
40	0.230	45.59	0.409	40.89	0.519	34.51
50	0.200	52.52	0.392	43.31	0.526	33.65
60	0.177	58.04	0.391	43.52	0.530	33.09
70	0.164	61.17	0.389	43.85	0.533	32.70
80	0.156	62.96	0.386	44.21	0.536	32.38
90	0.149	64.76	0.384	44.55	0.538	32.08
100	0.141	66.50	0.382	44.85	0.540	31.78
Uncontrolled	0.422	0.00	0.692	0.00	0.792	0.00

Table 5.7: Relative Velocity under Lomaprieta (PGA-0.6437g) EQ Excitation

Cd	Maximum Storey Velocity (m/sec)					
$kN \cdot sec/cm$	1^{st}	% Red.	2^{nd}	% Red.	Roof	% Red.
10	0.437	20.89	0.799	20.72	0.996	20.33
20	0.365	33.96	0.671	33.41	0.831	33.58
30	0.317	42.61	0.591	41.37	0.740	40.84
40	0.279	49.60	0.529	47.47	0.671	46.33
50	0.247	55.41	0.481	52.22	0.619	50.50
60	0.220	60.24	0.444	55.90	0.582	53.43
70	0.197	64.28	0.416	58.71	0.570	54.41
80	0.179	67.66	0.407	59.59	0.563	54.99
90	0.163	70.53	0.401	60.20	0.559	55.27
100	0.151	72.60	0.397	60.60	0.557	55.48
Uncontrolled	0.553	0.00	1.007	0.00	1.251	0.00

Table 5.8: Relative Velocity under Northridge (PGA-1.585g) EQ Excitation

Cd	Maximum Storey Velocity (m/sec)					
$kN \cdot sec/cm$	1^{st}	% Red.	2^{nd}	% Red.	Roof	% Red.
10	0.637	17.23	1.242	17.64	1.598	16.09
20	0.543	29.44	1.042	30.94	1.331	30.09
30	0.471	38.89	0.905	39.97	1.171	38.50
40	0.420	45.46	0.827	45.14	1.049	44.93
50	0.376	51.14	0.773	48.76	0.959	49.66
60	0.339	55.96	0.724	51.97	0.903	52.59
70	0.308	60.01	0.682	54.76	0.859	54.91
80	0.282	63.42	0.646	57.18	0.820	56.93
90	0.259	66.32	0.614	59.28	0.786	58.70
100	0.240	68.78	0.587	61.11	0.757	60.25
Uncontrolled	0.770	0.00	1.508	0.00	1.904	0.00

From results, it is evident that velocity of top storey is highest, so comparison of velocity is done at top of the structure. For controlled building with viscous damper a reduction of 10.4%, 2.04%, 20.33% and 16.09% in roof velocity is observed, when co-efficient of damping 'C_d' is 10 $kN \cdot sec/cm$ for El Centro, Kobe, Loma Prieta and Northridge earthquake excitation, respectively, with respect to uncontrolled structure. But for Kobe earthquake only 2.04% roof velocity reduction is observed, which is very less as compare to other three earthquake excitations for C_d=10 $kN \cdot sec/cm$. When co-efficient of damping 'C_d'=100 $kN \cdot sec/cm$, reduction of 32.7%, 31.78%, 55.48% and 60.25% in roof velocity is observed for El Centro, Kobe, Loma Prieta and Northridge earthquake excitation respectively.It is observed that, reduction in roof velocity above 50% is achieved when damper with co-efficient of damping 'C_d'=100 $kN \cdot sec/cm$ is used, under Loma Prieta and Northridge type of earthquake excitations.

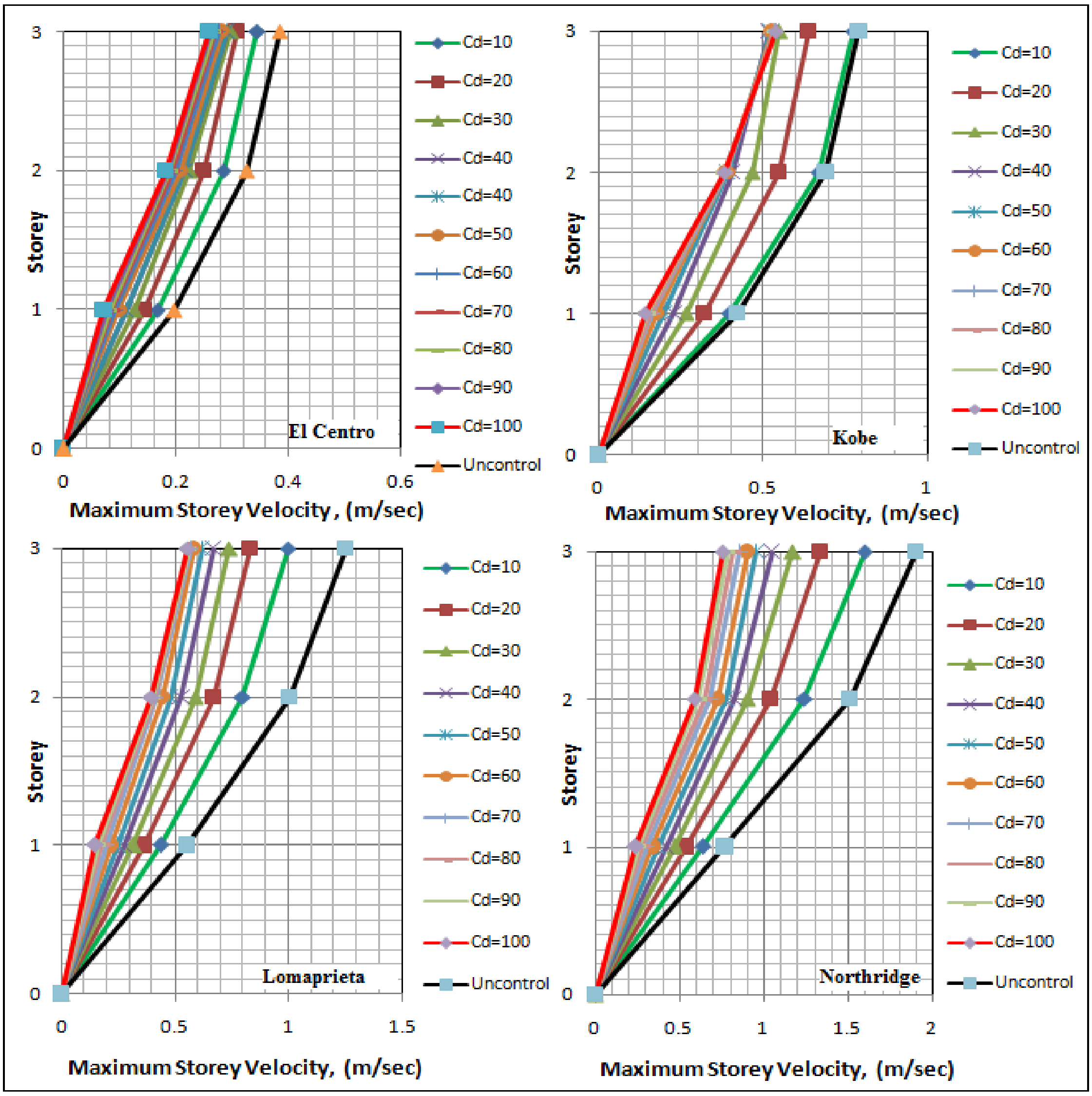

Figure 5.3: Comparison of Velocity for Different EQ Excitation

5.2.3 Comparison of Acceleration Response

The results of acceleration response of uncontrolled and controlled building for four earthquake excitation of different peak acceleration value, namely El Centro, Kobe, Loma Prieta and Northridge are given in Table 5.9 to 5.12 respectively. The graphical representations of comparison of acceleration response for uncontrolled and controlled structure are presented in Figure 5.4.

Table 5.9: Absolute Acceleration under El Centro (PGA-0.3129g) EQ Excitation

Cd	Maximum Storey Acceleration (m/sec^2)					
$kN \cdot sec/cm$	1^{st}	% Red.	2^{nd}	% Red.	Roof	% Red.
10	4.369	20.2	6.622	6.8	7.94	5.3
20	3.615	34.0	6.256	12.0	7.701	8.1
30	3.077	43.8	6.103	14.1	7.489	10.7
40	2.678	51.1	6.004	15.5	7.318	12.7
50	2.37	56.7	5.938	16.4	7.285	13.1
60	2.149	60.8	5.896	17.0	7.309	12.8
70	2.013	63.2	5.87	17.4	7.34	12.4
80	1.891	65.5	5.855	17.6	7.377	12.0
90	1.781	67.5	5.846	17.7	7.415	11.5
100	1.681	69.3	5.845	17.8	7.454	11.1
Uncontrolled	5.476	0.0	7.107	0.0	8.382	0.0

Table 5.10: Absolute Acceleration under Kobe (PGA-0.6936g) EQ Excitation

Cd	Maximum Storey Acceleration (m/sec^2)					
$kN \cdot sec/cm$	1^{st}	% Red.	2^{nd}	% Red.	Roof	% Red.
10	9.405	14.81	14.315	17.87	17.506	1.78
20	8.259	25.20	12.420	28.74	15.271	14.32
30	7.515	31.93	11.251	35.45	13.916	21.92
40	6.990	36.69	10.457	40.01	13.030	26.89
50	6.680	39.49	9.900	43.20	12.434	30.24
60	6.564	40.55	9.502	45.48	12.028	32.51
70	6.587	40.34	9.216	47.13	11.985	32.75
80	6.594	40.27	9.025	48.22	12.227	31.40
90	6.593	40.28	8.883	49.04	12.465	30.06
100	6.589	40.32	8.776	49.65	12.701	28.74
Uncontrolled	11.040	0.00	17.430	0.00	17.823	0.00

Table 5.11: Absolute Acceleration under Loma Prieta (PGA-0.6437g) EQ Excitation

Cd	Maximum Storey Acceleration (m/sec^2)					
$kN \cdot sec/cm$	1^{st}	% Red.	2^{nd}	% Red.	Roof	% Red.
10	9.441	8.15	14.383	14.34	16.941	19.78
20	8.708	15.28	13.273	20.95	15.656	25.87
30	8.140	20.81	12.438	25.93	14.686	30.46
40	7.711	24.98	11.804	29.70	13.964	33.88
50	7.393	28.08	11.329	32.53	13.411	36.50
60	7.139	30.54	10.952	34.78	12.983	38.53
70	6.953	32.35	10.666	36.48	12.663	40.04
80	6.815	33.70	10.444	37.80	13.029	38.31
90	6.702	34.80	10.262	38.88	13.378	36.65
100	6.609	35.70	10.111	39.78	13.706	35.10
Uncontrolled	10.279	0.00	16.791	0.00	21.119	0.00

Table 5.12: Absolute Acceleration under Northridge (PGA-1.585g) EQ Excitation

Cd	Maximum Storey Acceleration (m/sec^2)					
$kN \cdot sec/cm$	1^{st}	% Red.	2^{nd}	% Red.	Roof	% Red.
10	13.214	19.02	21.652	14.82	26.832	14.36
20	11.810	27.62	18.387	27.66	24.100	23.08
30	10.784	33.92	16.198	36.27	22.875	26.99
40	10.901	33.19	14.513	42.90	21.564	31.17
50	10.999	32.60	13.446	47.10	21.244	32.19
60	11.030	32.41	13.009	48.82	21.007	32.95
70	11.028	32.42	12.925	49.15	20.754	33.76
80	11.086	32.06	12.897	49.26	20.503	34.56
90	11.415	30.05	12.910	49.21	20.265	35.32
100	11.701	28.30	13.261	47.83	20.196	35.54
Uncontrolled	16.318	0.00	25.418	0.00	31.330	0.00

From results, it is evident that acceleration of top storey is highest, so comparison of acceleration is done at top of the structure. For controlled building with viscous damper reduction is 5.3%, 1.78%, 19.78% and 14.36% in roof acceleration is observed, when co-efficient of damping 'C_d' is 10 $kN \cdot sec/cm$ for El Centro, Kobe, Loma Prieta and Northridge earthquake excitation, respectively, with respect to uncontrolled structure. But for El Centro and Kobe earthquake reduction is only 5.3% and 1.78% in roof acceleration is observed, which is very less as compare to other two earthquake excitations for C_d=10 $kN \cdot sec/cm$. When co-efficient of damping 'C_d'=100 $kN \cdot sec/cm$, reduction is 11.1%, 28.74%, 35.10% and 35.54% in roof acceleration is observed for El Centro, Kobe, Loma Prieta and Northridge earthquake excitations, respectively. It is observed that, reduction in roof acceleration up to 35% is achieved when damper with co-efficient of damping 'C_d'=100 $kN \cdot sec/cm$ is used, under Loma Prieta and Northridge type of earthquake excitations.

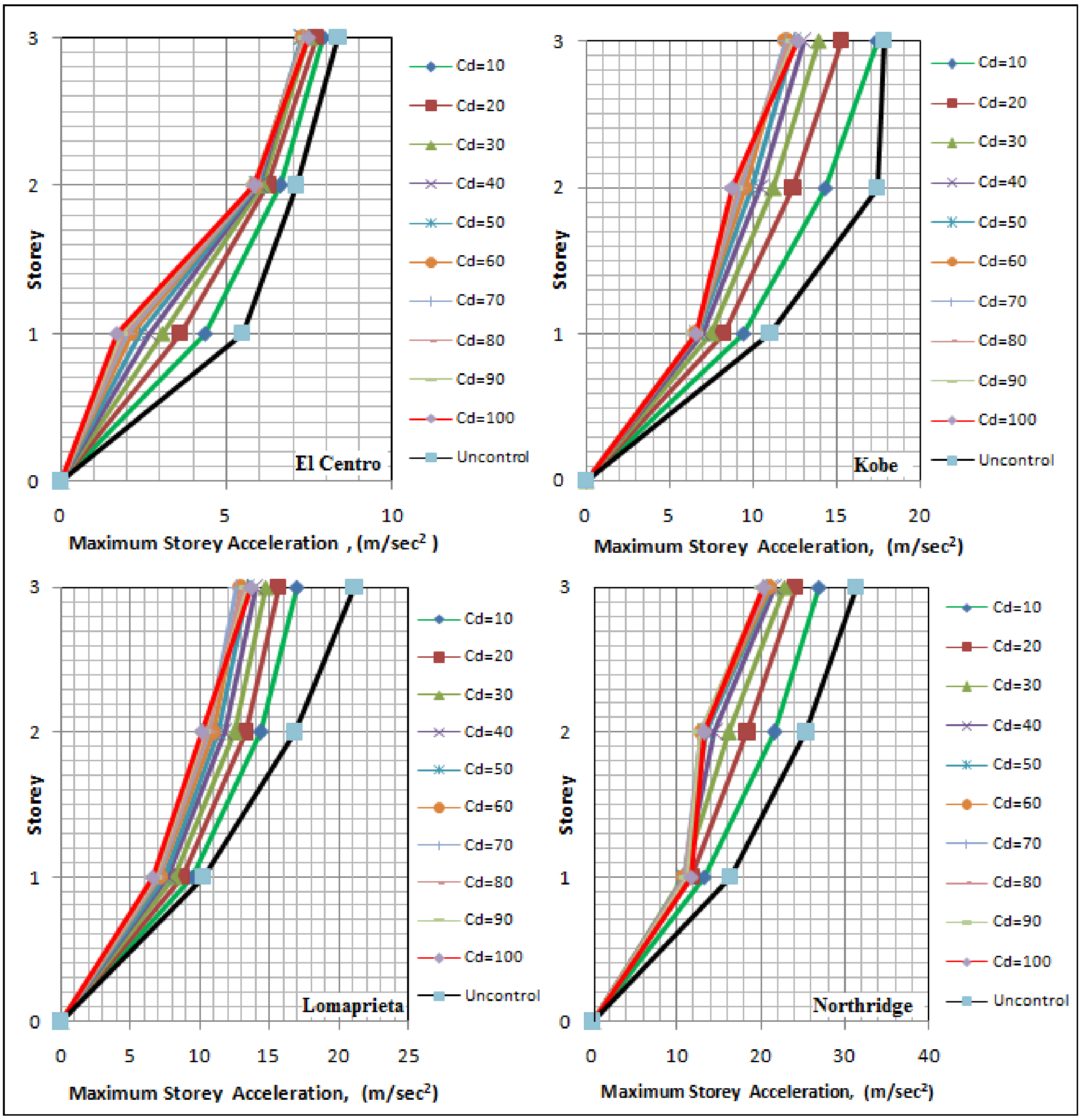

Figure 5.4: Comparison of Acceleration for Different EQ Excitation

5.2.4 Comparison of Inter Storey Drift

The results of inter storey drift of uncontrolled and controlled building for four earthquake excitation of different peak acceleration value, namely El Centro, Kobe, Loma Prieta and Northridge are given in Table 5.13 to 5.16 respectively. The graphical representations of comparison of inter storey drift for uncontrolled and controlled structure are presented in Figure 5.5.

Table 5.13: Inter Storey Drift under El Centro (PGA-0.3129g) EQ Excitation

Cd	Maximum Inter Storey Drift (m)					
$kN \cdot sec/cm$	1^{st}	% Red.	2^{nd}	% Red.	Roof	% Red.
10	0.0091	12.9	0.0069	17.1	0.0035	24.5
20	0.0079	24.5	0.0061	26.2	0.0032	31.1
30	0.0070	33.6	0.0059	28.8	0.0031	33.6
40	0.0063	40.4	0.0057	31.0	0.0031	34.3
50	0.0061	42.1	0.0056	32.1	0.0031	34.5
60	0.0059	44.2	0.0056	32.7	0.0031	34.5
70	0.0056	46.2	0.0055	33.1	0.0031	34.4
80	0.0054	48.4	0.0055	33.4	0.0031	34.0
90	0.0052	50.6	0.0055	33.4	0.0031	33.1
100	0.0050	52.8	0.0056	33.0	0.0032	32.3
Uncontrolled	0.0105	0.0	0.0083	0.0	0.0047	0.0

Table 5.14: Inter Storey Drift under Kobe (PGA-0.6936g) EQ Excitation

Cd	Maximum Inter Storey Drift (m)					
$kN \cdot sec/cm$	1^{st}	% Red.	2^{nd}	% Red.	Roof	% Red.
10	0.0251	18.62	0.0194	18.34	0.0097	18.01
20	0.0214	30.49	0.0168	29.31	0.0084	28.71
30	0.0188	38.98	0.0152	35.99	0.0076	35.43
40	0.0168	45.51	0.0142	40.39	0.0071	39.77
50	0.0153	50.47	0.0135	43.40	0.0068	42.46
60	0.0140	54.64	0.0130	45.51	0.0066	44.28
70	0.0129	58.03	0.0126	46.98	0.0065	44.78
80	0.0121	60.91	0.0124	48.02	0.0067	43.54
90	0.0113	63.44	0.0123	48.25	0.0068	42.33
100	0.0106	65.68	0.0125	47.34	0.0069	41.14
Uncontrolled	0.0308	0.00	0.0238	0.00	0.0118	0.00

Table 5.15: Inter Storey Drift under Lomaprieta (PGA-0.6437g) EQ Excitation

Cd	Maximum Inter Storey Drift (m)					
$kN \cdot sec/cm$	1^{st}	% Red.	2^{nd}	% Red.	Roof	% Red.
10	0.0248	13.71	0.0192	17.13	0.0093	19.86
20	0.0221	23.23	0.0176	23.80	0.0086	26.20
30	0.0197	31.51	0.0165	28.73	0.0081	30.93
40	0.0177	38.57	0.0156	32.46	0.0076	34.46
50	0.0159	44.68	0.0150	35.23	0.0073	37.13
60	0.0144	49.94	0.0145	37.35	0.0071	39.19
70	0.0131	54.50	0.0141	39.04	0.0069	40.73
80	0.0120	58.44	0.0138	40.27	0.0071	39.42
90	0.0110	61.90	0.0136	41.26	0.0073	37.65
100	0.0101	64.94	0.0139	40.10	0.0074	36.16
Uncontrolled	0.0288	0.00	0.0232	0.00	0.0117	0.00

Table 5.16: Inter Storey Drift under Northridge (PGA-1.585g) EQ Excitation

Cd	Maximum Inter Storey Drift (m)					
$kN \cdot sec/cm$	1^{st}	% Red.	2^{nd}	% Red.	Roof	% Red.
10	0.0366	16.63	0.0297	13.71	0.0148	13.53
20	0.0302	31.23	0.0253	26.54	0.0130	23.96
30	0.0257	41.59	0.0229	33.43	0.0125	26.99
40	0.0225	48.77	0.0216	37.14	0.0119	30.45
50	0.0198	54.89	0.0205	40.52	0.0113	33.71
60	0.0180	59.02	0.0199	42.13	0.0113	33.87
70	0.0165	62.37	0.0196	42.98	0.0113	34.16
80	0.0152	65.33	0.0194	43.75	0.0112	34.50
90	0.0141	67.94	0.0191	44.44	0.0111	34.87
100	0.0131	70.23	0.0189	45.05	0.0111	35.23
Uncontrolled	0.0439	0.00	0.0344	0.00	0.0171	0.00

From results, it is evident that storey drift is maximum at 1^{st} storey level, so comparison of storey drift is done at level of 1^{st} storey of the structure. It is clear from graphs that storey drift is constantly decreased by attaching viscous damper to structure for increasing the value of damping co-efficient C_d=10 $kN \cdot sec/cm$ to C_d=100 $kNsec/cm$ respectively. For controlled building with viscous damper reduction is 12.9%, 18.62%, 13.71% and 16.63% in inter storey drift is observed, when co-efficient of damping 'C_d' is 10 $kN \cdot sec/cm$ for El Centro, Kobe, Loma Prieta and

Northridge earthquake excitations, respectively, with respect to uncontrolled structure. When co-efficient of damping 'C_d'=100 $kN \cdot sec/cm$, reduction is 52.8%, 65.68%, 64.94% and 70.23% in storey drift is observed for El Centro, Kobe, Loma Prieta and Northridge earthquake excitations, respectively. From this results it is observed that, reduction in inter storey drift up to 50% to 70% is achieved using viscous damper with co-efficient of damping 'C_d'=100 $kN \cdot sec/cm$ is used, under four different types of earthquake excitations.

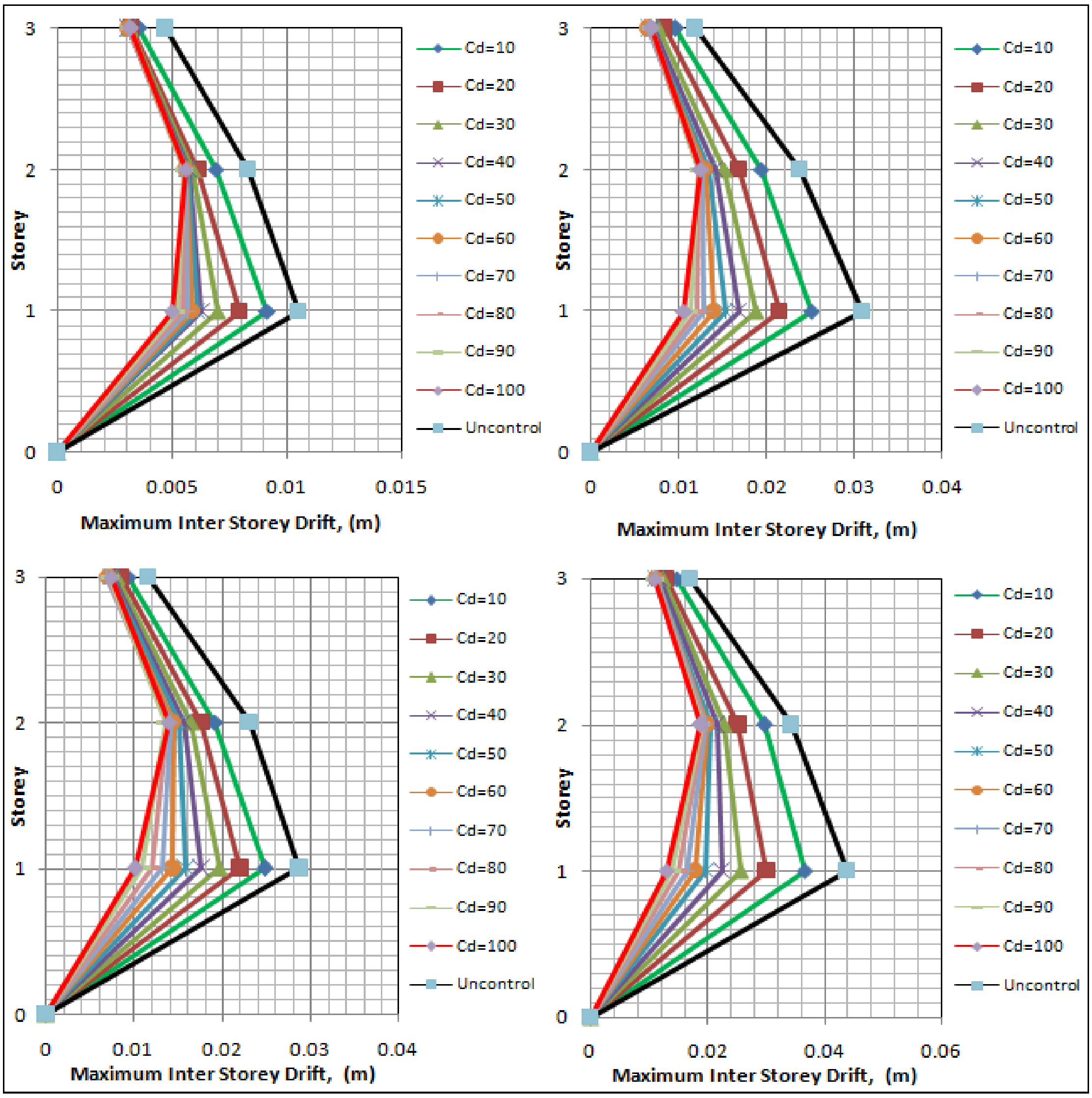

Figure 5.5: Comparison of Inter Storey Drift for Different EQ Excitation

5.2.5 Comparison of Time History

Figure 5.6 to 5.10 represents displacement, velocity and acceleration time history in horizontal direction of uncontrolled (for 5% inherent damping ratio) and controlled (for C_d=100 $kN \cdot sec/cm$) building for El Centro, Kobe, Loma Prieta and Northridge earthquake excitation respectively. The maximum response reduction is achieved when damping co-efficient 'C_d' is 100 $kN \cdot sec/cm$ in most of the response quantities. Therefore all the response quantities of control building with C_d=100 $kN \cdot sec/cm$ is compared to uncontrolled building. Out of time history plots obtained for all response quantities at each storey, only those time history plots are presents here, which shows maximum reduction in response quantities. Figure 5.6 to 5.10 shows the responses of building at the 1^{st} storey under El Centro earthquake excitation.

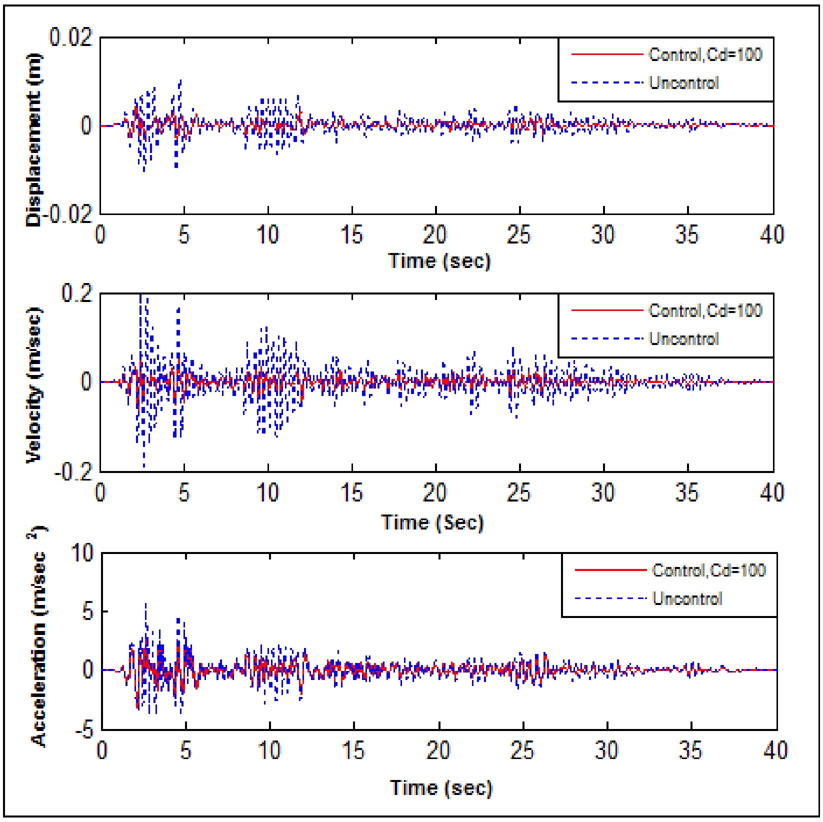

Figure 5.6: Time History Response at 1^{st} Storey under El Centro EQ

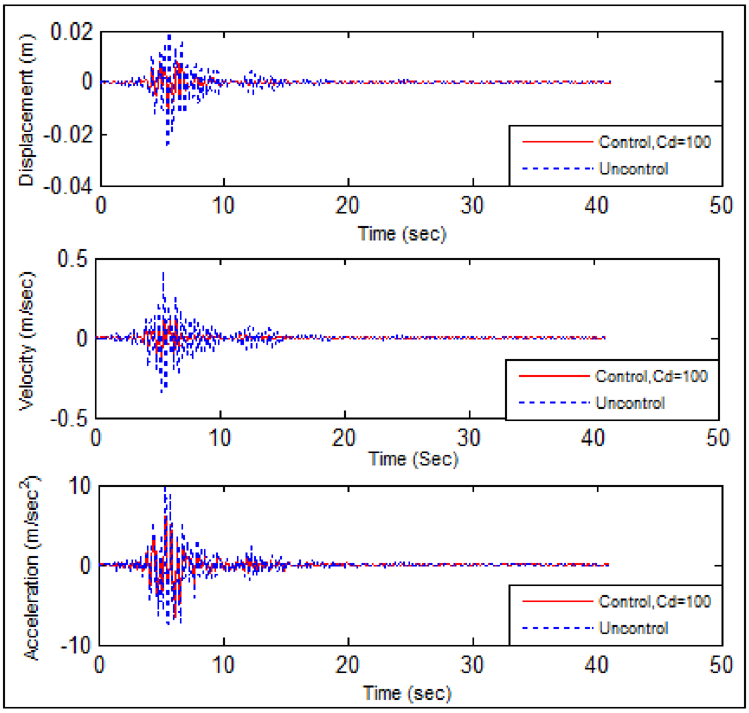

Figure 5.7: Time History Response at 1^{st} Storey under Kobe EQ

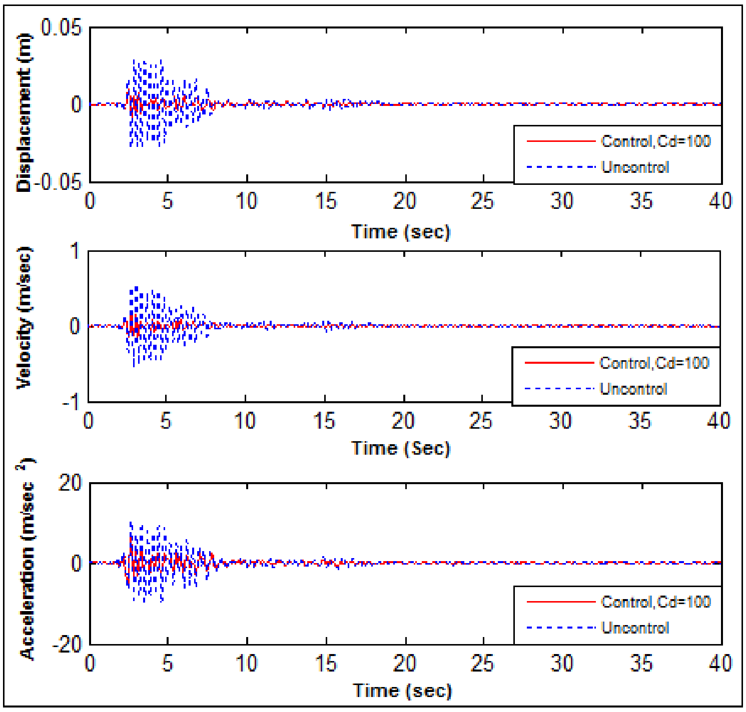

Figure 5.8: Time History Response at 1^{st} Storey under Lomaprieta EQ

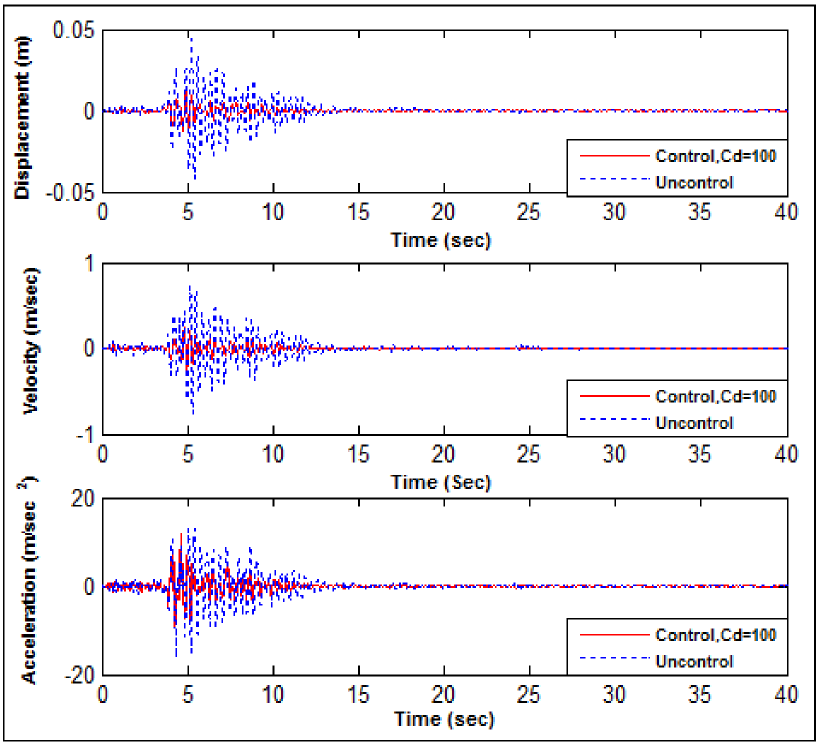

Figure 5.9: Time History Response at 1^{st} Storey under Northridge EQ

From results and graphs, it is evident that for controlled building maximum displacement reduce by of 70.23 % under the Northridge earthquake, maximum velocity reduce by 72.60 % under the Loma Prieta earthquake, maximum acceleration reduce by 69.3 % under the El Centro earthquake at 1^{st} storey level. From time history of above four earthquake excitations, it have been observed that viscous devices are equally effective under different types, i.e., strong motion and pulse type earthquake excitations.

5.2.6 Comparison of Damper Force

Table 5.17 shows the maximum damper force due to different earthquake excitation for damping co-efficient 'C_d' value 10 $kN \cdot sec/cm$ to 100 $kN \cdot sec/cm$. The graphical representation for comparison of maximum damper force with roof displacement, roof velocity, and roof acceleration for viscous damper added building under the El Centro, Kobe, Loma Prieta and Northridge earthquake excitations are presented in Figure 5.11 to **??** respectively.

Table 5.17: Maximum Viscous Damper Force under Four EQ Excitation

Cd	Maximum Damper Force at 1^{st} Storey (kN)			
$kN \cdot sec/cm$	El Centro	Kobe	Loma Prieta	Northridge
10	167.06	399.72	437.37	637.36
20	288.90	645.86	730.24	1086.65
30	377.86	806.19	951.89	1411.69
40	442.98	918.71	1114.52	1679.84
50	491.12	1002.00	1232.68	1881.08
60	552.00	1062.57	1318.95	2034.98
70	603.84	1147.30	1382.43	2155.77
80	646.73	1250.69	1430.51	2253.37
90	682.26	1338.86	1466.40	2334.56
100	711.80	1414.06	1514.63	2403.91

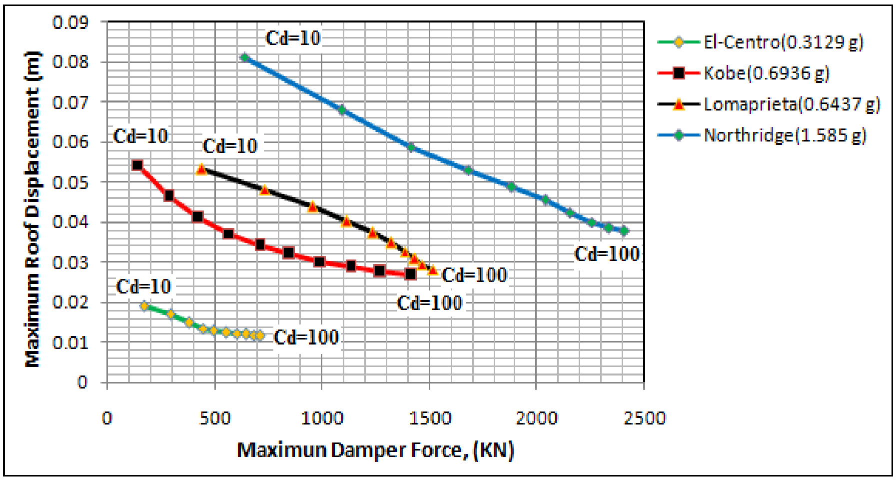

Figure 5.10: Comparison of Max. Roof Displacement with Max. Damper Force

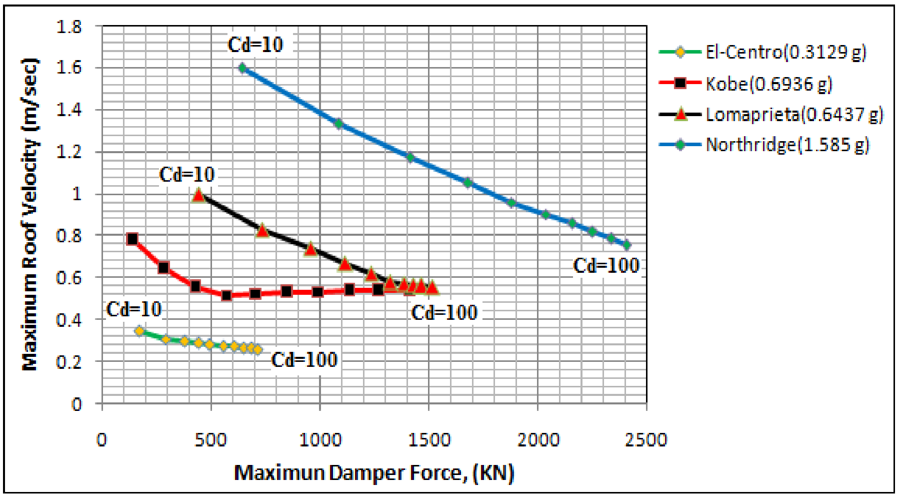

Figure 5.11: Comparison of Max. Roof Velocity with Max. Damper Force

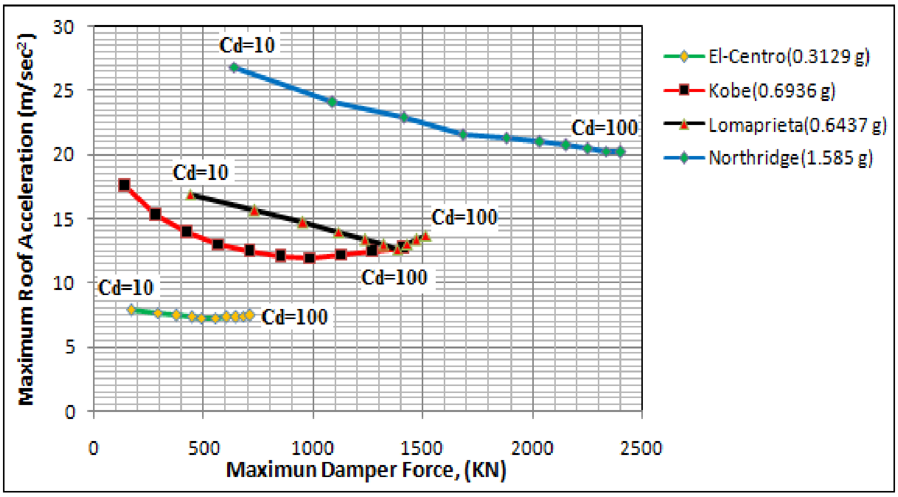

Figure 5.12: Comparison of Max. Roof Acceleration with Max. Damper Force

From graphical results, it can be said that as damping co-efficient increases for controlled structure maximum roof displacement, velocity and acceleration are decreases and maximum damper forces are increases for all types of earthquake. Damper damping co-efficient up to 60 $kN \cdot sec/cm$, is most effective for reduction of controlled building displacement, velocity and acceleration. It can be observed that, for damping co-efficient 'C_d' value between 60 to 100 $kN \cdot sec/cm$, shows very less reduction of response quantities as compare to 'C_d' value up to 60 $kN \cdot sec/cm$ for El Centro, Loma Prieta and Northridge earthquake respectively.

5.3 Summary

This chapter deals with the response of the three storey shear building using viscous damper by numerical method like Newmark-Beta for four different types of earthquake excitations through MATLAB. Response quantities of uncontrolled building like relative displacement, relative velocity, and absolute acceleration are compared with the controlled building for different values of damping co-efficient. Maximum Damper force are compared with the maximum value of roof responses for different values of damping co-efficient. Results obtained has shown that viscous damper is quit effective to reduce the all response quantities about 50 % for damping co-efficient 'C_d' value 100 $kN \cdot sec/cm$.

Chapter 6

Response of Building using VE Damper

6.1 General

The chapter deals with the response of three storey shear building using viscoelastic damper. Numerical method Newmark-Beta is used to find out the response quantity of controlled structure. Algorithm of Newmark-Beta method given in Table 4.1, is used to find out the different response quantity through MATLAB. Viscoelastic damper is design for different values of required damping ratio. Results of different response quantities are given in subsequent sections.

6.2 Parametric Study

To understand the influence of Viscoelastic Damper (VE), a three storey shear building has been considered as given in section 4.2, which was converted into a lump mass model. From this lump mass model of building without damper, mass matrix, stiffness matrix and damping matrix is determined, which is given Appendix-A. For response of controlled building, a viscoelastic damper is connected as diagonally at the first storey as shown in Figure 5.1. Here the stiffness of braces is to be neglected to simplify calculation, and the equation of motion for building with VE damper under the earthquake excitation is considered as given equation 4.13. Design steps of viscoelastic damper is given in following section.

6.2.1 Viscoelastic Damper Design

Following design procedure illustrate the parameters like number, size and required properties of damper for any structure to achieve target structural response.

(1) The required damping in general can be determined from the response spectra of the design earthquake. Prior to design it is required to decide, desired damping ratio that should be achieved to reduce prescribed response level of building. In this study, the required structural damping ratio 'ζ' is assumed for the initial goal.

(2) The selection of VE damper stiffness 'K_d' and loss factor is a trial and error procedure. This is determine from the modal strain energy method as,

$$\alpha_d K_d = \frac{2\varsigma}{(\eta - 2\varsigma)} K_s \tag{6.1}$$

Where, υ is the target added damping ratio; α_d is the attachment coefficient; η is the loss factor; and K_s is the storey stiffness of structure without damper.

(3) The thickness of VE material 't' can be determined based on the maximum allowable damper deformation to ensure that the maximum strain in the viscoelastic material is smaller than the maximum allowable value. Thickness of VE material can be determine as,

$$t = \frac{0.004 \cdot h_s \cdot Cos\theta}{\gamma_d} \tag{6.2}$$

Where, 't' is the thickness of one layer of VE material in the damper; 'h_s' is the typical storey height; 'γ_d' is the maximum design damper strain; 'θ' is the angel of inclination of VE device. In this study maximum design damper strain 'γ_d' of 60% allowed is assumed.

(4) The area of damper is determined from the following equation. Thus, damper size can be decided by assuming damper width and from the required length of damper.

$$A = \frac{K_d \cdot t}{G'} \tag{6.3}$$

Where, K_d is the damper stiffness; G' is the damper storage modulus; t is the thickness of one layer of VE material. The damping co-efficient 'C_d' of viscoelastic damper can be determine from following equation,

$$C_d = \frac{G'' \cdot A}{\omega t} \tag{6.4}$$

Where, G'' is the damper loss modulus; ω is the natural frequency of the structure.

(5) Properties of damper like Shear Modulus, Loss Factor can be decided as per the temperature for which damper is to be design. Maximum allowable strain in VE material will also change as per design temperature, to avoid the nonlinear behavior of VE material. In this study design temperature is assumed as 25^o C.

(6) The RC building can be analyzed now with added VE damper . We can find damping ratio achieved from the following equation.

$$\zeta = \frac{\eta}{2}(1 - \frac{\omega_d^2}{\omega_{dn}^2}) \tag{6.5}$$

Where, 'ω_d' and 'ω_{dn}' is the natural frequency and damped natural frequency of the system; 'η' is the loss factor.

For parametric study, different value of required damping ratio 'ζ' 12%, 14%, 16%, 18%, 20%, 22%, 24%, 26%, 28%, 30 are considered. VE damper is design for different value of 'ζ' as per above discussion, and find out the VE damper parameter like damper stiffness 'K_d', co-efficient of damper 'C_d', and size of damper, which is given in Table 6.1. Sample calculation of VE damper is given in Appendix-B. A three storey building with VE damper at first storey level is analyzed using Newmark-Beta Method for four different types of earthquake excitations as per Table 4.1 through MATLAB, and obtain the response quantity like relative displacement, relative velocity, absolute acceleration and damper force. Subsequent section deals with the results and discussion of VE damper equipped building with uncontrolled building.

Table 6.1: Viscoelastic Dampers Design Parameter

ζ	C_d	K_d	Damper Dimension		
(%)	(N Sec/m)	(N/m)	L(m)	B(m)	t(m)
12	1732345	25855250	0.4	0.25	0.016
14	2381974	35550969	0.55	0.25	0.016
16	2815061	42014781	0.65	0.25	0.016
18	3637925	54296025	0.7	0.3	0.016
20	4417480	65930888	0.85	0.3	0.016
22	4937183	73687463	0.95	0.3	0.016
24	5976590	89200613	1.15	0.3	0.016
26	6756146	100835475	1.3	0.3	0.016
28	7795553	116348625	1.5	0.3	0.016
30	9094812	135740063	1.5	0.35	0.016

6.3 Results and Discussion

This section presents the results obtained through Newmark-Beta direct integration method of three storey R.C. shear building with Viscoelastic damper for different value of required damping ratio. The response of shear building in the form of maximum displacement, maximum velocity, maximum acceleration, and maximum damper force is obtained. Efficiency of this damping systems is investigated for four earthquake excitations of different peak acceleration value. The uncontrolled building response was found out in order to compare its results with the results of the structures embedded with viscoelastic damper. There are various ways of assessing seismic response, but computation of top storey response are reasonable measure of the overall effects of seismic response. The reduction in the top storey displacement, velocity, acceleration, and damper resistance force are investigated.

6.3.1 Comparison of Displacement Response

The results of displacement response of uncontrolled and controlled shear building under the four earthquake excitations are presented in Table 6.2 to 6.5 respectively. From results, it is evident that displacement of top storey is highest, so comparison of displacement is done at top of the structure.

Table 6.2: Relative Displacement under El Centro (PGA-0.3129g) EQ Excitation

ζ	Maximum Storey Displacement (m)					
(%)	1^{st}	% Red.	2^{nd}	% Red.	Roof	% Red.
12	0.0071	32.19	0.0135	26.57	0.0164	27.88
14	0.0063	39.84	0.0124	32.84	0.0153	32.65
16	0.0058	44.39	0.0117	36.35	0.0149	34.54
18	0.0051	51.78	0.0110	40.21	0.0142	37.62
20	0.0045	57.32	0.0105	42.88	0.0138	39.48
22	0.0042	59.86	0.0102	44.42	0.0135	40.52
24	0.0038	63.82	0.0098	47.02	0.0131	42.27
26	0.0035	66.33	0.0095	48.33	0.0129	43.34
28	0.0032	69.21	0.0092	49.76	0.0126	44.52
30	0.0029	71.90	0.0090	51.22	0.0124	45.58
Uncontrolled	0.0105	0.00	0.0184	0.00	0.0228	0.00

Table 6.3: Relative Displacement under Kobe (PGA-0.6936g) EQ Excitation

ζ	Maximum Storey Displacement (m)					
(%)	1^{st}	% Red.	2^{nd}	% Red.	Roof	% Red.
12	0.0180	29.75	0.0350	22.95	0.0435	21.36
14	0.0155	39.84	0.0310	31.74	0.0388	29.79
16	0.0141	45.12	0.0290	36.29	0.0364	34.13
18	0.0121	52.95	0.0259	42.91	0.0329	40.42
20	0.0107	58.39	0.0239	47.50	0.0305	44.74
22	0.0099	61.32	0.0228	49.93	0.0293	47.00
24	0.0087	66.04	0.0210	53.72	0.0274	50.50
26	0.0080	68.86	0.0200	55.90	0.0263	52.48
28	0.0072	71.84	0.0190	58.19	0.0254	54.12
30	0.0065	74.79	0.0180	60.30	0.0252	54.34
Uncontrolled	0.0257	0.00	0.0455	0.00	0.0553	0.00

Table 6.4: Relative Displacement under Loma Prieta (PGA-0.6437g) EQ Excitation

ζ	Maximum Storey Displacement (m)					
(%)	1^{st}	% Red.	2^{nd}	% Red.	Roof	% Red.
12	0.01451	49.56	0.02689	47.21	0.03280	47.52
14	0.01316	54.25	0.02512	50.68	0.03087	50.61
16	0.01240	56.90	0.02415	52.59	0.02979	52.34
18	0.01118	61.14	0.02261	55.62	0.02807	55.08
20	0.01024	64.42	0.02142	57.95	0.02675	57.20
22	0.00969	66.30	0.02073	59.30	0.02601	58.39
24	0.00876	69.54	0.01957	61.58	0.02479	60.34
26	0.00817	71.58	0.01883	63.03	0.02401	61.58
28	0.00750	73.92	0.01802	64.64	0.02314	62.98
30	0.00680	76.36	0.01718	66.28	0.02222	64.45
Uncontrolled	0.02877	0.00	0.05094	0.00	0.06250	0.00

Table 6.5: Relative Displacement under Northridge (PGA-1.585g) EQ Excitation

ζ	Maximum Storey Displacement (m)					
(%)	1^{st}	% Red.	2^{nd}	% Red.	Roof	% Red.
12	0.0140	68.15	0.0267	65.95	0.0373	60.93
14	0.0126	71.27	0.0259	66.91	0.0367	61.54
16	0.0118	73.04	0.0255	67.49	0.0363	61.99
18	0.0106	75.87	0.0246	68.55	0.0355	62.83
20	0.0096	78.06	0.0242	69.08	0.0354	62.96
22	0.0091	79.31	0.0240	69.38	0.0352	63.09
24	0.0082	81.42	0.0235	69.97	0.0349	63.40
26	0.0076	82.75	0.0232	70.40	0.0347	63.66
28	0.0069	84.24	0.0230	70.67	0.0345	63.90
30	0.0063	85.76	0.0228	70.88	0.0346	63.80
Uncontrolled	0.0439	0.00	0.0784	0.00	0.0955	0.00

For controlled building with viscoelastic damper reduction of 27.88%, 21.36%, 47.52% and 60.93% in roof displacement is observed, when required damping ratio 'ζ' is 12% for El Centro, Kobe, Loma Prieta and Northridge earthquake excitation respectively, with respect to uncontrolled structure. When, required damping ratio 'ζ' is 30%, reduction is 45.58%, 54.34%, 64.45% and 63.80% in roof displacement is observed for El Centro, Kobe, Loma Prieta and Northridge earthquake excitations, respectively. It is observed that, top storey displacement in all four types of earthquake excitations are significantly reduces, when damping ratio 'ζ' is 30%. But, when 'ζ' is 12% displacement reduction is less under the El Centro and Kobe earthquake as compare to Loma Prieta and Northridge earthquakes. The graphical representa-

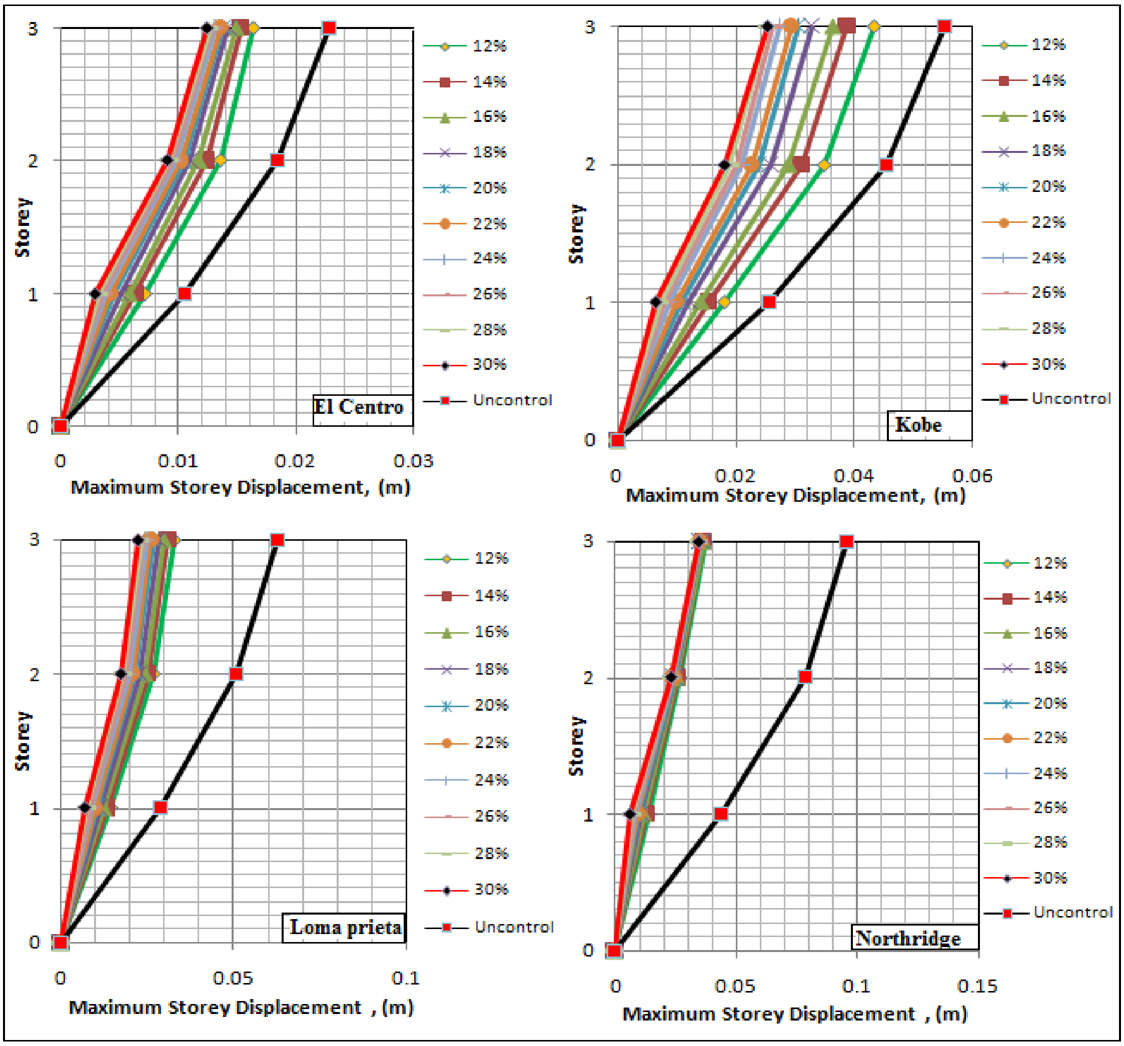

Figure 6.1: Comparison of Storey Displacement under Four EQ Excitation

tions of comparison of displacement response for uncontrolled and controlled building are presented in Figure 6.1. Figure clearly demonstrated that incorporation of the damper to the structure reduced maximum value of roof displacement under the all four earthquake excitations. On the other hand, the performance of the VE damper added structure obtained under different excitations varied significantly for different value of required damping ratio 'ζ'.

6.3.2 Comparison of Velocity Response

Results of the maximum storey velocity of building obtained under four earthquake excitation, namely El Centro, Kobe, Loma Prieta and Northridge are presented in Table 6.6 to 6.9 respectively, for different values of required damping ratio 'ζ'.

Table 6.6: Relative Velocity under El Centro (PGA-0.3129g) EQ Excitation

ζ	Maximum Storey Velocity (m/sec)					
(%)	1^{st}	% Red.	2^{nd}	% Red.	Roof	% Red.
12	0.1392	29.15	0.2603	20.29	0.3239	16.04
14	0.1253	36.26	0.2434	25.48	0.3081	20.14
16	0.1174	40.28	0.2354	27.93	0.2984	22.64
18	0.1048	46.69	0.2222	31.97	0.2888	25.14
20	0.0951	51.60	0.2135	34.64	0.2864	25.75
22	0.0896	54.40	0.2090	36.01	0.2863	25.78
24	0.0804	59.08	0.2013	38.38	0.2909	24.60
26	0.0749	61.88	0.1981	39.35	0.2939	23.81
28	0.0687	65.05	0.1947	40.37	0.2970	23.02
30	0.0623	68.32	0.1947	40.38	0.3005	22.12
Uncontrolled	0.1965	0.00	0.3266	0.00	0.3858	0.00

Table 6.7: Relative Velocity under Kobe (PGA-0.6936g) EQ Excitation

ζ	Maximum Storey Velocity (m/sec)					
(%)	1^{st}	% Red.	2^{nd}	% Red.	Roof	% Red.
12	0.273	35.26	0.490	29.16	0.599	24.37
14	0.230	45.62	0.457	33.93	0.582	26.47
16	0.208	50.79	0.446	35.60	0.572	27.79
18	0.183	56.70	0.431	37.80	0.563	28.98
20	0.168	60.16	0.422	39.01	0.558	29.55
22	0.160	62.12	0.418	39.63	0.556	29.76
24	0.146	65.41	0.412	40.50	0.555	29.88
26	0.137	67.47	0.409	40.93	0.556	29.78
28	0.127	69.81	0.406	41.29	0.560	29.32
30	0.117	72.24	0.406	41.29	0.568	28.26
Uncontrolled	0.422	0.00	0.692	0.00	0.792	0.00

Table 6.8: Relative Velocity under Lomaprieta (PGA-0.6437g) EQ Excitation

ζ	Maximum Storey Velocity (m/sec)					
(%)	1^{st}	% Red.	2^{nd}	% Red.	Roof	% Red.
12	0.169	69.43	0.316	68.66	0.383	69.39
14	0.148	73.31	0.283	71.88	0.345	72.40
16	0.136	75.41	0.266	73.62	0.325	73.99
18	0.118	78.64	0.239	76.26	0.295	76.42
20	0.105	81.02	0.220	78.15	0.273	78.19
22	0.098	82.33	0.210	79.19	0.261	79.15
24	0.086	84.48	0.193	80.85	0.241	80.70
26	0.079	85.77	0.183	81.83	0.230	81.60
28	0.071	87.19	0.172	82.89	0.218	82.57
30	0.063	88.61	0.162	83.91	0.206	83.49
Uncontrolled	0.553	0.00	1.007	0.00	1.251	0.00

Table 6.9: Relative Velocity under under Northridge (PGA-1.585g) EQ Excitation

ζ	Maximum Storey Velocity (m/sec)					
(%)	1^{st}	% Red.	2^{nd}	% Red.	Roof	% Red.
12	0.341	55.67	0.701	53.50	0.889	53.34
14	0.310	59.70	0.684	54.64	0.860	54.85
16	0.292	62.05	0.673	55.38	0.842	55.81
18	0.270	64.88	0.656	56.52	0.812	57.35
20	0.252	67.27	0.650	56.88	0.804	57.77
22	0.241	68.72	0.646	57.14	0.819	57.01
24	0.221	71.31	0.639	57.65	0.842	55.78
26	0.208	73.02	0.633	58.02	0.856	55.05
28	0.192	75.04	0.626	58.48	0.871	54.27
30	0.176	77.21	0.618	59.01	0.885	53.51
Uncontrolled	0.770	0.00	1.508	0.00	1.904	0.00

From results, it is evident that velocity of top storey is highest, so comparison of velocity is done at top of the structure. For controlled building with VE damper reduction of 16.04%, 24.37%, 69.39% and 53.34% in roof velocity is observed, when required damping ratio 'ζ' is 12% for El Centro, Kobe, Loma Prieta and Northridge earthquake excitation respectively, with respect to uncontrolled structure. When, required damping ratio 'ζ' is 30%, reduction of 22.12%, 28.26%, 83.49% and 53.51% in roof velocity is observed for El Centro, Kobe, Loma Prieta and Northridge earthquakes respectively. From results, it evident that for El Centro and Kobe earthquake, less reduction of roof velocity is observed as compare to Loma Prieta and Northridge earthquake excitations for all values of required damping ratio 'ζ'. Figure 6.2 illus-

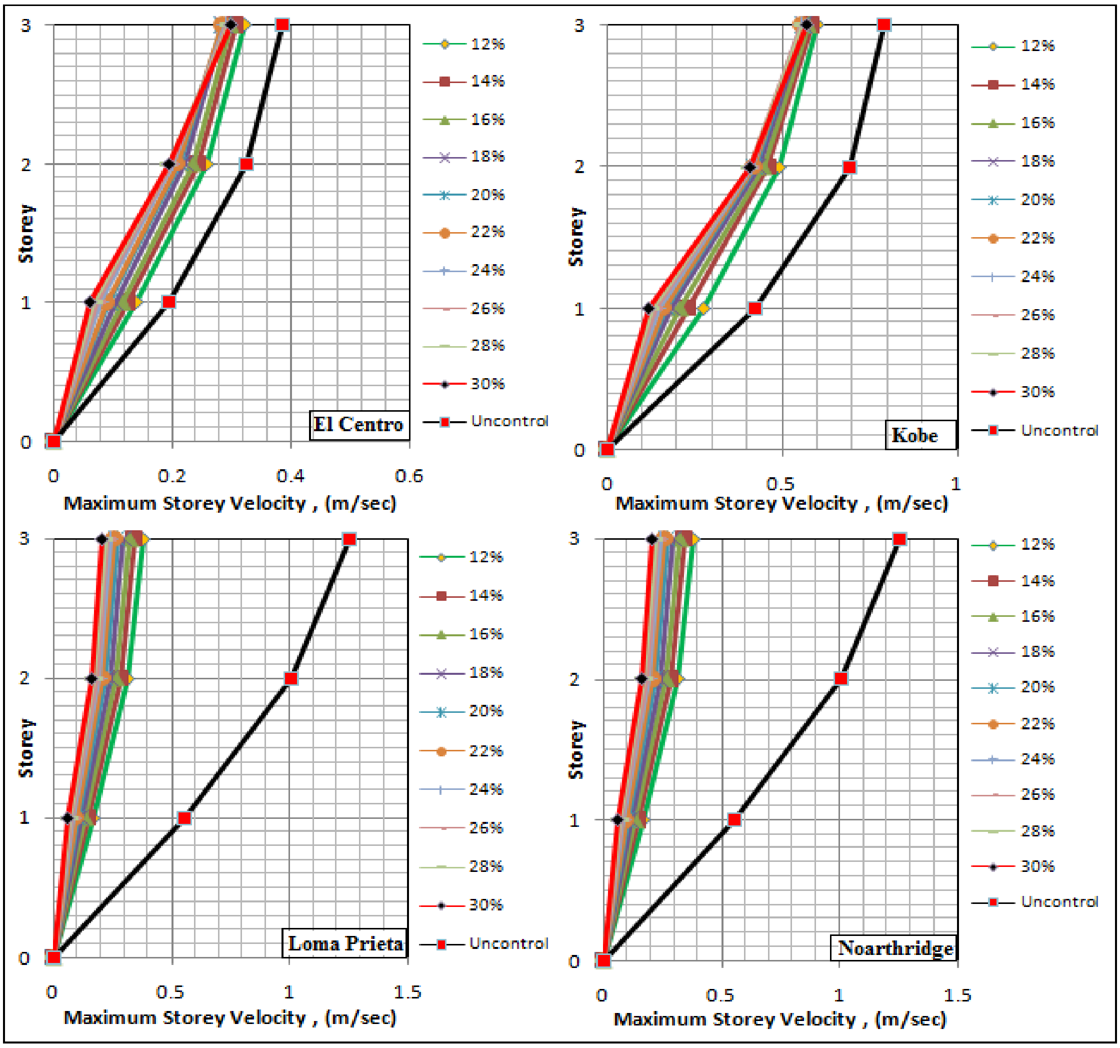

Figure 6.2: Comparison of Storey Velocity under Four EQ Excitation

trates the comparison of maximum storey velocity at each storey of uncontrolled and controlled building under four earthquake excitations. From Figure 6.2, it is observed that maximum storey velocity at all storey are significantly reduces in controlled building under the Loma Prieta and Northridge earthquakes as compare to El Centro and Kobe earthquakes for 12% damping ratio 'ζ'.

6.3.3 Comparison of Acceleration Response

Results of maximum storey acceleration of uncontrolled and controlled shear building for different value of damping ratio under the four earthquake excitations of different peak acceleration value are presented in Table 6.10 to 6.13.

Table 6.10: Absolute Acceleration under under El Centro (PGA-0.3129g) EQ Excitation

ζ	Maximum Storey Acceleration (m/sec^2)					
(%)	1^{st}	% Red.	2^{nd}	% Red.	Roof	% Red.
12	4.200	23.31	5.425	23.66	6.472	22.79
14	4.008	26.80	5.249	26.15	6.476	22.74
16	3.950	27.86	5.105	28.17	6.476	22.74
18	3.837	29.93	4.883	31.29	6.477	22.72
20	3.727	31.94	4.712	33.70	6.481	22.68
22	3.654	33.28	4.605	35.21	6.485	22.63
24	3.589	34.47	4.527	36.30	6.553	21.82
26	3.554	35.09	4.494	36.77	6.611	21.13
28	3.502	36.05	4.483	36.92	6.682	20.28
30	3.433	37.31	4.525	36.33	6.761	19.34
Uncontrolled	5.476	0.00	7.107	0.00	8.382	0.00

Table 6.11: Absolute Acceleration under Kobe (PGA-0.6936g) EQ Excitation

ζ	Maximum Storey Acceleration (m/sec^2)					
(%)	1^{st}	% Red.	2^{nd}	% Red.	Roof	% Red.
12	8.902	19.37	12.708	27.09	15.236	14.51
14	8.423	23.70	11.750	32.59	14.043	21.21
16	8.158	26.11	11.246	35.48	13.457	24.50
18	7.749	29.82	10.511	39.70	12.630	29.14
20	7.464	32.40	10.007	42.59	12.221	31.43
22	7.339	33.53	9.745	44.09	12.334	30.80
24	7.141	35.32	9.345	46.39	12.579	29.42
26	7.026	36.36	9.123	47.66	12.770	28.35
28	6.906	37.45	8.956	48.62	13.025	26.92
30	6.793	38.47	9.053	48.06	13.335	25.18
Uncontrolled	11.040	0.00	17.430	0.00	17.823	0.00

Table 6.12: Absolute Acceleration under Lomaprieta (PGA-0.6437g) EQ Excitation

ζ	Maximum Storey Acceleration (m/sec^2)					
(%)	1^{st}	% Red.	2^{nd}	% Red.	Roof	% Red.
12	7.786	24.26	9.472	43.58	10.787	48.92
14	7.629	25.78	9.194	45.25	10.472	50.42
16	7.544	26.61	9.049	46.11	10.296	51.25
18	7.410	27.91	8.827	47.43	10.021	52.55
20	7.308	28.90	8.661	48.42	9.850	53.36
22	7.250	29.46	8.568	48.97	9.757	53.80
24	7.153	30.41	8.424	49.83	9.599	54.55
26	7.092	31.01	8.335	50.36	9.499	55.02
28	7.023	31.68	8.234	50.96	9.384	55.57
30	6.952	32.37	8.139	51.52	9.266	56.12
Uncontrolled	10.279	0.00	16.791	0.00	21.119	0.00

Table 6.13: Absolute Acceleration under Northridge (PGA-1.585g) EQ Excitation

ζ	Maximum Storey Acceleration (m/sec^2)					
(%)	1^{st}	% Red.	2^{nd}	% Red.	Roof	% Red.
12	8.368	48.72	10.489	58.73	19.486	37.80
14	8.025	50.82	10.262	59.63	19.454	37.91
16	7.856	51.86	10.144	60.09	19.563	37.56
18	7.899	51.59	10.496	58.71	20.001	36.16
20	8.815	45.98	11.050	56.53	20.249	35.37
22	9.315	42.92	11.352	55.34	20.357	35.02
24	10.112	38.03	11.846	53.40	20.487	34.61
26	11.047	32.30	12.475	50.92	21.103	32.64
28	11.479	29.65	12.879	49.33	21.462	31.50
30	10.572	35.22	12.144	52.22	20.727	33.84
Uncontrolled	16.318	0.00	25.418	0.00	31.330	0.00

For controlled building with viscoelastic damper reduction of 22.79%, 14.51%, 48.92% and 37.80% in roof acceleration is observed, when required damping ratio 'ζ' is 12% for El Centro, Kobe, Loma Prieta and Northridge earthquake excitations, respectively, with respect to uncontrolled structure. When, required damping ratio 'ζ' is 30%, reduction od 19.34%, 25.18%, 56.12% and 33.84% in roof acceleration is observed for El Centro, Kobe, Loma Prieta and Northridge earthquake excitation respectively. It is observed that, top storey displacement in all four types of earthquake excitations produced significant reductions when damping ratio 'ζ' is 30%. But, when 'ζ' is 12% reduction in acceleration response is more under the El Centro and Northridge earthquake as compare to Kobe and Loma Prieta earthquakes. Figure 6.3

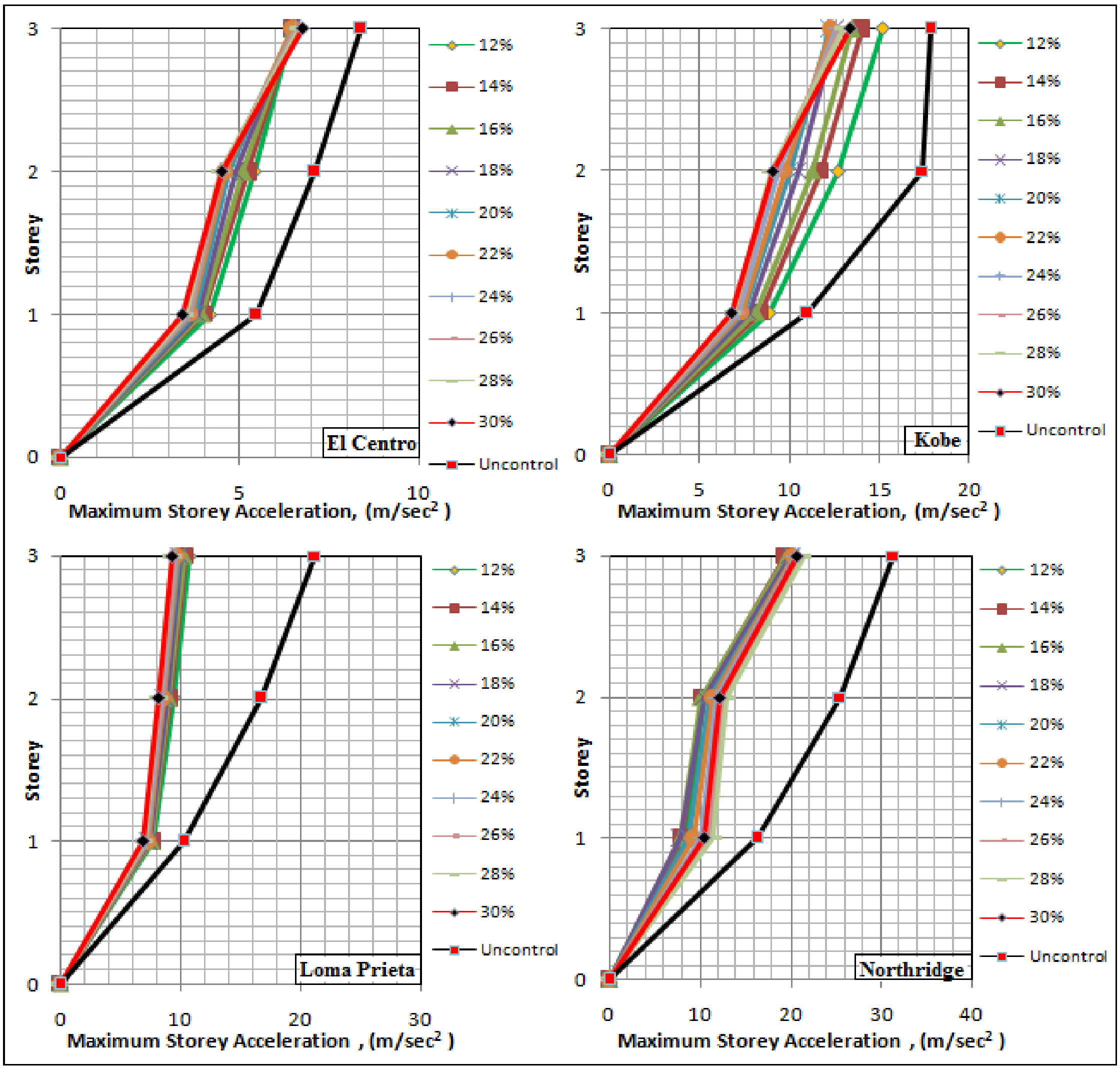

Figure 6.3: Comparison of Storey Acceleration under Four EQ Excitation

illustrates the comparison of maximum storey acceleration at each storey of uncontrolled and controlled building under four earthquake excitations. From Figure 6.3, it is evident that maximum storey acceleration at all storey are significantly reduces in controlled building under all the earthquake excitations for 12% damping ratio 'ζ'. When damping ratio 'ζ' is 14% to 30%, less reduction is observed.

6.3.4 Comparison of Inter Storey Drift

The results of maximum inter storey drift of uncontrolled and controlled building for four earthquake excitation of different peak acceleration value, namely El Centro, Kobe, Loma Prieta and Northridge are given in Table 6.14 to 6.16 respectively.

Table 6.14: Inter Storey Drift at First Storey

ζ	Inter Storey Drift at 1^{st} Storey							
(%)	El Cen.	% Red.	Kobe	% Red.	Lomapri.	% Red.	Northridge	% Red.
12	0.00711	32.26	0.01805	41.50	0.01451	49.56	0.01399	68.15
14	0.00631	39.90	0.01545	49.90	0.01316	54.25	0.01262	71.27
16	0.00583	44.44	0.01410	54.30	0.01240	56.90	0.01184	73.04
18	0.00506	51.82	0.01209	60.82	0.01118	61.14	0.01060	75.87
20	0.00448	57.36	0.01069	65.35	0.01024	64.42	0.00964	78.06
22	0.00421	59.89	0.00994	67.79	0.00969	66.30	0.00909	79.31
24	0.00380	63.85	0.00872	71.72	0.00876	69.54	0.00816	81.42
26	0.00353	66.37	0.00800	74.07	0.00817	71.58	0.00758	82.75
28	0.00323	69.24	0.00723	76.55	0.00750	73.92	0.00692	84.24
30	0.00295	71.92	0.00648	79.00	0.00680	76.36	0.00626	85.76
Uncont.	0.01050	0.00	0.03085	0.00	0.02877	0.00	0.04393	0.00

Table 6.15: Inter Storey Drift at Second Storey

ζ	Inter Storey Drift at 2^{nd} Storey							
(%)	El Cen.	% Red.	Kobe	% Red.	Lomapri.	% Red.	Northridge	% Red.
12	0.00655	21.10	0.01699	28.55	0.01247	46.15	0.01534	55.42
14	0.00648	21.89	0.01568	34.05	0.01208	47.83	0.01540	55.25
16	0.00644	22.39	0.01500	36.90	0.01188	48.70	0.01541	55.24
18	0.00641	22.76	0.01403	40.98	0.01160	49.92	0.01566	54.51
20	0.00642	22.70	0.01338	43.71	0.01138	50.85	0.01586	53.92
22	0.00642	22.66	0.01305	45.11	0.01126	51.37	0.01596	53.63
24	0.00643	22.56	0.01256	47.18	0.01106	52.24	0.01631	52.62
26	0.00643	22.48	0.01270	46.60	0.01096	52.69	0.01657	51.87
28	0.00644	22.37	0.01289	45.77	0.01084	53.21	0.01685	51.05
30	0.00650	21.66	0.01317	44.59	0.01071	53.75	0.01713	50.24
Uncont.	0.00830	0.00	0.02377	0.00	0.02316	0.00	0.03442	0.00

Table 6.16: Inter Storey Drift at Roof

ζ	Inter Storey Drift at Roof							
(%)	El Cen.	% Red.	Kobe	% Red.	Lomapri.	% Red.	Northridge	% Red.
12	0.00353	24.90	0.00845	28.43	0.00595	49.01	0.01066	37.66
14	0.00349	25.68	0.00779	34.05	0.00575	50.66	0.01078	36.98
16	0.00349	25.72	0.00745	36.88	0.00567	51.41	0.01081	36.84
18	0.00351	25.26	0.00699	40.83	0.00553	52.60	0.01090	36.27
20	0.00353	24.87	0.00669	43.36	0.00542	53.51	0.01113	34.93
22	0.00354	24.62	0.00670	43.20	0.00536	54.03	0.01124	34.27
24	0.00357	24.14	0.00684	42.05	0.00528	54.74	0.01141	33.32
26	0.00358	23.78	0.00695	41.09	0.00523	55.16	0.01149	32.83
28	0.00361	23.27	0.00710	39.84	0.00517	55.64	0.01157	32.37
30	0.00366	22.09	0.00728	38.32	0.00511	56.14	0.01174	31.38
Uncont.	0.00470	0.00	0.01180	0.00	0.01166	0.00	0.01711	0.00

From results, it is evident that inter storey drift is maximum at 1^{st} storey level, so comparison of inter storey drift is done at level of 1^{st} storey of the building. It is clear from results that inter storey drift is constantly decreased by attaching viscoelastic damper to structure as increasing the value of damping ratio 'ζ' from 12% to 30%, respectively at first storey. For controlled building with viscoelastic damper, reduction of 32.26%, 41.56%, 49.56% and 68.15% in inter storey drift is observed, when required damping ratio'ζ' is 12% for El Centro, Kobe, Loma Prieta and Northridge earthquake excitation respectively, with respect to uncontrolled structure. When required damping ratio 'ζ' is equal to 30%, reduction of 71.92%, 79.92%, 76.36% and 85.76% in storey drift is observed at 1^{st} storey for El Centro, Kobe, Loma Prieta and Northridge earthquake excitations respectively.

The graphical representations of comparison of inter storey drift for uncontrolled and controlled structure are presented in Figure 6.4. It is observed that inter storey drift at 1^{st} storey for all earthquake excitations are reduces as required damping ratio 'ζ' increases from 12% to 30%. At 2^{nd} storey, inter storey drift reduction variation is less for El Centro, Loma Prieta, and Northridge earthquake as compare to Kobe earthquake excitations as required damping ratio 'ζ' increases from 12% to 30%.

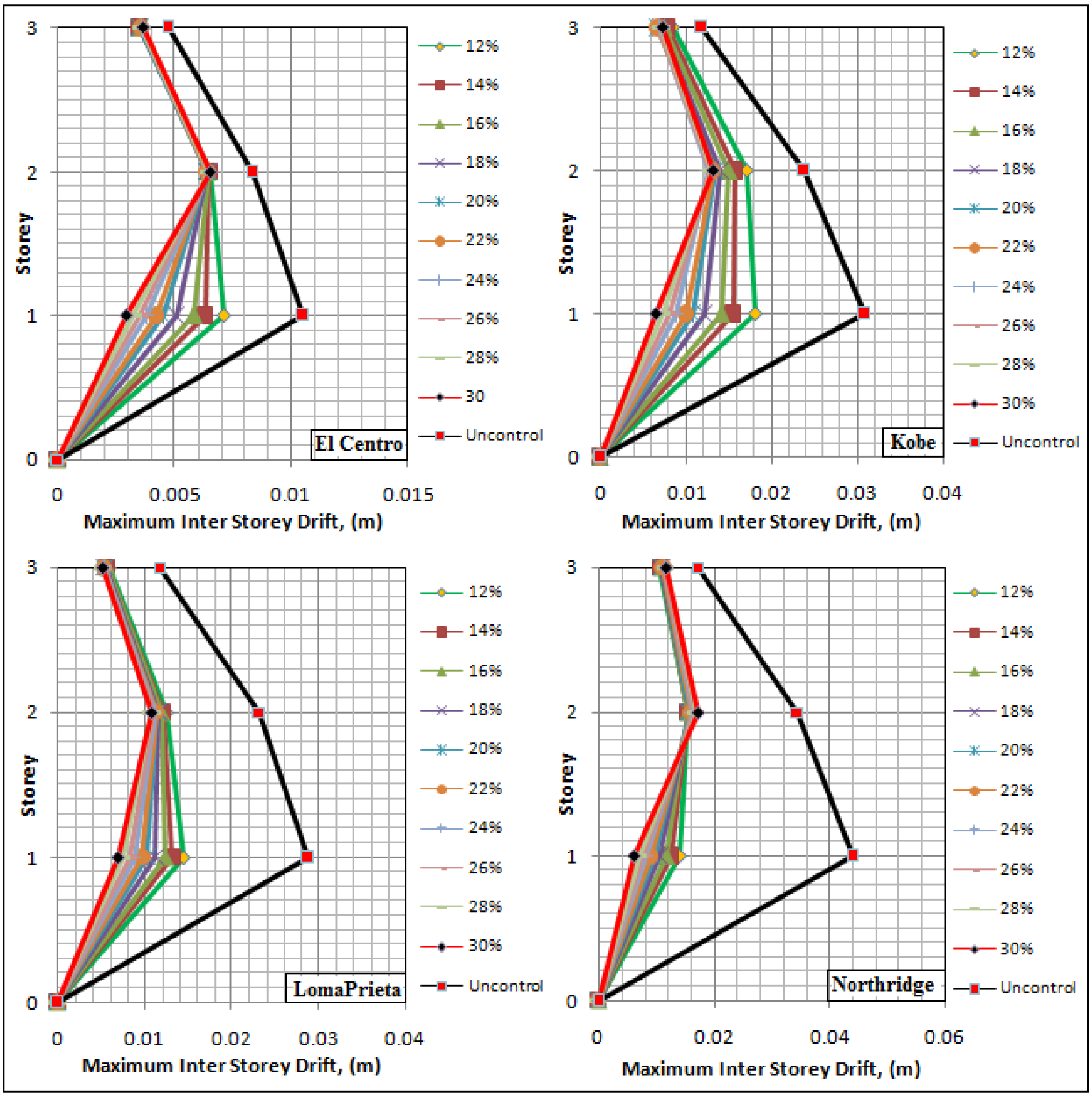

Figure 6.4: Comparison of Inter Storey Drift under Four EQ Excitation

At 3^{rd} storey, inter storey drift reduction variation is more for Kobe, Loma Prieta, and Northridge earthquake as compare to El Centro earthquake excitations as required damping ratio 'ζ' increases from 12% to 30%.

6.3.5 Comparison of Time History

Figure 6.5 to 6.8 represents displacement, velocity and acceleration time history in horizontal direction of uncontrolled (for 5% inherent damping ratio) and controlled (for 'ζ'=30%) building for El Centro, Kobe, Loma Prieta and Northridge earthquake excitations, respectively. There is maximum response reduction is achieved when damping required damping ratio 'ζ' is 30% in most of response quantity. Therefore all the response quantity of viscoelastic damper added structure is compared to uncontrolled structure for 'ζ' is equal to 30%. Figure 6.5 to 6.8 shows the responses of building at the 1^{st} level under El Centro, Kobe, Loma Prieta and Northridge earthquake excitation.

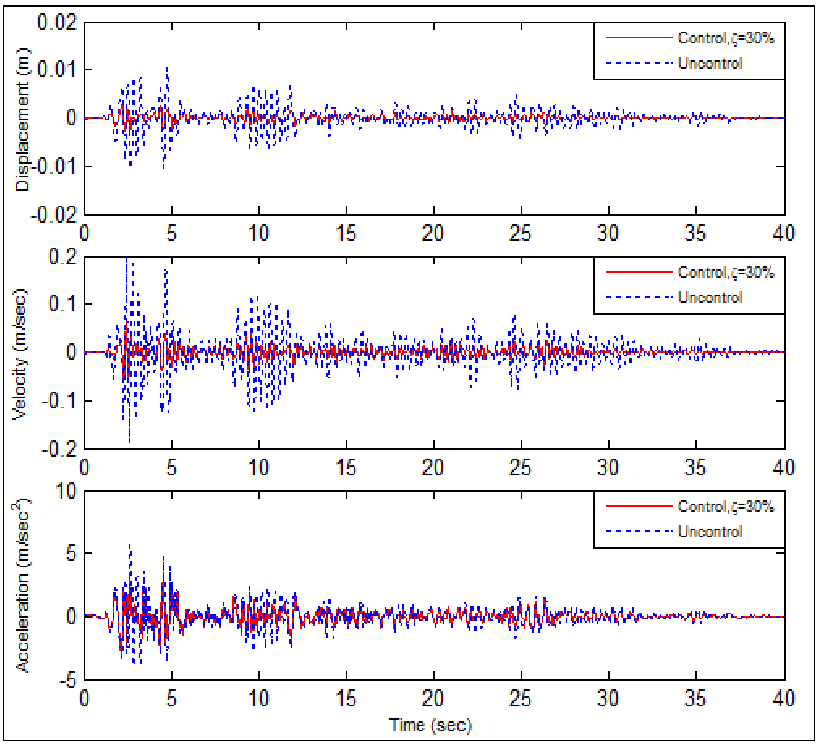

Figure 6.5: Time History Response at 1^{st} Storey under El Centro EQ

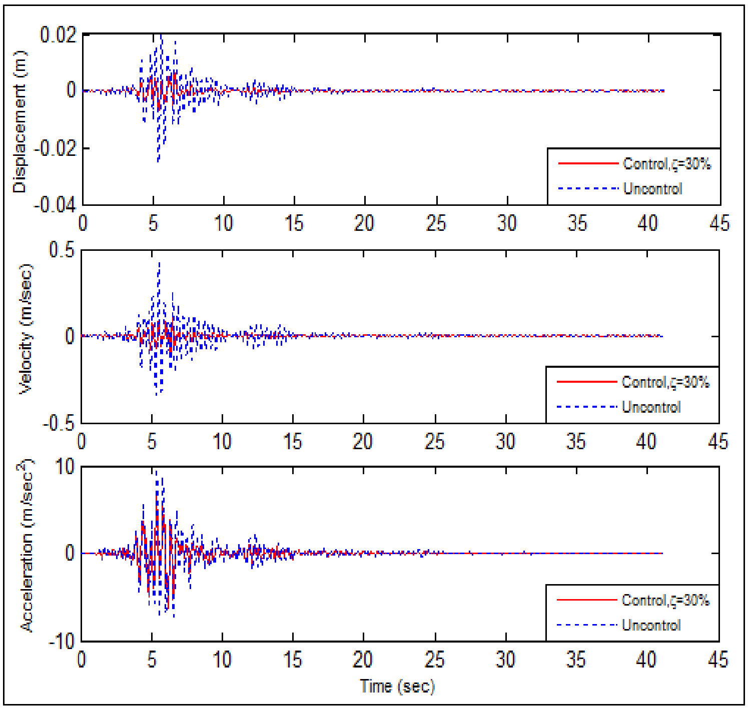

Figure 6.6: Time History Response at 1st Storey under Kobe EQ

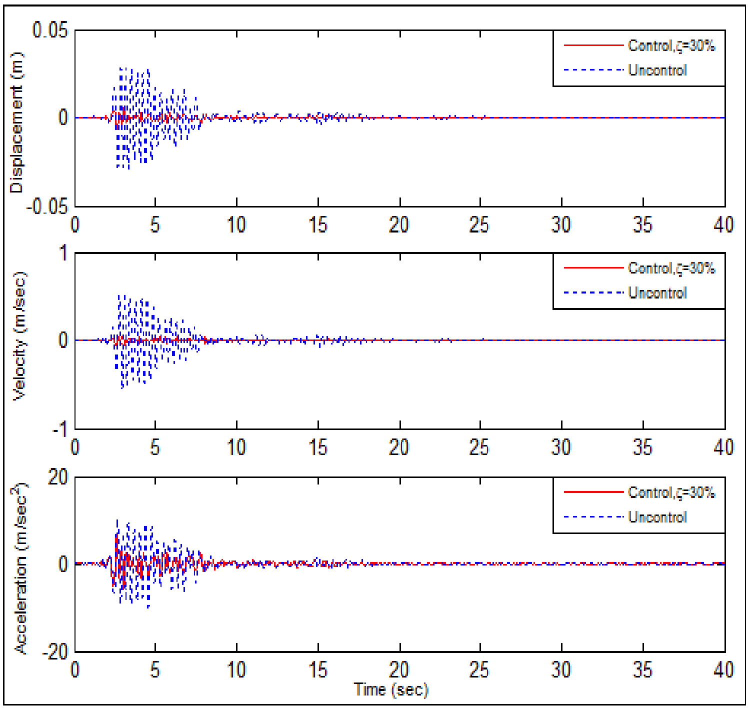

Figure 6.7: Time History Response at 1st Storey under Lomaprieta EQ

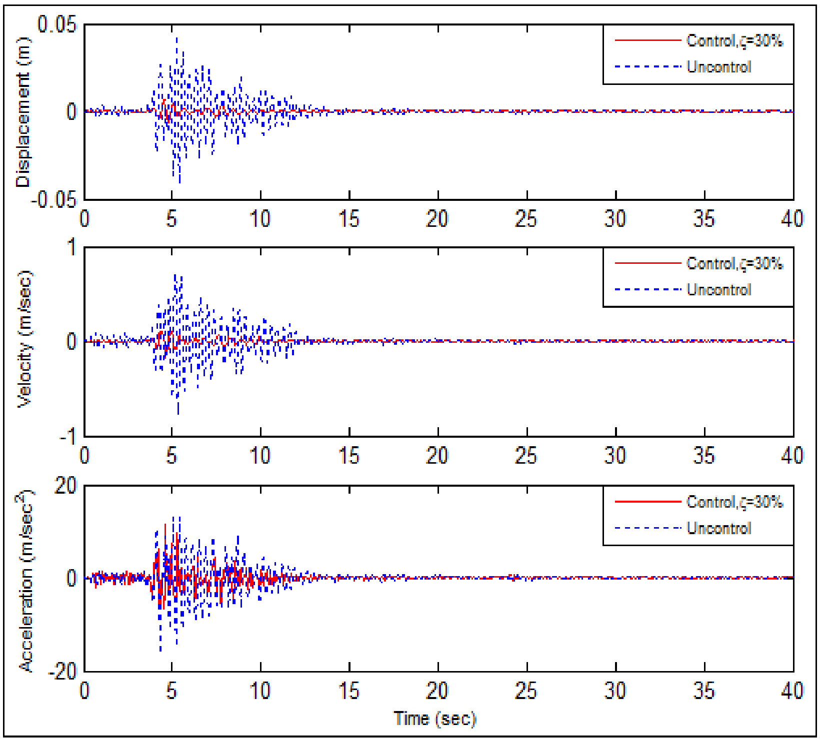

Figure 6.8: Time History Response at 1^{st} Storey under Northridge EQ

Figure 6.5 to 6.8 illustrates the comparison of time history response of building equipped with viscoelastic damper with uncontrolled building at the 1^{st} storey for four different earthquake excitations. From this time history plots, it is evident that, in all the earthquake excitations, significantly reduced to storey displacement, velocity, and acceleration through out the duration of strong motion. From this time history, it can be seen that maximum value of 1^{st} storey displacement and velocity reduction is more than half, on the other hand 1^{st} storey acceleration is less than half under all four earthquake excitations.

6.3.6 Comparison of damper Force

Table 6.17 illustrated the maximum damper force due to different earthquake excitation for damping ratio 'ζ' is equal to 30%. From results it is evident that as 'ζ' increases, damper stiffness 'K_d', co-efficient of damper 'C_d' and damper resistance force also increases.

Table 6.17: Maximum Viscoelastic Damper Force under Four EQ Excitation

ζ	C_d	K_d	Maximum Damper Force at 1st Storey (kN)			
(%)	(N Sec/m)	N/m	El Centro	Kobe	lomaprieta	Northridge
12	1732345	25855250	314.98	661.26	461.05	564.62
14	2381974	35550969	351.83	771.87	572.91	723.42
16	2815061	42014781	383.83	827.44	636.73	819.05
18	3637925	54296025	440.97	907.53	740.04	981.54
20	4417480	65930888	489.88	974.77	821.12	1115.37
22	4937183	73687463	518.40	1030.52	868.07	1195.12
24	5976590	89200613	567.86	1128.90	948.54	1334.93
26	6756146	100835475	599.67	1193.56	999.45	1424.87
28	7795553	116348625	636.61	1270.28	1057.53	1528.18
30	9094812	135740063	675.86	1357.08	1117.84	1641.07

Graphical representation of comparison of maximum damper force with roof displacement, roof velocity, and roof acceleration for viscoelastic damper added building under the El Centro, Kobe, Loma Prieta and Northridge earthquake excitations are presented in Figure 6.9 to 6.11 respectively. From Figure 6.9 to 6.11, it is observed

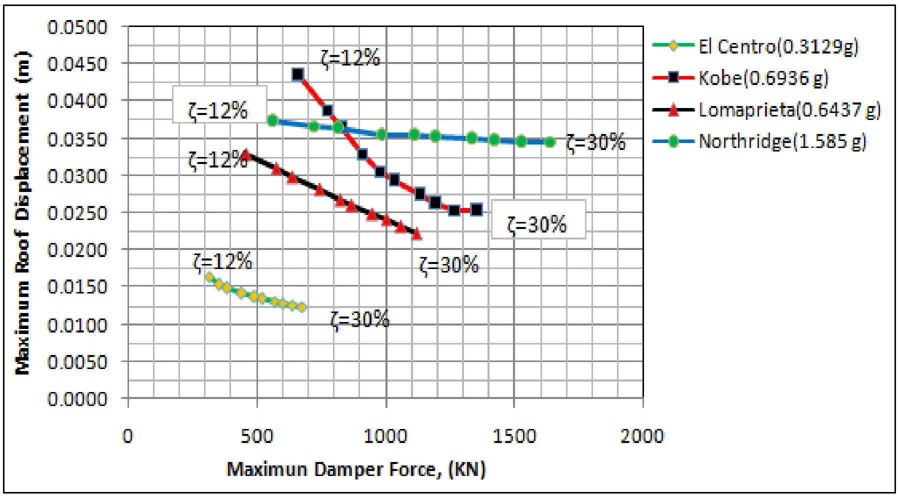

Figure 6.9: Comparison of Max. Roof Displacement with Max. Damper Force

that, as required damping ratio 'ζ' increases damper force also increases for all earthquake excitations. Figure6.9 shows the maximum roof displacement are significantly reduces for El Centro, Kobe, and Loma Prieta earthquake as compare to Northridge earthquake, as required damping ratio 'ζ' increases. Figure 6.10 shows the maximum roof velocity are significantly reduces for Kobe earthquake, as compare to El Centro, Loma Prieta, and Northridge earthquake, as required damping ratio 'ζ' increases.

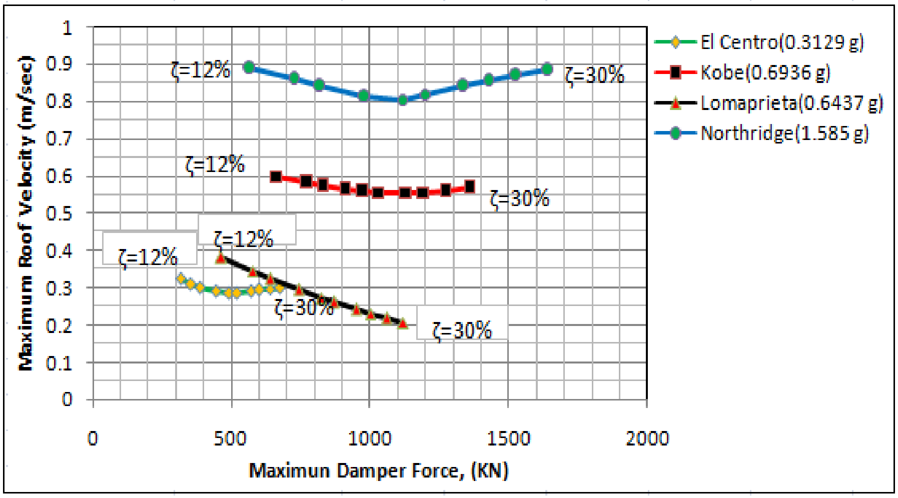

Figure 6.10: Comparison of Max. Roof Velocity with Max. Damper Force

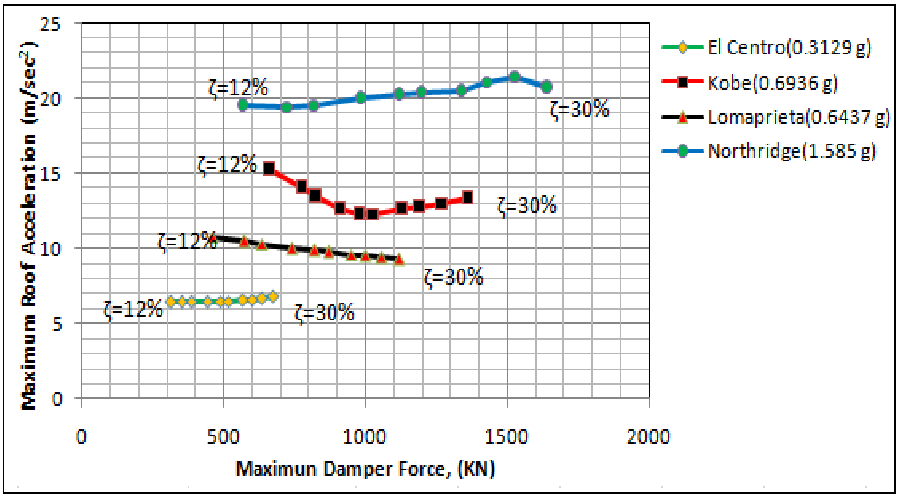

Figure 6.11: Comparison of Max. Roof Acceleration with Max. Damper Force

Figure 6.11 shows the maximum roof acceleration reduction are less for El Centro earthquake as compare to other three earthquakes, as required damping ratio 'ζ' increases.

6.4 Summary

This chapter deals with the response of the three storey shear building using viscoelastic damper by numerical method Newmark-Beta for four types of earthquake excitations through MATLAB. Response quantities of uncontrolled building like relative displacement, relative velocity, and absolute acceleration are compared with the controlled building for different values of required damping ratio 'ζ'. For different value of 'ζ' viscoelastic damper was design, and damper stiffness, co-efficient of damper, and size of damper was determined. Maximum Damper force was compared with the maximum value of roof responses for different values required damping ratio 'ζ'. From the results, it can be depicted that viscoelastic damper is significantly effective to reduce the all response quantity above 50 % for required damping ratio 'ζ' is equal to 30%.

Chapter 7

Response of Building using Metallic Damper

7.1 General

The chapter deals with the response of three storey shear building using metallic yield damper. Numerical method Newmark-Beta is used to find out the response quantity of controlled structure. Algorithm of Newmark-Beta method given in Table 4.1, is used to find out the different response quantity through MATLAB. Results of different response quantities are given in subsequent sections.

7.2 Metallic Yield Damper Design Considerations

Even if the metallic yield damper acts as a structural member the design may need to be based on damper design procedures rather than usual methods for the design of strengthening elements. This is because the metallic yield damper will usually be designed to yield before the existing structure. There will be non-linearity at the design load level, whereas linear elastic behavior may be assumed for conventional design. In present study, Added Damping and Stiffness (ADAS) type of metallic yield damper is considered. Figure 7.1 represents a lump mass Model with a ADAS damper. For controlled building, an ADAS damper is connected at the first storey as shown in Figure 7.1. The equation of motion for three story shear building with ADAS damper under the earthquake excitation is considered as given in equation 4.14. To find out the response shear building, equation of motion under the different earthquake excitations are solved using Newmark-Beta method as given in Table4.1 through MATLAB.

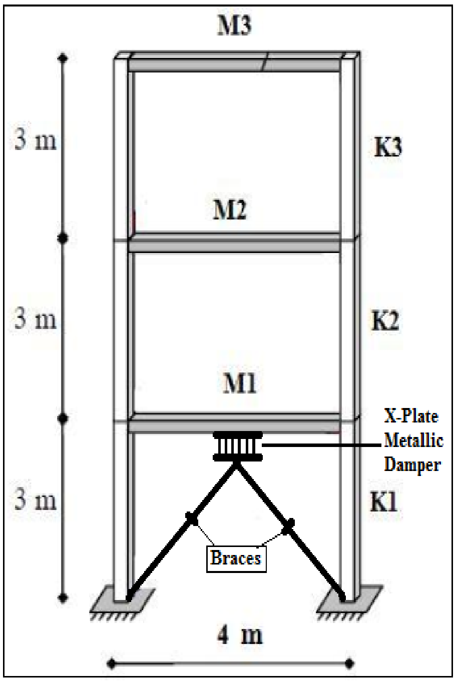

Figure 7.1: Shear building Lump Mass Model with ADAS Damper

Figure 3.24 shows, a simple bilinear hysteretic forcing model is used to identify the parameters involved in the design of a typical metallic yield damper.

Design parameters of ADAS damper are considered as follows,

1) SR represents the ratio of brace-damper stiffness 'Ka' to that of the corresponding bare structural stiffness 'Ks'. In present study, SR is equal to 2, B/D is equal to 2, and Δ_y is equal to 0.005 m are considered. Where B/D is the ratio of brace stiffness to damper stiffness and Δ_y is the yield displacement of damper respectively.

2) From the lump mass model of building, compute the lateral storey stiffness 'K_s' of the structure.

3) By using structure storey stiffness 'K_s' and Stiffness Ratio 'SR', It is possible to find out the brace assembly stiffness 'Ka' using Equation 3.12. So, the value of K_a is equal to 270000000 N/m, which is used in equation of motion to find out the Stiffness matrix due to addition of ADAS damper.

4) Equivalent viscous damping ratio 'β', calculated using Equation 3.18 is equal to 16.5 %, which is used to calculate the equivalent structural damping matrix due to inherent damping ratio (i,e., 5%) and viscous damping ratio (i,e,.16.5 %) provided by ADAS damper.

5) Damper yield force 'P_y' is calculated using Equation 3.13, which is 1800 kN.

7.3 Results and Discussion

This section deals with the response obtained through Newmark-Beta direct integration method of three storey R.C. shear building with added damping and stiffness (ADAS) damper for Stiffness Ratio 'SR' is equal to 2. The response of shear building in the form of relative displacement, relative velocity, absolute acceleration, and inter storey drift are obtained. Efficiency of this damping system is investigated for four earthquakes of different peak acceleration value. The uncontrolled building response is find out in order to compare response of the building embedded with ADAS damper. There are various ways of assessing seismic response, but computation of top storey response are reasonable measure of the overall effects of seismic response.

7.3.1 Comparison of Displacement Response

Table 7.1 to 7.4 are shows the response quantity of uncontrolled and controlled building under the El cento, Kobe, Loma Prieta, and Northridge earthquake respectively. From results, it is evident that displacement of top storey is highest, so comparison of displacement is done at top of the structure.

For controlled building with added damping and stiffness (ADAS) damper reduction of 50%, 58.6%, 67.5% and 66.9% in roof displacement is observed, when Stiffness Ratio 'SR' is equal to 2 for El Centro, Kobe, Loma Prieta and Northridge earthquake excitation respectively, with respect to uncontrolled structure. From results, it is evident that maximum 67.5 % reduction of displacement at roof is achieved under the Loma Prieta earthquake excitations for controlled building with ADAS damper.

Table 7.1: Relative Displacement under El Centro (PGA-0.3129g) EQ Excitation

SR	Maximum Storey Displacement (m)					
	1^{st}	% Red.	2^{nd}	% Red.	Roof	% Red.
2	0.00237	77.4	0.00805	56.3	0.01138	50.0
Uncontrolled	0.01049	0.0	0.01841	0.0	0.02276	0.0

Table 7.2: Relative Displacement under Kobe (PGA-0.6936g) EQ Excitation

SR	Maximum Storey Displacement (m)					
	1^{st}	% Red.	2^{nd}	% Red.	Roof	% Red.
2	0.00504	80.4	0.01653	63.6	0.02286	58.6
Uncontrolled	0.02569	0.0	0.04545	0.0	0.05527	0.0

Table 7.3: Relative Displacement under Lomaprieta (PGA-0.6437g) EQ Excitation

SR	Maximum Storey Displacement (m)					
	1^{st}	% Red.	2^{nd}	% Red.	Roof	% Red.
2	0.00496	82.7	0.01536	69.9	0.02029	67.5
Uncontrolled	0.02877	0.0	0.05094	0.0	0.06250	0.0

Table 7.4: Relative Displacement under Northridge (PGA-1.585g) EQ Excitation

SR	Maximum Storey Displacement (m)					
	1 st	% Red.	2 nd	% Red.	Roof	% Red.
2	0.00536	87.80	0.02148	72.58	0.03159	66.91
Uncontrolled	0.04393	0.0	0.07835	0.0	0.09546	0.0

7.3.2 Comparison of Velocity Response

Results of the maximum storey velocity of building obtained under four earthquake excitation, namely El Centro, Kobe, Loma Prieta and Northridge are presented in Table 7.5 to 7.8 respectively.

From results, controlled building with ADAS damper reduction of 28.7%, 35.3%, 84.7% and 57.8% in maximum roof velocity is observed, for El Centro, Kobe, Loma Prieta and Northridge earthquake excitation respectively, with respect to uncontrolled structure. From results it is observed that for El Centro and Kobe earthquake, less reduction of roof velocity is observed as compare to Loma Prieta and Northridge earthquake excitations.

Table 7.5: Relative Velocity under El Centro (PGA-0.3129g) EQ Excitation

SR	Maximum Storey Velocity (m/sec)					
	1^{st}	% Red.	2^{nd}	% Red.	Roof	% Red.
2	0.06718	65.8	0.1860	43.0	0.27488	28.7
Uncontrolled	0.19650	0.0	0.3266	0.0	0.38580	0.0

Table 7.6: Relative Velocity under Kobe (PGA-0.6936g) EQ Excitation

SR	Maximum Storey Velocity (m/sec)					
	1^{st}	% Red.	2^{nd}	% Red.	Roof	% Red.
2	0.09610	77.2	0.37216	46.24	0.51223	35.3
Uncontrolled	0.42210	0.0	0.69221	0.0	0.79216	0.0

Table 7.7: Relative Velocity under Lomaprieta (PGA-0.6437g) EQ Excitation

SR	Maximum Storey Velocity (m/sec)					
	1^{st}	% Red.	2^{nd}	% Red.	Roof	% Red.
2	0.04864	91.2	0.1459798	85.5	0.19082	84.7
Uncontrolled	0.55285	0.0	1.0072377	0.0	1.25053	0.0

Table 7.8: Relative Velocity under under Northridge (PGA-1.585g) EQ Excitation

SR	Maximum Storey Velocity (m/sec)					
	1^{st}	% Red.	2^{nd}	% Red.	Roof	% Red.
2	0.27525	64.3	0.59973	60.2	0.80400	57.8
Uncontrolled	0.77006	0.0	1.50825	0.0	1.90446	0.0

7.3.3 Comparison of Acceleration Response

Table 7.9 to 7.12 shows the maximum value of storey acceleration of building under the four earthquake excitation for uncontrolled and added damping and stiffness damper (ADAS) added structure.

For controlled building with ADAS damper reduction of 23.9%, 31.3%, 57.3% and 36.8% in roof acceleration is observed, when Stiffness Ratio 'SR' is equal to 2 for El Centro, Kobe, Loma Prieta and Northridge earthquake excitation respectively, with respect to uncontrolled structure. For Loma Prieta earthquake, significant roof acceleration reduction is achieved as compare to other earthquake. However, 4.2% acceleration increase at 1^{st} storey under the Northridge earthquake in controlled building with compare to uncontrolled building.

Table 7.9: Absolute Acceleration under El Centro (PGA-0.3129g) EQ Excitation

SR	Maximum Storey Acceleration (m/sec^2)					
	1^{st}	% Red.	2^{nd}	% Red.	Roof	% Red.
2	3.60290	34.2	4.2356	40.4	6.38211	23.9
Uncontrolled	5.47600	0.0	7.1070	0.0	8.38200	0.0

Table 7.10: Absolute Acceleration under Kobe (PGA-0.6936g) EQ Excitation

SR	Maximum Storey Acceleration (m/sec^2)					
	1^{st}	% Red.	2^{nd}	% Red.	Roof	% Red.
2	7.62109	31.0	8.97820	48.5	12.23872	31.3
Uncontrolled	11.04048	0.0	17.43023	0.0	17.82295	0.0

Table 7.11: Absolute Acceleration under Lomaprieta (PGA-0.6437g) EQ Excitation

SR	Maximum Storey Acceleration (m/sec^2)					
	1^{st}	% Red.	2^{nd}	% Red.	Roof	% Red.
2	6.72234	34.6	8.07954	51.9	9.02618	57.3
Uncontrolled	10.27897	0.0	16.79059	0.0	21.11921	0.0

Table 7.12: Absolute Acceleration under Northridge (PGA-1.585g) EQ Excitation

SR	Maximum Storey Acceleration (m/sec^2)					
	1^{st}	% Red.	2^{nd}	% Red.	Roof	% Red.
2	16.99849	4.2(%Inc.)	15.21016	40.2	19.79599	36.8
Uncontrolled	16.31813	0.0	25.41820	0.0	31.33038	0.0

7.3.4 Comparison of Inter Storey Drift

For the reason of effective damage control and safety measure of the structures, code IS 1893:2002 specified the upper limit of the storey drift as a 0.004 H where, H is the storey height. Inter storey drift obtained from uncontrolled and controlled structure are given in Table 7.13 to 7.16.

From results, it is evident that inter storey drift is maximum at 2^{nd} storey level, so comparison of inter storey drift is done at level of 2^{nd} storey of the building. It is clear from results that inter storey drift is constantly decreased by attaching ADAS damper to structure. For controlled building with ADAS damper, reduction of 29.6%, 49.8%, 55.1% and 51.6% in inter storey drift is observed under the El Centro, Kobe, Loma Prieta and Northridge earthquake excitations respectively, with respect to uncontrolled structure. It is observed that the inter storey drift is within the limiting the value which is recommended by the IS 1893:2002.

Table 7.13: Inter Storey Drift under El Centro (PGA-0.3129g) EQ Excitation

SR	Maximum Inter Storey Drift (m)					
	1^{st}	% Red.	2^{nd}	% Red.	Roof	% Red.
2	0.00237	77.4	0.00585	29.6	0.00333	29.1
Uncontrolled	0.01050	0.0	0.00830	0.0	0.00470	0.0

Table 7.14: Inter Storey Drift under Kobe (PGA-0.6936g) EQ Excitation

SR	Maximum Inter Storey Drift (m)					
	1^{st}	% Red.	2^{nd}	% Red.	Roof	% Red.
2	0.00504	83.7	0.01192	49.8	0.00653	44.6
Uncontrolled	0.03085	0.0	0.02377	0.0	0.01180	0.0

Table 7.15: Inter Storey Drift under Lomaprieta (PGA-0.6437g) EQ Excitation

SR	Maximum Inter Storey Drift (m)					
	1^{st}	% Red.	2^{nd}	% Red.	Roof	% Red.
2	0.00496	82.7	0.01039	55.1	0.00494	57.6
Uncontrolled	0.02877	0.0	0.02316	0.0	0.01166	0.0

Table 7.16: Inter Storey Drift under Northridge (PGA-1.585g) EQ Excitation

SR	Maximum Inter Storey Drift (m)					
	1^{st}	% Red.	2^{nd}	% Red.	Roof	% Red.
2	0.00536	87.8	0.01666	51.6	0.01080	36.9
Uncontrolled	0.04393	0.0	0.03442	0.0	0.01711	0.0

7.3.5 Comparison of Time History

Figure 7.2 to 7.5 shows 1^{st} storey displacement, velocity and acceleration time history in horizontal direction of uncontrolled and controlled building for El Centro, Kobe, Loma Prieta and Northridge earthquake excitations respectively.

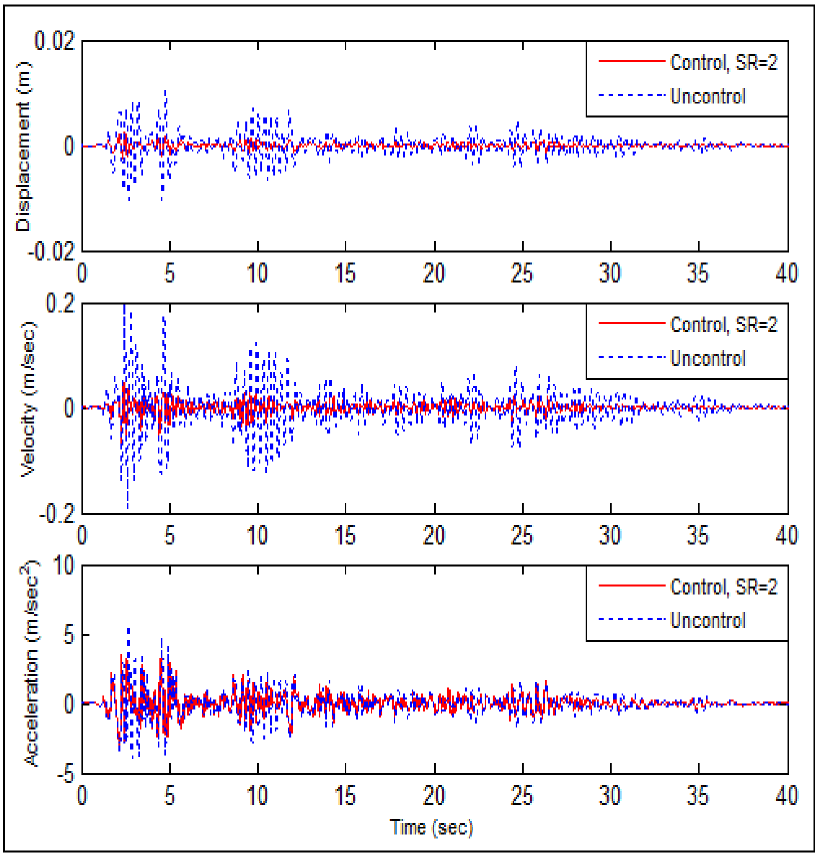

Figure 7.2: Time History Response at 1^{st} Storey under El Centro EQ

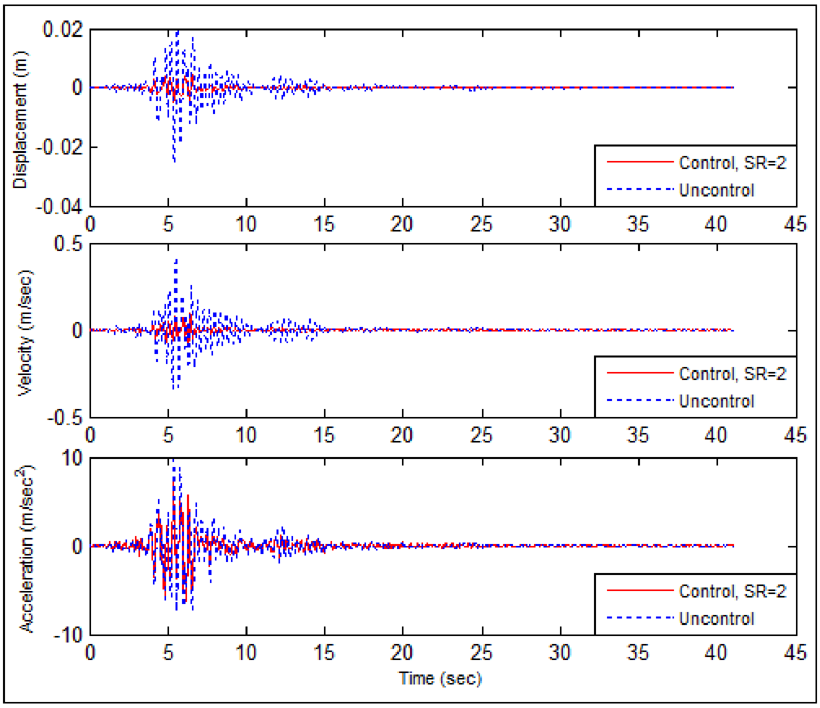

Figure 7.3: Time History Response at 1^{st} Storey under Kobe EQ

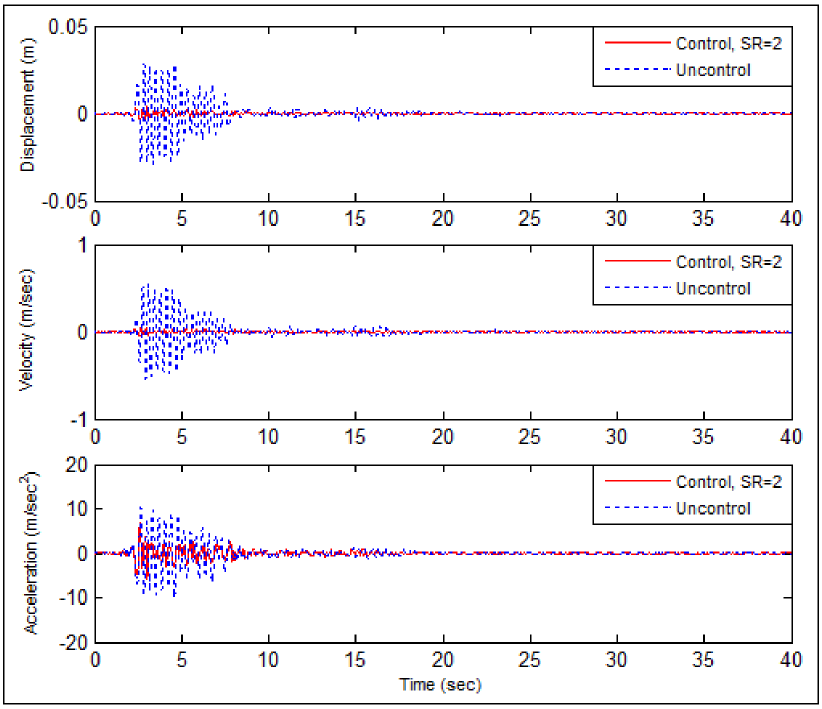

Figure 7.4: Time History Response at 1^{st} Storey under Lomaprieta EQ

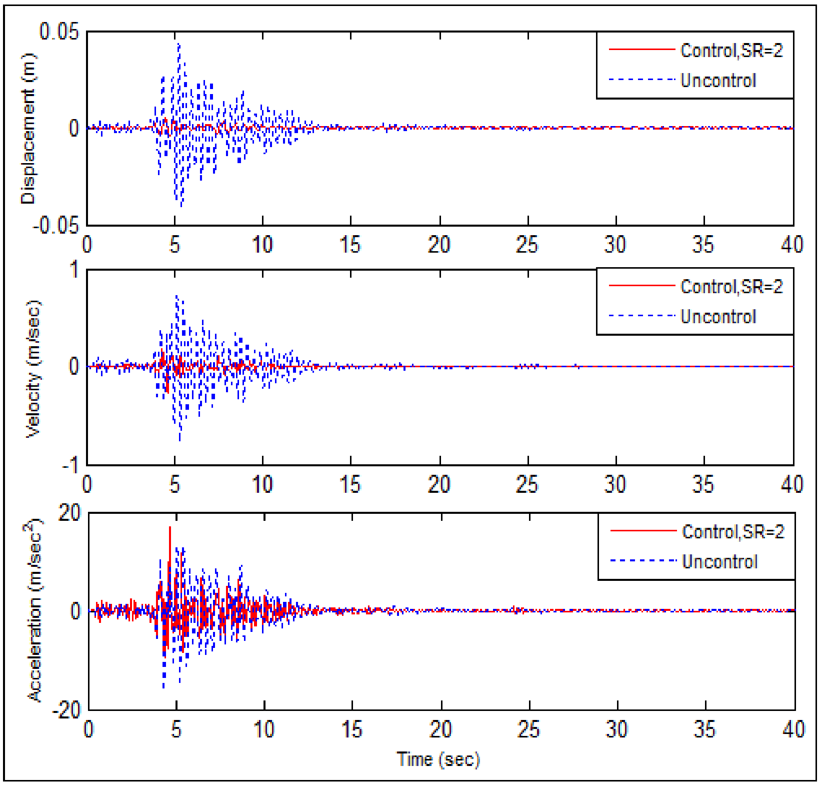

Figure 7.5: Time History Response at 1^{st} Storey under Northridge EQ

From this time history plots, it is evident that, in all the earthquake excitations, significantly reduced to storey displacement, and velocity throughout the strong motion of earthquake. However, Maximum acceleration reduction at 1^{st} storey of ADAS damper attached building is considerable under the El Centro, Kobe and Northridge earthquake. However, 4.2% acceleration is increases in the controlled building under the Loma Prieta earthquake with respect to uncontrolled building.

7.4 Summary

This chapter deals with the response of shear building using Added Damping and Stiffness (ADAS) damper by numerical method like Newmark-Beta under the EL Centro, Kobe, Loma Prieta, and Northridge earthquake excitations through MATLAB. Design parameters of ADAS damper are discussed, which is used in present study to find out the response of ADAS damper equipped building. Response quantities of controlled building like maximum displacement, maximum velocity, and maximum acceleration are compared with the uncontrolled building.

Chapter 8

Summary and Conclusions

8.1 Summary

Special techniques are required to design buildings rather than conventional seismic design, such that they remain practically undamaged even in a severe earthquake. For structures subjected to strong earthquake motions, the inherent damping in the structure is not sufficient to mitigate the structural response, therefore extra damping is required in the form of energy dissipating systems. Three basic technologies are used to protect buildings from damaging earthquake effects. These are Base Isolation, Passive Energy Dissipation Devices and Active Control Devices. In passive energy dissipation systems the motion of structure is controlled by adding devices to structure in the form of stiffness, mass and damping.

In this work, the main focuses was on the passive energy dissipation devices like, viscous, viscoelastic and metallic yield dampers. To understand the behavior of viscous and viscoelastic damper, characterization of this dampers have been carried out under the sinusoidal and different earthquake excitations, namely El Centro, Kobe, Loma Prieta, and Northridge excitations.

A three storey shear building has been considered. This building is converted to lump mass model and, mass matrix and stiffness matrix are derived. A rayleigh's damping is assumed and damping matrix are obtained. Equation of motion for multi degree of freedom system subjected to earthquake excitations are derived. Also, equation of motion for shear building with passive devices like viscous, viscoelastic and metallic yield dampers are derived. These equation of motions are solved using numerical method like Newmark-Beta for uncontrolled and controlled building under the different earthquake excitations through MATLAB. Response quantities like maximum displacement, maximum velocity, maximum acceleration and maximum inter storey drift has been obtained for uncontrolled and controlled building. These response quantities of uncontrolled building has been compared with the controlled building. Time history plot for displacement, velocity, acceleration and damper forces are also obtained.

8.2 Conclusions

The main aim of the work was to understand the mathematical model and behavior of viscous, viscoelastic, and metallic damper. From mathematical model of viscous and viscoelastic damper characterization of viscous and viscoelastic damper has been carried out under the sinusoidal and random earthquake excitations. Three storey shear building analysis has been done using time stepping numerical method Newmark-Beta for uncontrolled and the building equipped with passive energy dissipation devices, and extract the response quantities like maximum storey displacement, velocity, acceleration and damper force for four earthquake excitations through MATLAB.
Based on the work carried out following conclusions are made.

- Numerical results of three storey shear building equipped with viscous damper clearly indicate that the maximum roof displacement, maximum roof velocity, maximum roof acceleration and maximum inter storey drift are significantly reduces as co-efficient of damper 'C_d' increases, under four different types of earthquake excitations.

  a. Maximum roof displacements are reduced by 60.49 % under the Northridge earthquake excitation when damping co-efficient is 100 $kNsec/cm$.

b. Maximum roof velocity are reduced by 60.25 % under the Northridge earthquake excitation when damping co-efficient is 100 $kNsec/cm$.

c. Maximum roof acceleration are reduced by 40.04 % under the Loma Prieta earthquake excitation when damping co-efficient is 70 $kNsec/cm$.

d. Maximum inter storey drift at first storey are reduced by 70.23 % under the Northridge earthquake when damping co-efficient is 100 $kNsec/cm$.

e. This result indicates that amount of damping directly influence the responses by reducing it.

- It can be concluded that viscoelastic damper are effective in reducing all response quantities of building as required damping ratio 'ζ' increases under the earthquake excitations. This result indicates that amount of damping and stiffness directly influence the responses by reducing it.

a. Maximum roof displacements are reduced by 64.45 % under the Loma Prieta earthquake when required damping ratio is 30 %.

b. Maximum roof velocity are reduced by 83.49 % under the Loma Prieta earthquake when required damping ratio is 30 %.

c. Maximum roof acceleration are reduced by 56.12 % under the Loma Prieta earthquake when required damping ratio is 30 %.

d. Maximum inter storey drift at first storey are reduced by 85.76 % under the Northridge earthquake when required damping ratio is 30 %.

e. As higher level of damping is not feasible in all types of earthquakes. It is found from the study that, even 12 % of required damping ratio had achieved great influence on response reduction.

- It is found from the results of three storey shear building equipped with added damping and stiffness damper (ADAS) that, ADAS device is more effective in reducing the response quantity for Stiffness Ratio 'SR' is equal to 2, as compare to viscous damper.

a. Maximum roof displacements are reduced by 67.5 % under the Loma Prieta earthquake for Stiffness Ratio is equal to 2.

b. Maximum roof velocity are reduced by 84.7 % under the Loma Prieta earthquake for Stiffness Ratio is equal to 2.

c. Maximum roof acceleration are reduced by 57.3 % under the Loma Prieta earthquake for Stiffness Ratio is equal to 2.

d. Maximum inter storey drift are reduced by 57.6 % under the Loma Prieta earthquake for Stiffness Ratio is equal to 2.

- From all the results of different passive damper added three storey shear building, it is concluded that all are good enough to reduces all response quantities. It can be also concluded that viscous damper are more effective under the Northridge type of earthquake excitations, however viscoelastic and ADAS damper are suitable for Loma Prieta type of earthquake excitations.

8.3 Future Scope of the Work

The present work can be used as an input for further work explained as follows.

- Present study has considered only Maxwell and Kelvin Model. However more precise mathematical model can be taken up for analysis.

- In this study three storey building with passive devices equipped at first storey is considered, however the effectiveness of more passive dampers placed at different different storey can be studied.

- The optimal locations of damper placement can be obtained through various optimization techniques.

- Comparative study of cost analysis of different passive energy dissipation devices can help in appropriate selection of proper damper for various buildings in various seismic excitations.

Appendix A

Calculation of Eigenvalue and Eigenvector

As discussed earlier, three storey shear building is shown in Figure 4.1 is converted in to a Lump mass model, which is given in Figure 4.2. Calculation of Eigenvalues, Eigenvectors, Mass Matrix [M], Stiffness Matrix [K], Damping Matrix [D] of this lump mass model are found out as follows,

Building Configuration

Number of Stories	3 No.
Floor height (c/c)	3 m
Imposed load	3 kN/m^2
Percentage of Imposed Load	0.75 kN/m^2
Characteristics Strength of Concrete, f_{ck}	25 N/mm^2
Characteristics Strength of Steel, f_y	415 N/mm^2
No. of Bays In X-Direction	3 No.
No. of Bays In Y-Direction	3 No.
Bay Width In X-Direction	4 m
Bay Width In Y-Direction	4 m

Column size,	(0.3 x 0.3) m
Beam size,	(0.23 x 0.3) m
Depth of slab	0.12 m
Specific weight of R.C.C	25 kN/m^3
Specific weight of infill	0
Inherent Damping Ratio for Concrete Structure	5%

Lump Mass Calculation

At Roof Level		At Typical Storey	
Weight of Infill	0	Weight of Infill	0
Weight of Columns	54 kN	Weight of Columns	108 kN
Weight of Beams	165.6 kN	Weight of Beams	165.6 kN
Weight of Slab	432 kN	Weight of Slab	432 kN
Imposed Load	0 (IS 1893:2002)]	Imposed Load	108 kN
Total Roof Load	651.6 kN	Total Floor Load	1627.2 kN

Total Seismic Weight of Building, W = 2278.8 kN

Calculation of Eigenvalues and Eigenvectors

Mass Matrix of lumped mass model of building, M

$$[\mathrm{M}]= \begin{vmatrix} M_1 & 0 & 0 \\ 0 & M_2 & 0 \\ 0 & 0 & M_3 \end{vmatrix} \mathrm{Kg}$$

$$[\mathrm{M}]= \begin{vmatrix} 82935.78 & 0 & 0 \\ 0 & 82935.78 & 0 \\ 0 & 0 & 66422.02 \end{vmatrix} \mathrm{Kg}$$

Stiffness Matrix of lumped mass model of building, K

Column stiffness in X and Y direction, k=12EI/l^3

Total lateral stiffness of each story = No of columns in a story × k = 120000000 N/m

$$[K]= \begin{vmatrix} K_1+K_2 & -K_2 & 0 \\ -K_2 & K_2+K_3 & -K_3 \\ 0 & -K_3 & K_3 \end{vmatrix}$$

$$[K]= \begin{vmatrix} 240000000 & -120000000 & 0 \\ -120000000 & 240000000 & -120000000 \\ 0 & -120000000 & 120000000 \end{vmatrix} \text{N/m}$$

For the above stiffness and mass matrices, eigenvalue and eigenvector are worked out using MATLAB as follows,

$$[K] \times [M]^{-1} = \begin{vmatrix} 2893.81 & -1446.9027 & 0 \\ -1446.9 & 2893.80531 & -1806.6298 \\ 0 & -1446.9027 & 1806.62983 \end{vmatrix}$$

Eigenvalues or natural frequencies of various modes are,

$$[\omega^2] = \begin{vmatrix} 320.82 & 0 & 0 \\ 0 & 2438.17 & 0 \\ 0 & 0 & 4835.25 \end{vmatrix}$$

ω_1=17.92 rad/sec, ω_2=49.38 rad/sec, ω_3=69.54 rad/sec,

The eigenvector (mode shapes) and natural periods corresponding to each natural frequency are,

$$[\phi] =[\phi_1\ \phi_2\ \phi_2] = \begin{vmatrix} 0.3364 & -0.7234 & -0.5391 \\ 0.5982 & -0.2278 & 0.7233 \\ 0.7273 & 0.6517 & -0.4315 \end{vmatrix}$$

$$T = \begin{vmatrix} 0.351 & 0 & 0 \\ 0 & 0.127 & 0 \\ 0 & 0 & 0.351 \end{vmatrix} \text{sec}$$

Evaluate the Rayleigh Damping Matrix

By considering first mass-proportional damping and stiffness-proportional damping, C = $a_0M + a_1K$

Where, C is the rayleigh damping matrix; a_0 and a_1 are the co-efficient; M and K are the mass and stiffness matrix of building respectively. The co-efficient a_0 and a_1 can be determine from specified damping ratios ξ_i and ξ_j for the i th and j th modes, respectively. If all modes are to have the same damping ratio ξ, which is reasonable based on experiment data, therefore

$$a_0 = \frac{\xi\omega_i\omega_j}{\omega_i + \omega_j}$$

$$a_1 = \frac{2\xi}{\omega_i + \omega_j}$$

Where, ξ is the inherent damping ratio of the structure, ω_i and ω_j are the i th and j th natural frequency of of the building. Therefore, damping matrix of three storey building as per rayleigh's damping 'C' is,

$$C = \begin{vmatrix} 465677.03 & -178334.3 & 0 \\ -178334.3 & 465677.027 & -178334.3 \\ 0 & -178334.3 & 265637.512 \end{vmatrix} \text{N Sec/m}$$

Appendix B

Design of Viscoelastic Damper

- The design of Viscoelastic damper is an iterative process. Many iteration were performed to achieve the exact area of Viscoelastic material pad. The design is carried out according to R. D. Hanson and T. T. Soong [20], which recommends Kelvin Model for analysis. To support the iterative calculations Microsoft Excel Sheet was used.

- The procedure for design was given in chapter 6 Section 6.2.1 with various equations. Calculation usually comprise of estimating additional stiffness and damping provided by the damper which were calculated by Equations 6.1, 6.3 and 6.4 explained in Chapter 6.

- Prior to design it is required to decide, desired damping ratio that should be achieved to reduce prescribed response level of building. In this study, the required structural damping ratio 'ζ' is assumed for the initial goal.

- Here sample calculation of design of damper is carried out for required damping ratio 'ζ' is equal to 20 %.

Data Taken:

Fundamental Frequency of the Building, ω	17.91 rad/sec
Inherent Damping Ratio of Building	5%
Storey Drift Ratio	0.40%
Operating Temperature, T	25^{o}C
Storey Height, h	3 m
Required Damping Ratio, ζ	20%
Angel Between Bracing Member and Floor, θ	36.86
Target Added damping Ratio, ς	15%
Assumed Loss Factor, η	1.2

1) From modifying modal strain energy method,

$$\alpha_d K_d = \frac{2\varsigma}{(\eta - 2\varsigma)} K_s$$

where, α_d is the attachment co-efficient is equal to $cos^2\theta$ for diagonally attached damper, and K_s = 120000000 N/m is the typical storey stiffness of the building. Therefore damper stiffness K_d is equal to 62490235.90 N/m

2) In this study of VE damper design, Maximum design damper deformation is $0.004 \times h \times cos\theta = 0.0096$ m.

3) If the maximum design damper strain of 60 % is allowed, then the damper thickness t is $0.0096/0.6 = 0.016$ m.

4) Simplified relationship for shear storage and shear loss modulus is given by soong and dargush [11], from this relationship shear storage modulus, $G^{'} = 2068420$ N/m^2 and shear loss modulus, $G^{''} = 2482104$ N/m^2 are determined.

5) Area of viscoelastic damper is calculated using Equation 6.3. Therefore, area of viscoelastic damper $A = 0.48338527$ m^2 for one layer.

6) If two VE layers are used per damper, then the selected dimension of each damper pad are, $A = 0.241692\ m^2$, Length of damper pad $L = 0.85$ m, Width of damper $B = 0.3$ m, and thickness of damper $t = 0.016$ m.

7) From area of VE damper, final stiffness of damper $K_d = 65930887.5$ N/m and co-efficient of damper $C_d = 4417479.899$ N sec/m are calculated using Equation 6.3 and Equation 6.4 respectively.

8) Similarly, VE damper design is carries out for different value of required damping ratio 'ζ', and damper stiffness K_d, co-efficient of damper C_d, and size of damper are find out, which is given in Table 6.1.

Appendix C

MATLAB Code

A) MATLAB Code for Response of Viscous Damper Subjected to Sinusoidal Input (for varying value of amplitude)

```
% For linear viscous damper
w=6.28; % Frequency is constant in rad/sec
cd=160; % Damping co efficient in N*S/mm
for a = 20:5:40 %Amplitudes are varying(in mm)
t=0:0.002:2; %Time in Sec
x=a*sin(w*t); %Displacement in mm
x1=a*w*cos(w*t); % Velocity in mm/sec
f=(cd*x1); % Force in Damper in N
subplot(2,2,1:2)
plot(t,f,'g'); % Plot of Force Vs Time
grid on
xlabel('Time(sec)')
ylabel('Force(N)')
hold on
subplot(2,2,3)
plot(x,f,'g'); % Plot of Force Vs Displacement
grid on
```

```
xlabel('Displacement(mm)')
ylabel('Force(N)')
hold on
subplot(2,2,4)
plot(x1,f,'g'); % Plot of Force Vs Velocity
grid on
xlabel('Velocity(mm/sec)')
ylabel('Force(N)')
hold on
end
```

B) MATLAB Code for Response of Viscous Damper Subjected to Earthquake Excitations

```
cd=160000 ; % Damping coefficient in NS/m
t=0:0.01:40; %Time in Sec
fid1 = fopen('.txt file of El Centro Displacement Data');
x=fscanf(fid1,'%g'); %Displacement in cm
x=[0 ; x];
x=x.*0.01; %in m
fid2 = fopen('.txt file of El Centro Velocity Data');
x1=fscanf(fid2,'%g'); % Velocity in cm/sec
x1=[0 ; x1];
x1=x1.*0.01; % in m/sec
f=(cd*x1); % Force in Damper in N
subplot(2,2,1:2)
plot(t,f,'k');% Plot of Force Vs Time
title('Response of Viscous Damper');
grid on
xlabel('Time(sec)')
```

```
ylabel('Force(N)')
hold on
subplot(2,2,3)
plot(x,f,'k'); % Plot of Force Vs Displacement
grid on
xlabel('Displacement(m)')
ylabel('Force(N)')
hold on
subplot(2,2,4)
plot(x1,f,'k'); % Plot of Force Vs Velocity
grid on
xlabel('Velocity(m/sec)')
ylabel('Force(N)')
hold on
```

C) MATLAB Code for Response of Viscoelastic Damper Subjected to Sinusoidal Motion (for varying value of amplitude)

```
w=6.28; % Frequency is constant in rad/sec
kd=486.85; % Stiffness co efficient for VE Damper in N/mm
cd=93.093; % Damping co efficient in N*S/mm
for a=0.75:0.25:2; %Amplitudes are varying(in mm)
t=0:0.001:3; %Time in Sec
x=a*sin(w*t); %Displacement in mm
x1=a*w*cos(w*t); % Velocity in mm/sec
f=(kd*x)+(cd*x1); % Force in Damper in N
subplot(2,2,1:2)
plot(t,f); % Plot of Force Vs Time
grid on
xlabel('Time(sec)')
```

```
ylabel('Force(N)')
hold on
subplot(2,2,3)
plot(x,f); % Plot of Force Vs Displacement
grid on
xlabel('Displacement(mm)')
ylabel('Force(N)')
hold on
subplot(2,2,4)
plot(x1,f); % Plot of Force Vs Velocity
grid on
xlabel('Velocity(mm/sec)')
ylabel('Force(N)')
hold on
end
```

D) MATLAB Code for Response of Viscoelastic Damper Subjected to Earthquake Excitations

```
kd=468850; % Stiffness co efficient for VE Damper in N/m
cd=93093; % Damping co efficient in N*S/m
t=0:0.01:40; %Time in Sec
fid1 = fopen('.txt file of earthquake displacement data ');
x=fscanf(fid1,'%g'); %Displacement in cm
x=[0 ; x];
x=x.*0.01; %in m
fid2 = fopen('.txt file of earthquake velocity data ');
x1=fscanf(fid2,'%g'); % Velocity in cm/sec
x1=[0 ; x1];
x1=x1.*0.01; % in m/sec
```

```
f=(kd*x)+(cd*x1);% Force in Damper in N
x1max = max(abs(f))
subplot(2,2,1:2)
plot(t,f,'k'); % Plot of Force Vs Time
grid on
xlabel('Time(sec)')
ylabel('Force(N)')
hold on
subplot(2,2,3)
plot(x,f,'k'); % Plot of Force Vs Displacement
grid on
xlabel('Displacement(m)')
ylabel('Force(N)')
hold on
subplot(2,2,4)
plot(x1,f,'k'); % Plot of Force Vs Velocity
grid on
xlabel('Velocity(m/sec)')
ylabel('Force(N)')
hold on
```

E) MATLAB Code for Seismic Response of Uncontrolled Building to Find out Maximum Roof Displacement, Velocity and Acceleration using Newmark-Beta Method (El Centro EQ Excitation)

```
%Seismic Response of Three storey uncontrolled Building using newmark-Beta method
(El centro) clc;
close all
%mass matrix
m=[82935.78 0 0;0 82935.78 0;0 0 66422.02];
```

```
disp('mass matrix')
m
[ns,ms] = size(m);
fid=fopen('.txt file of El Centro Acceleration Data');
di = fscanf(fid,'%g');
di=[0 ; di];
di=di.*9.81; %in m/sec^2
for i=1:ns
f(:,i)=-di*m(i,i);
end
%damping matrix in N sec/m
c=[465677.0273 -178334.295 0;-178334.295 465677.0273 -178334.295;0 -178334.295 265637.5122];
disp('damping matrix')
c
%stiffness matrix in N/m
k=[240000000 -120000000 0;-120000000 240000000 -120000000;0 -120000000 120000000];
k
kim=inv(m)*k;
for i=1:ns
omega(i)=sqrt(ev(i,i));
end
disp('natural frequency')
omega
%specify integration parameter for constant acceleration method
beta=1/4;
gamma=0.5;
%specify increment in time
dt=0.01;
%specify initial displacement
u0=[0 0 0];
```

```
v0=[0 0 0];
for i=1:ns
a0=inv(m)*(f(1,:)'-c*v0'-k*u0');
end
kba=k+(gamma/(beta*dt))*c+(1/(beta*dt*dt))*m;
kin=inv(kba);
aa=(1/(beta*dt))*m+(gamma/beta)*c;
bb=(1/(2*beta))*m+dt*(gamma/(2*beta)-1)*c;
u(1,:)=u0;
v(1,:)=v0;
a(1,:)=a0;
for i=2:4001
df(i,:)=f(i,:)-f(i-1,:)+v(i-1,:)*aa'+a(i-1,:)*bb';
du(i,:)=df(i,:)*kin;
dv(i,:)=(gamma/(beta*dt))*du(i,:)-(gamma/beta)*v(i-1,:)+dt*(1-gamma/(2*beta))*a(i-
1,:);
da(i,:)=(1/(beta*dt^2))*du(i,:)-(1/(beta*dt))*v(i-1,:)-(1/(2*beta))*a(i-1,:);
u(i,:)=u(i-1,:)+du(i,:);
v(i,:)=v(i-1,:)+dv(i,:);
a(i,:)=a(i-1,:)+da(i,:);
end
tt=linspace(0,40,4001);
%find total acceleration
at3 = a(:,3) + di;
at2 = a(:,2) + di;
at1 = a(:,1) + di;
subplot(3,1,1)
plot(tt,u(:,3),'k');
xlabel('Time(sec)');
ylabel('Roof Disp.(m)');
```

```
title('Displacement Response at Roof');
subplot(3,1,2)
plot(tt,v(:,3),'k');
xlabel('Time(Sec)');
ylabel('Roof Velo.(m/sec)');
title(' Velocity Response at Roof');
subplot(3,1,3)
plot(tt,at3,'k');
xlabel('Time(sec)');
ylabel('Roof Accel.(m/sec^2)');
title('Acceleration Response at Roof');
```

F) MATLAB Code for Seismic Response of Building Equipped with Viscous Damper (for C_d = 100 Kn s/cm) to Find out Maximum Roof Displacement, Velocity and Acceleration using Newmark-Beta Method (El Centro EQ Excitation)

```
clc;
close all
%mass matrix m=[82935.78 0 0;0 82935.78 0;0 0 66422.02];
disp('mass matrix')
m
[ns,ms] = size(m);
fid=fopen('.txt file of El Centro Acceleration Data');
di = fscanf(fid,'%g');
di=di.*9.81; %in m/sec^2
di=[0 ; di];
for i=1:ns
f(:,i)=-di*m(i,i);
end
```

```
%damping matrix in N sec/m
cs=[465677.0273 -178334.295 0;-178334.295 465677.0273 -178334.295;0 -178334.295
265637.5122];
disp('damping matrix')
cs
%stiffness matrix in N/m
k=[240000000 -120000000 0;-120000000 240000000 -120000000;0 -120000000 120000000];
k
%column vector of ones
l=[1 1 1];
%Matrix determined by the placement of VE dampers in the structure
b=[1 0 0]';
%damping matrix due to viscous damper in N sec/m
cd=[10000000 0 0;0 0 0;0 0 0];
c=cs+cd;
format long;
kim=inv(m)*k;
for i=1:ns
omega(i)=sqrt(ev(i,i));
end
disp('natural frequency')
omega
%specify integration parameter for constant acceleration method
beta=1/4;
gamma=0.5;
%specify increment in time
dt=0.01;
%specify initial displacement
u0=[0 0 0];
v0=[0 0 0];
```

```
for i=1:ns
a0=inv(m)*((f(1,:)*l'-c*v0'-k*u0'));
end
kba=k+(gamma/(beta*dt))*c+(1/(beta*dt*dt))*m;
kin=inv(kba);
aa=(1/(beta*dt))*m+(gamma/beta)*c;
bb=(1/(2*beta))*m+dt*(gamma/(2*beta)-1)*c;
u(1,:)=u0;
v(1,:)=v0;
a(1,:)=a0;
for i=2:4001
df(i,:)=f(i,:)-f(i-1,:)+v(i-1,:)*aa'+a(i-1,:)*bb';
du(i,:)=df(i,:)*kin;
dv(i,:)=(gamma/(beta*dt))*du(i,:)-(gamma/beta)*v(i-1,:)+dt*(1-gamma/(2*beta))*a(i-
1,:);
da(i,:)=(1/(beta*dt^2))*du(i,:)-(1/(beta*dt))*v(i-1,:)-(1/(2*beta))*a(i-1,:);
u(i,:)=u(i-1,:)+du(i,:);
v(i,:)=v(i-1,:)+dv(i,:);
a(i,:)=a(i-1,:)+da(i,:);
end
tt=linspace(0,40,4001);
at3 = a(:,3) + di;%total acceleration
subplot(3,1,1)
plot(tt,u(:,3),'k');
xlabel('Time(sec)');
ylabel('Roof Disp.(m)');
title('Displacement Response at Roof');
subplot(3,1,2)
plot(tt,v(:,3),'k');
xlabel('Time(Sec)');
```

```
ylabel('Roof Velo.(m/sec)');
title('Velocity Response at Roof');
subplot(3,1,3)
plot(tt,a(:,3),'k');
xlabel('Time(sec)');
ylabel('Roof Accel.(m/sec^2)');
title('Acceleration Response at Roof');
```

G) MATLAB Code for Seismic Response of Building Equipped with Viscoelastic Damper (for ζ = 30 %) to Find out Maximum Roof Displacement, Velocity and Acceleration using Newmark-Beta Method (El Centro EQ Excitation)

```
clc;
close all
%mass matrix
m=[82935.78 0 0;0 82935.78 0;0 0 66422.02];
disp('mass matrix')
m
[ns,ms] = size(m);
fid=fopen('.txt file of El Centro Acceleration Data');
di = fscanf(fid,'%g');
di=di.*9.81; %in m/sec^2
di=[0 ; di];
for i=1:ns
f(:,i)=-di*m(i,i);
end
%damping matrix in N sec/m
cs=[465677.0273 -178334.295 0;-178334.295 465677.0273 -178334.295;0 -178334.295
265637.5122];
```

```
disp('damping matrix')
%damping matrix due to viscous damper in N sec/m
cd=[9094811.558 0 0;0 0 0;0 0 0];
c=cs+cd;
disp('damping matrix')
c
%Storey stiffness matrix in N/m ks=[240000000 -120000000 0;-120000000 240000000
-120000000;0 -120000000 120000000];
%Stiffness matrix due to Damper added
kd=[135740062.5 0 0;0 0 0;0 0 0];
%Stiffness matrix due to storey stiffness and VE damper
k=ks+kd
%column vector of ones
l=[1 1 1];
%Matrix determined by the placement of VE dampers in the structure
b=[1 0 0]';
format long;
kim=inv(m)*k;
[evec,ev] = eig(kim);
for i=1:ns
omega(i)=sqrt(ev(i,i));
end
disp('natural frequency')
omega
%specify integration parameter for constant acceleration method
beta=1/4;
gamma=0.5;
%specify increment in time
dt=0.01;
%specify intial displacement
```

```
u0=[0 0 0];
v0=[0 0 0];
for i=1:ns
a0=inv(m)*((f(1,:)*l'-c*v0'-k*u0'));
end
%calculate the following constants
kba=k+(gamma/(beta*dt))*c+(1/(beta*dt*dt))*m;
kin=inv(kba);
aa=(1/(beta*dt))*m+(gamma/beta)*c;
bb=(1/(2*beta))*m+dt*(gamma/(2*beta)-1)*c;
u(1,:)=u0;
v(1,:)=v0;
a(1,:)=a0;
for i=2:4001
df(i,:)=f(i,:)-f(i-1,:)+v(i-1,:)*aa'+a(i-1,:)*bb';
du(i,:)=df(i,:)*kin;
dv(i,:)=(gamma/(beta*dt))*du(i,:)-(gamma/beta)*v(i-1,:)+dt*(1-gamma/(2*beta))*a(i-
1,:);
da(i,:)=(1/(beta*dt^2))*du(i,:)-(1/(beta*dt))*v(i-1,:)-(1/(2*beta))*a(i-1,:);
u(i,:)=u(i-1,:)+du(i,:);
v(i,:)=v(i-1,:)+dv(i,:);
a(i,:)=a(i-1,:)+da(i,:);
end
tt=linspace(0,40,4001);
at3 = a(:,3) + di;%total acceleration
at2 = a(:,2) + di;%total acceleration
at1= a(:,1) + di;%total acceleration
%inter storey drift d1=u(:,1);
d2=(u(:,2)-u(:,1));
d3=(u(:,3)-u(:,2));
```

```
d1max = max(abs(d1))
d2max = max(abs(d2))
d3max = max(abs(d3))
%Maximum displacement di1max = max(abs(u(:,1)))
di2max = max(abs(u(:,2)))
di3max = max(abs(u(:,3)))
%Maximum velocity ve1max = max(abs(v(:,1)))
ve2max = max(abs(v(:,2)))
ve3max = max(abs(v(:,3)))
%Maximum accleration
ac1max = max(abs(at1))
ac2max = max(abs(at2))
ac3max = max(abs(at3))
subplot(3,1,1)
plot(tt,u(:,3),'k');
xlabel('Time(sec)');
ylabel('Roof Disp.(m)');
title('Displacement Response at roof');
subplot(3,1,2)
plot(tt,v(:,3),'k');
xlabel('Time(Sec)');
ylabel('Roof Velo.(m/sec)');
title('Velocity Response at roof');
subplot(3,1,3)
plot(tt,at3,'k');
xlabel('Time(sec)');
ylabel('Roof Accel.(m/sec^2)');
title('Acceleration Response at roof')
```

H) MATLAB Code for Seismic Response of Building Equipped with Added Damping and Stiffness Damper (for SR = 2) to Find out Maximum Roof Displacement, Velocity and Acceleration using Newmark-Beta Method (El Centro EQ Excitation)

```
clc;
close all
%mass matrix m=[82935.78 0 0;0 82935.78 0;0 0 66422.02];
disp('mass matrix')
m
[ns, ms] = size(m);
fid=fopen('.txt file of El Centro Acceleration Data');
di = fscanf(fid,'%g');
di=di.*9.81; %in m/sec^2
di=[0 ; di];
for i=1:ns
f(:,i)=-di*m(i,i);
end
%damping matrix due to equivalent viscous damping ratio in N sec/m
c=[1583301.9 -606336.6 0; -606336.6 1583301.9 -606336.6; 0 -606336.6 903167.5];
disp('damping matrix')
disp('damping matrix')
c
%Storey stiffness matrix in N/m
ks=[240000000 -120000000 0;-120000000 240000000 -120000000;0 -120000000 120000000];
%Stiffness matrix due to ADAS Damper added
kd=[240000000 0 0;0 0 0;0 0 0];
%Stiffness matrix due to storey stiffness and VE damper
k=ks+kd
%column vector of ones
```

```
l=[1 1 1];
%Matrix determined by the placement of VE dampers in the structure
b=[1 0 0]';
format long;
kim=inv(m)*k;
[evec,ev]=eig(kim); for i=1:ns
omega(i)=sqrt(ev(i,i));
end
disp('natural frequency')
omega %specify integration parameter for constant acceleration method beta=1/4;
gamma=0.5;
%specify increment in time
dt=0.01;
%specify initial displacement
u0=[0 0 0];
v0=[0 0 0];
for i=1:ns
a0=inv(m)*((f(1,:)*l'-c*v0'-k*u0'));
end
kba=k+(gamma/(beta*dt))*c+(1/(beta*dt*dt))*m;
kin=inv(kba);
aa=(1/(beta*dt))*m+(gamma/beta)*c;
bb=(1/(2*beta))*m+dt*(gamma/(2*beta)-1)*c;
u(1,:)=u0;
v(1,:)=v0;
a(1,:)=a0;
for i=2:4001
df(i,:)=f(i,:)-f(i-1,:)+v(i-1,:)*aa'+a(i-1,:)*bb';
du(i,:)=df(i,:)*kin;
dv(i,:)=(gamma/(beta*dt))*du(i,:)-(gamma/beta)*v(i-1,:)+dt*(1-gamma/(2*beta))*a(i-
```

```
1,:); da(i,:)=(1/(beta*dt^2))*du(i,:)-(1/(beta*dt))*v(i-1,:)-(1/(2*beta))*a(i-1,:);
u(i,:)=u(i-1,:)+du(i,:);
v(i,:)=v(i-1,:)+dv(i,:);
a(i,:)=a(i-1,:)+da(i,:);
end
tt=linspace(0,40,4001);
at3 = a(:,3) + di;%total acceleration
at2 = a(:,2) + di;%total acceleration
at1= a(:,1) + di;%total acceleration
x1=u(:,1);
x2=(u(:,2)-u(:,1));
x3=(u(:,3)-u(:,2));
w1max = max(abs(x1))
w2max = max(abs(x2))
w3max = max(abs(x3))
x1max = max(abs(u(:,3)))
x2max = max(abs(v(:,3)))
x3max = max(abs(at3))
y1max = max(abs(u(:,2)))
y2max = max(abs(v(:,2)))
y3max = max(abs(at2))
z1max = max(abs(u(:,1)))
z2max = max(abs(v(:,1)))
z3max = max(abs(at1))
subplot(3,1,1)
plot(tt,u(:,3),'k');
xlabel('Time(sec)');
ylabel('Roof Disp.(m)');
title('Displacement Response at Roof');
%figure(2);
```

```
subplot(3,1,2)
plot(tt,v(:,3),'k');
xlabel('Time(Sec)');
ylabel('Roof Velo.(m/sec)');
title('Velocity Response at Roof');
%figure(3)
subplot(3,1,3)
plot(tt,at3,'k');
xlabel('Time(sec)');
ylabel('Roof Accel.(m/sec^2)');
title('Acceleration Response at Roof');
```

References

[1] T. K. Caughey R. E. Skelton T. T. Soong B. F. Spencer J. P. Yao. G. W. Housner, L. A. Bergman. Structural control: past, present, and future. *Journal of Engineering Mechanics*, (Vol:123):897–971, 1997.

[2] A. Mortezaei & S.M. Zahrai. Seismic response of reinforced concrete building with viscoelastic damper under near feild earthquake. *Asian Journal of Civil Engineering*, (Vol:9), 2009.

[3] David Thambiratnam Julius Marko and Nimal Perera. Study of viscoelastic and friction damper configurations in medium rise structures. *Journal of Mechanics of Materials and Structures*, (Vol:1(6)), 2006.

[4] B. Samali & K. C. S. Kwok. Use of viscoelastic dampers in reducing wind and earthquake induced motion of building. *Engineering Structures*, (Vol:17), 1995.

[5] M. S. Jaafar M. Seifi E. Yazdan Panah, J. Noorzaei. Earthquake response of steel building with viscous brace damper. *Internatinal Conference on Building and Construction*, (Vol:5):59–68, 2008.

[6] Chuan Xia & Robert D. Hanson. Influence of adas element parameters on building seismic response. *Journal of Structural Engineering*, (Vol:118), July 1992.

[7] & H Pourmohammad S. M. S. Alehashem, A. Keyhani. Behavior and performance of structures equipped with adas & tadas dampers (a comparison with conventional structures). *Shahrood University of Technology, Shahrood, IRAN*, Oct 2008.

[8] C.L. Thompson L. J. Alonso A. S. Whittaker, V. V. Bertero. Seismic testing of steel plate energy dissipation devices. *Earthquake Spectra*, (Vol:7(4)):553–604, 1991.

[9] C. P. Hong Y. F. Su K. C. Tsai, H. W. Chen. Design of steel triaguler plate energy absorbers for seismic-resistance construction. *Earthquake Spectra*, (Vol:9(3)), 1993.

[10] T.T. Soong & M.C. Constantinou. Passive and active structural vibration control in civil engineering. *Vienna and new york: Springer-Verlag*, 1994.

[11] T.T.Soong and G.F Dargush. Passive energy dissipation systems in structural engineering. *University of New York at Buffalo, USA. John Willey & Sons*, 1997.

[12] N. Makris & M. C. Constantinou. Viscous dampers: testing, modeling and application in vibration and seismic isolation. *National Center for Earthquake Engineering Research, Buffalo, NY. NCEER Report*, 1990.

[13] P. Tsopelas D. P. Taylor M. C. Constantinou, M. D. Saymans. Fluid viscous dampers in applications of seismic energy dissipation and seismic isolation. *Proceeding ATC 17-1 on Seismic Isolaion Energy Dissipation and Active Control San Francisco, CA*, (Vol:2), 1993.

[14] FEMA 273 NEHRP Guidelines for the Seismic Rehabilitation of Buildings. Department of homeland security federal emergency management agency. *Ch-9 Seismic Isolation and Energy Dissipation*, pages 9.1–9.27, Oct 1997.

[15] T. T. Soong D. S. Hao K. C. Chang, M. L. Lai. Seismic behavoir and design guidelines for steel frame structures with added viscoelastic dampers. *National Centre For Earthquake Engineering Research*, 1993.

[16] A. J. Heine J. M. Kelly, R. I. Skinner. Mechanisms of energy absorption in special devices for use in earthquake resistanant structures. *Earthquake Engineering*, (Vol:5(3)), 1972.

[17] I. G. Buckle. Passive control of structures for seismic loads. *University of Nevada, USA*, 2000.

[18] N. M. Newmark. A method of computation for structural dynamics. *ASCE Journol of Engineering Mechanics Division*, (Vol:85), 1959.

[19] A. K. Chopra. Dynamics of structures. theory and appliction to earthquake engineering. *Pearson Education, Inc.*, 2007.

[20] Robert D.Hanson and T.T Soong. Seismic design with supplementary energy dissipation devices, monograph series, eeri. 2001.